UNIVERSITÀ DEGLI STUDI DI SASSARI

Doctoral Dissertation
Doctoral Program in Biomedical Sciences (35th Cycle)

Methods for real-world gait analysis based on wearable sensors.

Mobility assessment on healthy and pathological subjects

By

Francesca Salis

Supervisor:
Prof. A. Cereatti

Reviewers:
Prof. G. Vannozzi, Referee, University of Rome "Foro Italico"
Prof. A. Parachiv Ionescu, Referee, Ecole Polytechnique Federale de Lausanne

University of Sassari
2023

Declaration

I hereby declare that the contents and organization of this dissertation constitute my own original work and do not compromise in any way the rights of third parties, including those relating to the security of personal data.

Francesca Salis

2023

Statement of authorship

The works reported and described in this thesis have been published in scientific international journals:

1. F. Salis, S. Bertuletti, T. Bonci, U. Della Croce, C. Mazzà, & A. Cereatti, (2021). *A method for gait events detection based on low spatial resolution pressure insoles data*. Journal of Biomechanics, 127, 110687.

2. F. Salis, et al. (2023) *A multi-sensor wearable system for the assessment of diseased gait in real-world conditions*. Frontiers in Bioengineering and Biotechnology, 11, 518.

Acknowledgements

I would like to express my heartfelt gratitude to all those who have contributed to the completion of this doctoral thesis. First and foremost, I extend my deepest appreciation to my supervisor, Prof. Andrea Cereatti, for his invaluable guidance and mentorship throughout this research. His expertise, constructive feedback, and unwavering commitment have shaped this thesis in countless ways. Furthermore, I want to thank Prof. Giuseppe Vannozzi, and Prof. Anisoara P. Ionescu for their insightful feedback and recommendations that significantly improved the quality of this work.

To my dear colleagues, Rachele, Diletta, Paolo, Marco, Stefano, Roberto, and all the thesis students. Thank you for the moments of sharing and laughter. Our lunches together, gelato breaks, and coffee sessions have been more than just enjoyable occasions; they have been essential for fostering a supportive environment that has enriched my academic journey.

A huge thank to my colleagues from the Mobilise-D project for the multidisciplinary perspectives and valuable inputs, which contributed to the significance of my research findings. A special thanks to Tecla, who provided unwavering support and encouragement during challenging times.

Thanks to my colleagues at the University of Sassari, Gianluca, Lucia, Nicola, Francesca and all the others, for creating a supportive and nurturing academic environment and for welcoming me as a family. A huge thank to Andrea, who has believed in me since I was still in high school.

To my parents, your unconditional love and unwavering belief in my potential have been my driving force. I am forever grateful for your sacrifices and constant encouragement.

To my beloved Francesco, your patience, understanding, and support have been my anchor during the highs and lows of this challenging endeavor. I am truly blessed to have you by my side.

Lastly, to all my dear friends near and far, especially Giovanni, Daniel, Sara and Melissa and all my lindy-hop friends. Your presence in my life has been a source of joy and inspiration and your friendship has made this journey all the more memorable.

Francesca Salis

Abstract

The deterioration of walking ability has a huge impact on the quality of life, as low gait speed is associated with mortality, dementia, cognitive decline and fall risk. This is valid not only in people affected by diseases linked to motor impairments, but also in healthy elderly with advancing age. Conversely, the maintenance of a good mobility level guarantees the preservation of individual independency and wellness in the everyday life. For this reason, the assessment of gait in ecological scenarios, that account for internal and external confounding factors, may be beneficial to study and try to prevent this condition. In fact, gait analysis conducted with the most traditional laboratory technologies is not sufficient, alone, to obtain a complete evaluation, since it allows to only evaluate motor capacity; therefore, it should be integrated with performance measures. In this sense, wearable sensors represent the optimal solution to make this transition: in particular, inertial measurement units allow to extract both temporal and spatial gait variables, minimizing costs and encumbrance. However, their validation is still performed in the laboratory, while it should be carried out in conditions comparable to those of end use. In this sense, a technically valid wearable solution that provides accurate gait parameters to be used as reference in real-world conditions is still missing.

A fundamental step to perform an accurate gait assessment is the correct identification of gait events to segment the walking sequence into gait cycles and their subphases (i.e. stance and swing). Despite the high number of IMU-based algorithms, they are based on indirect methods and should not be considered a proper reference. On the other hand, the available technologies providing a direct estimate are often time-consuming (e.g. body cameras), expensive (e.g. pressure mapping insoles) or affected by a low spatial resolution (e.g. foot switches). Therefore, the first contribution regarded the development and validation of a new algorithm based on wearable low-cost pressure insoles for accurate gait events detection. Two pressure insoles, including 16 sensing elements each (element area = 310 mm2), with a sample frequency of 100 Hz were employed in the study. The proposed algorithm used the pressure insoles data as input to detect gait events through a cluster-based approach, assuming that at least three sensors in the same foot region should be activated or deactivated to have an initial (IC) or final contact (FC), respectively. The method was tested on nine healthy participants against the force platforms, for a total of 801 IC and 801 FC included in the

analysis. Performance was evaluated in terms of average root mean square error, which resulted low for both gait events (about 20 ms for IC and 10 ms for FC) and temporal parameters (20 ms for stance duration and <10 ms for step duration). The results obtained on healthy participants suggest that this solution can be used as an accurate wearable reference. However, the study should be extended to pathological cohorts including also non-rectilinear walking.

The pressure insoles allow to obtain a temporal characterization of gait, but a complete description also requires the estimation of spatial variables. In this perspective, a new algorithmic pipeline based on a multi-sensor wearable system (INDIP) was developed and validated on both healthy young and elderly subjects and patients affected by five different diseases (Parkinson's Disease, Multiple Sclerosis, Proximal Femoral Fracture, Congestive Heart Failure, Chronic obstructive pulmonary disease). The INDIP comprised two pressure insoles, three IMUs positioned on feet and lower back and two distance sensors. The algorithmic pipeline, based on state-of-art algorithms, was developed exploiting system redundancy. The system was validated against the stereophotogrammetric system in a laboratory experimental protocol, including structured tests of different complexity levels and a simulation of daily life activities, specifically designed to stress the system. A total of 128 participants from seven different cohorts were involved in the study; in addition, they were asked to perform 2.5h real-world unsupervised activity, while wearing the INDIP, to evaluate its usability. In the structured tests results were excellent for all cohorts and DMOs (ICC > 0.95; mean absolute errors: cadence ≤ 0.61 steps/min, stride length ≤ 0.02 m, walking speed ≤ 0.02 m/s). As regards the SDA test, errors were larger but still limited (cadence 2.72–4.87 steps/min, stride length 0.04–0.06m, walking speed 0.03–0.05 m/s). The validation proved that the INDIP is a feasible solution to be used as reference for the analysis of gait in real-world settings. In addition, results on stride-level parameters were reported in the present thesis and confirmed the accuracy of the system. Nevertheless, further improvements can be made in the sensor fusion process (e.g. better exploiting the distance sensors information) and in the stride selection process to increase specificity.

The same multi-sensor system designed to be used as a wearable reference can be used as a mobile gait laboratory in clinical and rehabilitation applications. For example, it can be used to verify the efficacy of a medical treatment during supervised real-world conditions. The third work presented in this thesis regarded the use of the INDIP system to quantify gait changes in people with Multiple Sclerosis before and after physical rehabilitation. The study involved nine patients

who were asked to perform activities of daily living while wearing the INDIP system. Primary gait parameters were extracted using the INDIP pipeline; in addition, gait variability and gait symmetry were estimated for each primary outcome. The clinical relevance of the extracted variables was investigated through statistical analysis, comparing the outcomes obtained from the two sessions (before and after the treatment). Meaningful differences were noticed in stride duration, stride length, swing length and stride speed for a subset of tasks. In particular, stride duration showed an average decrease, while the other parameters increased their average after the treatment. This work suggests that the INDIP system can be used to obtain relevant gait measures and to investigate their relevance in clinical applications. However, further studies are required, with a higher number of participants and a control group for reference values, to confirm the results of this preliminary study.

In conclusion, this thesis aims at providing effective solutions to transfer the validation and the complete assessment of gait in real-world conditions. The first two contributions enable the estimation of reference temporal and spatial gait parameters based on affordable wearable solutions. The third contribution presents the use of the validated solution as a mobile gait laboratory for clinical applications and investigates the effective significance of the extracted gait outcomes.

Contents

List of Abbreviations

Abbreviation	Description
ADL	Activities of Daily Living
CHF	Congestive heart failure
COPD	Chronic obstructive pulmonary disease
DMO	Digital mobility outcome
FC	Final contact
FSR	Force sensitive resistor
HYA	Healthy young adults
HOA	Healthy older adults
IC	Initial contact
ICC	Intraclass correlation coefficient
INDIP	Inertial module with distance sensors and pressure insoles
IMU	Inertial measurement unit
IR	Infrared
MEMS	Micro-electro-mechanical systems
MS	Multiple sclerosis
PD	Parkinson’s disease
PFF	Proximal femoral fracture
SDA	Simulated daily activities
SP	Stereophotogrammetric
ToF	Time of flight

List of Figures

List of Tables

Chapter 1

Introduction

1.1 General introduction

Walking is a simple gesture, characterized by periodic and standardized movements, which is part of our everyday life. The ability to walk has a great impact on individual well-being, as it is strictly connected to the mobility and quality of life in general [1], [2]. Its deterioration can occur not only due to diseases characterized by specific motor dysfunctions but also, merely, with advancing age [3], [4]. This problem is becoming more and more present with the increase of both longevity of world's population and probability of survival to chronic and disabling diseases. As such, losing motor ability is equivalent to a loss of independence in the everyday life. Moreover, a low level of physical activity, as also slow walking, is associated with high mortality, dementia, cognitive decline and fall risk [5], [6]. It has been demonstrated that walking speed can be considered the sixth vital sign after body temperature, heart rate, respiratory rate, blood pressure and oxygen saturation [7]. For this reason, it is fundamental to have valid instruments to measure the individual level of mobility, in order to detect and, eventually, prevent, this kind of condition. The use of technologies for the analysis of gait in a clinical or rehabilitation field allows to obtain an objective characterization of the degree of mobility of the individual, which can help the clinical specialist to evaluate the pathological conditions, the disease progression and the efficacy of a medical treatment [8], [9].

It is well known that individual mobility is the combination of what a person can do (motor capacity) and what he/she actually does (motor performance) [10].

Therefore, a complete assessment should include not only conventional analyses in a standardized setting, but also, a quantitative characterization of person's mobility performance in its ecological environment [11]–[15]. However, real-world gait analysis is an ongoing challenge due to a series of contextual factors which can deeply increase gait complexity, such as the presence of breaks (leading to more frequent initiation and termination phases), short walking bouts, increased number of changes in speed and direction of progression, walking on different surfaces, passing obstacles and non-walking activities [16]. The situation can be even more complicated in case of people with impaired mobility, due to slower walking, use of walking aids and less repeatable gait patterns. This requires the development of an algorithmic pipeline specifically conceived to address gait in real-world scenarios.

In some cases, it can be interesting to analyze gait and, in general, mobility during task-oriented real-world acquisitions [17]. Unlike unsupervised real-world experiments, where the participants do not follow a proper scheme, here they are asked to perform a specific set of daily life activities [18] that can be useful, for example, to evaluate the efficacy of a treatment. The choice of an appropriate treatment is particularly relevant in patients with neurodegenerative diseases such as multiple sclerosis [19]. Pharmacological therapies are used in multiple sclerosis patients to reduce the relapse rate [20], but robust evidence on their clinical effectiveness in disability progression is still lacking [21]–[23]. Conversely, recent studies report the clinical efficacy of physical rehabilitation and suggest its use as a proper therapeutic treatment [24]. Specifically, improvements have been observed in quality of life and activities of daily life [25], [26] but also gait [27]–[29]. However, changes in walking function after rehabilitation are usually evaluated during standard tests [27]–[33] and have been not properly investigated in more challenging conditions. In this sense, changes in gait performance can be assessed looking at the variation of some relevant gait parameters during two or more repetitions of the same activity (e.g. before and after the rehabilitation). For example, gait symmetry allows to quantify the differences between right and left side and is considered as a relevant measure to monitor rehabilitation progresses [34]. Moreover, it can help the clinician in the identification of gait pattern changes according to the different type of activities or to the severity of the disease [35]. These changes can be also quantified through the computation of gait variability, that accounts for the stride-by-stride differences [36], [37].

Moving the analysis "out of the laboratory" requires the use of wearable sensors that, compared to the most traditional technologies employed in gait

analysis (i.e., stereophotogrammetric systems, instrumented mats, and force platforms) are low cost, fully portable and do not require an ad-hoc laboratory for their usage [38].

In this perspective, a single inertial measurement unit (IMU), typically positioned on the trunk or wrist, represents the most suitable solution in terms of comfort and usability [39], [40], making them particularly convenient for long term monitoring applications. However, those locations are quite far from the contact point with the ground, making the estimation of gait-related spatial-temporal parameters more difficult. Conversely a bilateral approach, with IMUs mounted on shanks or feet, guarantees more accurate estimations. However, in both cases, the gait events are indirectly identified from the accelerometer and gyroscope signals. Therefore, IMU-based approaches should be accounted for as silver standard solutions and the validity of IMU-based methods should be assessed in the same conditions in which they are supposed to be used.

Despite the strong interest in using wearable sensors for mobility assessment, most of the studies still limit the validation to straight walking tasks [41]–[45]. Further efforts are hence required to make the transition from laboratory to real-world settings, adding more complexity to the validation protocols, such as curvilinear walking [46] and supervised or unsupervised tasks [47]–[49], to simulate what is commonly observed in real-world conditions. The validation in unsupervised settings could be extremely beneficial in case of machine learning based methods, which require a huge amount of data for a proper testing [17], [50].

Among the technological solutions adopted to detect reference gait events, there are body-worn cameras pointing to the subject's feet [51]–[53]. Nevertheless, the labelling of foot contacts is labor-intensive and the resolution is strictly linked to camera frame rate. Other options are foot switches [54]–[58] and plantar pressure insoles [59], [60]. However, the first ones include two or three sensors, limiting the temporal resolution of the detected gait events, especially in case of impaired gait [61]. On the other side, plantar pressure insoles usually include a high number of sensing elements, resulting in more expensive devices with high computational costs. Those limitations might be overcome reducing the number of sensing elements: some studies used pressure insoles with a limited number of sensing units [62]–[65], but their work was mainly focused on the estimation of temporal gait parameters different from IC and FC. Therefore, a

validated method to detect gait events based on a more affordable wearable technology, e.g. low-cost pressure insoles, is currently missing.

The above-mentioned solutions can only provide a reference for temporal parameters, but they do not provide any information on spatial gait parameters, which are crucial for a complete description of walking patterns in both healthy and pathological subjects [66]–[68]. The estimation of reference temporal and spatial parameters of gait requires the combination of different wearable sensor technologies, in order to exploit the complementary characteristics and redundancy of information provided. Such a system would be sufficiently robust and accurate to be used to assess the performances of other wearable devices, working as a mobile gold standard (mGS). On the other side, it could be employed as a mobile laboratory to obtain a complete movement analysis in an ecological environment, without the temporal and spatial limitations enforced by the traditional non-wearable technologies [69], [70]. Until today, few multi-sensor systems integrating IMUs and pressure insoles have been proposed, as the result of academic [71], [72] or commercial [73], [74] research. Nevertheless, further efforts should be made in validating those solutions not only on healthy participants but also on diseased cohorts with potential motor impairments, including more complex motor tasks different from basic straight walking tests. In addition, the commercial solutions follow a black box approach that does not allow the access to the algorithms, logic, and inner components. Conversely, a fully transparent, accessible, and configurable measurement system would facilitate its extensive usage and help the final user in satisfying all the project requirements [75].

1.2 Aim of the thesis

A complete gait analysis in real-world conditions can provide a quantitative description of how a person walks in his/her everyday environment, including social and personal factors. This is even more significant in case of diseased people, potentially affected by motor disorders, to target mobility loss and try to prevent it, as also to evaluate the efficacy of a treatment. In this perspective, activity monitors (i.e. devices including a single IMU) represent the best available solution, as they allow for long-term monitoring measurements without causing discomfort. However, their validation is still performed in standardized laboratory environments, while it should be carried out in the same conditions of end use (i.e. real-world unsupervised settings). In fact, those devices are conventionally

validated on very simple tasks, including a limited number of strides, which is far from what happens in a real-world context.

The real-world assessment of the above-mentioned devices requires robust and reliable gait measures to be used as reference. In case of temporal gait parameters, a wearable low-cost solution which provides a direct measure of foot to ground contact is needed. In addition, a novel algorithm based on the previous solution should be developed and tested against a ground truth before being used for the validation of third-party devices.

On the other hand, the validation of both temporal and spatial parameters calls for a system integrating multiple complementary technologies to directly estimate foot contacts and displacements and improve the statistical accuracy of such variables. Moreover, a structured computational pipeline should be developed and validated according to an experimental protocol including motor tasks of different complexity level in order to stress the system. Another relevant point is the assessment on different populations characterized by various gait patterns to ensure the robustness of the method and evaluate its applicability on a wide range of speeds and motor impairments.

The same multi-sensor technology can be used as a mobile laboratory for assessing mobility in ecological conditions. For example, it can be employed to estimate gait-related parameters during task-oriented experiments conducted before and after a rehabilitation treatment. This would allow to obtain an accurate evaluation even without the use of the most traditional laboratory technologies, thus minimizing the costs, encumbrance and complexity.

Based on the above, the aims of the here presented thesis are the following:

1. The development and validation of a new algorithm for accurate gait events detection based on wearable low-cost pressure insoles data.

2. The development of a new algorithmic pipeline for real-world gait analysis using a multi-sensor wearable system and its validation on both healthy young and elderly subjects and patients with different diseases.

3. The extraction of gait related parameters to quantify changes in gait before and after physical rehabilitation in people with multiple sclerosis while performing Activities of Daily Living (ADL).

1.3 Contributions

This section lists the major contributions addressing the objectives of the present thesis, the conference publications and the co-authored in the field of human movement analysis.

1.3.1 Major contributions

1. **F. Salis**, S. Bertuletti, T. Bonci, U. Della Croce, C. Mazzà, & A. Cereatti, (2021). A method for gait events detection based on low spatial resolution pressure insoles data. Journal of Biomechanics, 127, 110687.

2. **F. Salis,** et al. (2023) A multi-sensor wearable system for the assessment of diseased gait in real-world conditions. Frontiers in Bioengineering and Biotechnology, 11, 518.

1.3.2 Conference contributions

1. **F. Salis**, S. Bertuletti, M. Caruso, T. Bonci, K. Scott, R. Rossanigo, U. Della Croce, C. Mazzà, A. Cereatti (2020). A novel multi-sensor system for gait assessment in real-world conditions: preliminary results (GNB 2020, conference proceeding).

2. R. Rossanigo, M. Caruso, **F. Salis**, S. Bertuletti, U. Della Croce, & A. Cereatti, (2021, June). An Optimal Procedure for Stride Length Estimation Using Foot-Mounted Magneto-Inertial Measurement Units. In 2021 IEEE International Symposium on Medical Measurements and Applications (MeMeA) (pp. 1-6). IEEE.

3. **F. Salis**, S. Bertuletti, K. Scott, M. Caruso, T. Bonci, E. Buckley, U. Della Croce, C. Mazzà and A. Cereatti (2021). Accuracy of a multi-sensor system in stride parameters estimation: comparison of straight and curvilinear portions. SIAMOC Conference 2021.

4. **F. Salis**, S. Bertuletti, K. Scott, M. Caruso, T. Bonci, E. Buckley, U. Della Croce, C. Mazzà, A. Cereatti (2021). A wearable multi-sensor system for real world gait analysis. EMBC Conference 2021.

5. M. E. Micò Amigo et al, “Validation and Ranking of Algorithms for Gait Sequence Detection in Healthy Controls and People With Parkinson’s

Disease" in Proceedings of ICAMPAM Conference 2022, Keystone (CO), USA, June 2022, doi: 10.1123/jmpb.2022-0032.

6. **F. Salis**, T. Bonci, S. Bertuletti, M. Caruso, K. Scott, E. Buckley, ... & A. Cereatti (2022). Performance of a multi-sensor wearable system for validating gait assessment: preliminary results on patients and healthy. Gait & Posture, 97, 13, Proceedings of SIAMOC Conference 2022.

7. A. Manca, L. Ventura, G. Martinez, A. Cano, F. Ginatempo, A. Cereatti, **F. Salis**, F. Deriu. Measuring the impact of common exercise programs on subjective and objective fatigue during daily living activities in people with multiple sclerosis. FISM Annual Congress 2022, Roma, 24-26 Maggio 2022.

8. L. Ventura, G. Martinez, A. Boi, M. Morrone, A. Cano, F. Ginatempo, A. Cereatti, **F. Salis**, F. Deriu, A. Manca. Measuring the impact of common exercise programs on subjective fatigue and metabolic efficiency during daily living activities in people with multiple sclerosis: a randomized controlled pilot trial. ECTRIMS 2022 – ePoster. Multiple Sclerosis Journal. 2022;28(3_suppl):692-945. doi:10.1177/13524585221123682

1.3.3 Co-author contributions

1. G. Pavei, **F. Salis**, A. Cereatti, & E. Bergamini, (2020). Body center of mass trajectory and mechanical energy using inertial sensors: a feasible stride? *Gait & Posture*.

2. A. M. Polhemus, R. Bergquist, M. B. de Basea, G. Brittain, S. C. Buttery, N. Chynkiamis, G. dalla Costa, L. Delgado Ortiz, H. Demeyer, K. Emmert, J. G. Aymerich, H. Gassner, C. Hansen, N. Hopkinson, J. Klucken, F. Kluge, S. Koch, L. Leocani, W. Maetzler, M. E. Micó-Amigo, S. Mikolaizak, P. Piraino, **F. Salis**, C. Schlenstedt, L. Schwickert, K. Scott, B. Sharrack, K. Taraldsen, T. Troosters, B. Vereijken, I. Vogiatzis, A. Yarnall, C. Mazza, C. Becker, L. Rochester, M. A. Puhan, A. Frei (2020). Walking-related digital mobility outcomes as clinical trial endpoint measures: protocol for a scoping review. *BMJ open, 10(7), e038704.*

3. A. M. Polhemus, L. Delgado Ortiz, G. Brittain, N. Chynkiamis, **F. Salis**, H. Gaßner, M. Gross, C. Kirk, R. Rossanigo, K. Taraldsen, D. Balta, S. Breuls, S. Buttery, G. Cardenas, C. Endress, J. Gugenhan, A. Keogh, F. Kluge, S. Koch, M. E. Micó-Amigo, C. Nerz, C. Sieber, P. Williams, R. Bergquist, M. Bosch

de Basea, E. Buckley, C. Hansen, A. S. Mikolaizak, L. Schwickert, K. Scott, S. Stallforth, J. van Uem, B. Vereijken, A. Cereatti, H. Demeyer, N. Hopkinson, W. Maetzler, T. Troosters, I. Vogiatzis, A. Yarnall, C. Becker, J. Garcia-Aymerich, L. Leocani, C. Mazzà, L. Rochester, B. Sharrack, A. Frei, M. Puhan & Mobilise-D (2021). Walking on common ground: a cross-disciplinary scoping review on the clinical utility of digital mobility outcomes. NPJ digital medicine, 4(1), 1-14.

4. C. Mazzà, L. Alcock, K. Aminian, C. Becker, S. Bertuletti, T. Bonci, P. Brown, M. Brozgol, E. Buckley, A. Carsin, M. Caruso, B. Caulfield, A. Cereatti, L. Chiari, N. Chynkiamis, F. Ciravegna, S. Del Din, B. Eskofier, J. Evers, J. Garcia Aymerich, E. Gazit, C. Hansen, J. M Hausdorff, J. L Helbostad, H. Hiden, E. Hume, A. Paraschiv-Ionescu, N. Ireson, A. Keogh, C. Kirk, F. Kluge, S. Koch, A. Küderle, V. Lanfranchi, W. Maetzler, M. E. Micó-Amigo, A. Mueller, I. Neatrour, M. Niessen, L. Palmerini, L. Pluimgraaff, L. Reggi, **F. Salis**, L. Schwickert, K. Scott, B. Sharrack, H. Sillen, D. Singleton, A. Soltani, K. Taraldsen, M. Ullrich, L. Van Gelder, B. Vereijken, I. Vogiatzis, E. Warmerdam, A. Yarnall, L. Rochester (2021). Technical validation of real-world monitoring of gait: a multicentric observational study. BMJ open, 11(12), e050785.

5. T. Bonci, **F. Salis**, K. Scott, L. Alcock, C. Becker, S. Bertuletti, E. Buckley, M. Caruso, A. Cereatti, S. Del Din, E. Gazit, C. Hansen, J. M. Hausdorff, W. Maetzler, L. Palmerini, L. Rochester, L. Schwickert, B. Sharrack, I. Vogiatzis and C. Mazzà, on behalf of the Mobilise-D consortium (2022). An algorithm for accurate marker-based gait event detection in healthy and pathological populations during complex motor tasks. Frontiers in bioengineering and biotechnology, 10.

6. K. Scott, T. Bonci, **F. Salis**, L. Alcock, E. Buckley, E. Gazit, C. Hansen, L. Schwickert, K. Aminian, S. Bertuletti, M. Caruso, L. Chiari, B. Sharrack, W. Maetzler, C. Becker, J. M. Haussdorff, I. Vogiatzis, P. Brown, S. Del Din, B. Eskofier, A. Paraschiv-Ionescu, A. Keogh, C. Kirk, F. Kluge, M. E. Micó-Amigo, A. Mueller, I. Neatrur, M. Niessen, L. Palmerini, H. Sillen, D. Singleton, M. Ullrich, B. Vereijken, M. Froelich, G. Brittan, B. Caulfield, S. Koch, A. Carsin, J. Garcia-Aymerich, A. Kuederle, A. Yarnall, A. Cereatti, C. Mazzà (2022). Design and validation of a multi-task, multi-context protocol for real-world gait simulation. Journal of NeuroEngineering and Rehabilitation, *19*(1), 1-12.

7. L. Palmerini, L. Reggi, T. Bonci, S. Del Din, M. E. Micó-Amigo, **F. Salis**, S. Bertuletti, M. Caruso, A. Cereatti, E. Gazit, A. Paraschiv-Ionescu, A. Soltani, F. Kluge, A. Küderle, M. Ullrich, C. Kirk, H. Hiden, I. D'Ascanio, C. Hansen, L. Rochester, C. Mazzà & L. Chiari (2023). Mobility recorded by wearable devices and gold standards: the Mobilise-D procedure for data standardization. Scientific Data, 10(1), 38.

8. G. Prigent, K. Aminian, A. Cereatti, **F. Salis**, T. Bonci, K. Scott, C. Mazzà, L. Alcock, S. Del Din, E. Gazit, C. Hansen and A. Paraschiv-Ionescu for the Mobilise-D consortium (2023). A robust walking detection algorithm using a single foot-worn inertial sensor: validation in real-life settings. Medical & Biological Engineering & Computing.

9. M. E. Micó-Amigo, T. Bonci, A. Paraschiv-Ionescu, M. Ullrich, C. Kirk, A. Soltani, A. Küderle, E. Gazit, **F. Salis**, L. Alcock, K. Aminian et al. (2023). Assessing real-world gait with digital technology? Validation, insights and recommendations from the Mobilise-D consortium. Journal of Neuroengineering and Rehabilitation.

10. L. M.A. van Gelder, T. Bonci, E. E. Buckley, K. Price, F. Salis, M. Hadjivassiliou, C. Mazzà, and C. Hewamadduma. A single sensor approach to quantify gait in patients with hereditary spastic paraplegia. *Accepted in* Sensors.

11. R. Romijnders, **F. Salis**, C. Hansen, A. Küderle, A. Paraschiv-Ionescu, A. Cereatti, L. Alcock, K. Aminian, C. Becker, S. Bertuletti, T. Bonci, P. Brown, E. Buckley, A. Cantu, A. Carsin, M. Caruso, B. Caulfield, L. Chiari, I. D'Ascanio, S. Del Din, B. Eskofier, S. Fernstad, M. Fröhlich, J. Garcia-Aymerich, E. Gazit, J. Hausdorff, H. Hiden, E. Hume, A. Keogh, C. Kirk, F. Kluge, S. Koch, C. Mazzà, D. Megaritis, E. Micó-Amigo, A. Müller, L. Palmerini, L. Rochester, L. Schwickert, K. Scott, B. Sharrack , H. Sillén, D. Singleton, A. Soltani, M. Ullrich, B. Vereijken, I. Vogiatzis, A. Yarnall, G. Schmidt, and W. Maetzler, and Mobilise-D consortium. Ecological validity of a deep learning algorithm to detect gait events from real-life walking bouts in mobility-limiting diseases. *Submitted to* Digital Health.

12. J. Buekers, D. Megaritis, S. Koch, L. Alcock, N. Ammour, C. Becker, S. Bertuletti, T. Bonci, P. Brown, E. Buckley, S. C. Buttery, B. Caulfied, A. Cereatti, N. Chynkiamis, H. Demeyer, C. Echevarria, A. Frei, C. Hansen, J.

M. Hausdorff, N. S. Hopkinson, E. Hume, A. Kuederle, W. Maetzler, C. Mazzà, E. M. Micó-Amigo, A. Mueller, L. Palmerini, **F. Salis**, K. Scott, T. Troosters, B. Vereijken, H. Watz, L. Rochester, S. Del Din, I. Vogiatzis, J. Garcia-Aymerich. Laboratory and free-living gait performance in adults with COPD and healthy controls. *Submitted to* ERJ Open Research.

1.4 Outline of the thesis

This section illustrates the organization of the present thesis.

Chapter 1 (current chapter) introduces the general motivation and objectives of the thesis, also including the list of contributions and the outline.

Chapter 2 introduces the basic notions necessary to understand the background of the here presented work: the concept of human gait, differences between normal and pathological gait, motor characteristics of the pathological cohorts involved in this study and consequences on gait patterns, gait related parameters including the most traditional ones and those necessary to move the analysis in real-world. Finally, an overview on the technologies used for gait analysis purposes, both non-portable and wearable, is given.

Chapter 3 illustrates the current state of the art. A first section regards the estimation of gait events using wearable technologies. Then, the most relevant methods for gait assessment based on wearable technologies are presented, together with an overview of the validation process and its transition from standardized to real-world settings. Finally, the state of the art regarding the main studies based on activities of daily living for the mobility assessment is described.

Chapter 4 presents the sensors employed in the current study, with a focus on the working principle of the different technologies and a detailed description of the multi-sensor system used, i.e. the INDIP system.

Chapter 5 reports the abstract of the contribution regarding the development and validation of a new algorithm for accurate gait events detection based on wearable low-cost pressure insoles data. The full contribution is reported in Appendix A in its original form.

Chapter 6 regards the second aim of the thesis, i.e. the development of a new algorithmic pipeline for real-world gait analysis using a multi-sensor wearable

system (INDIP) and its validation. The first part describes the design of the algorithmic pipeline, followed by the abstract of the main contribution including the algorithm workflow and the validation of WB level DMOs on both healthy and pathological subjects. The full contribution is reported in Appendix B in its original form. Then, results of the validation of stride level DMOs is presented and discussed.

Chapter 7 illustrates the third aim of the thesis, regarding the estimation of gait-related parameters during Activities of Daily Living in multiple sclerosis patients using the validated INDIP system pipeline to quantify changes in mobility after physical rehabilitation.

Chapter 8 summarizes the findings of the present thesis with an outlook to limitations and future perspectives.

Chapter 2

Basic notions

2.1 Human gait

The term gait indicates the bipedal locomotion characterizing the way in which human beings move from one place to another. It consists in moving forward the center of mass thanks to the alternating movement of the lower limbs [76], [77]. Gait is a physical activity that every human being usually learns to perform around one year old, getting soon to the minimum energy expenditure required [78]. Despite the seeming simplicity, human locomotion involves different body parts such as muscles, cortical and subcortical structures [78]. An objective and instrumented analysis of gait requires a quantitative description of the movement. Physiological gait is a cyclic and periodic activity, defined by the repetition of the same functional sequence, called gait cycle [77], [79]. The gait cycle, or stride, is defined as the time interval between two consecutive initial contacts of the same foot (i.e. ipsilateral contacts). The interval between two consecutive initial contacts of opposite feet (i.e. contralateral contacts) is instead called step. A stride includes two distinct phases of the foot: a phase of support, or stance phase (about 60% of the gait cycle), and a phase of oscillation, or swing phase (about 40% of the gait cycle). During the gait cycle the feet alternate their support and oscillation phases. Figure 1 shows, as an example, a temporal description of one stride of the right foot. In particular, the gait cycle starts with the initial contact (IC) of the right foot, followed by:

- A first 10% of double support phase (i.e. both feet are in contact with the ground) which finishes with the final contact (FC) of the left foot.
- A swing phase of the left foot starts with the left FC and stops with the left IC, getting to the 50% of the cycle.
- At this stage, both feet are in contact with the ground (second 10% double support phase) that finishes with the right FC (60% of the gait cycle).
- A swing phase of the right foot starts with the right FC and stops with the right IC, getting to the end of the cycle.

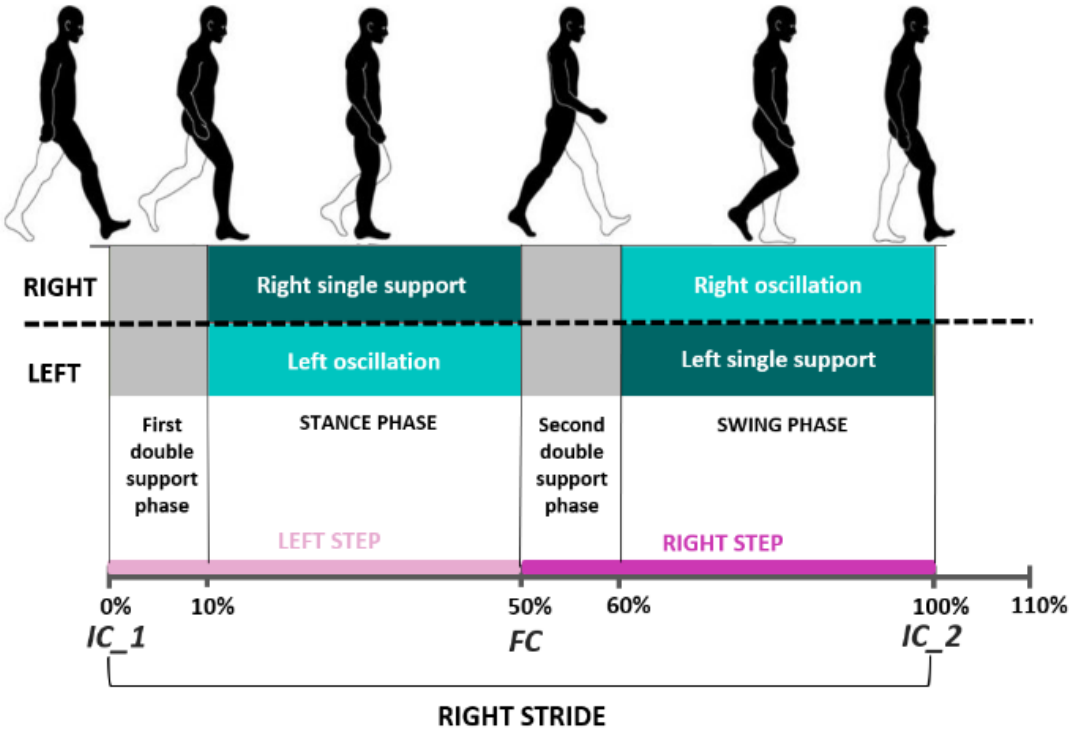

Figure 1: Gait cycle phases, example on right foot.

2.2 Normal gait versus pathological gait

Normal gait is distinguished by the regular and periodic repetition of the same sequence described above. The lower limbs alternate their movement, while the body maintains its erect posture, balance, and stability [80].

In pathological gait, the regularity of the movement depends on the disease and the specific level of motor impairment. In general, pathological gait patterns can be characterized by modified gait cycles, asymmetry, failure to maintain the

alternating movement. This results in a higher energy expenditure, loss of balance and joints fatigue due to the excessive loads, with major implications in life quality [80], [81]. Gait impairments can be a consequence of different diseased conditions, such as neurological disorders [82], cardiovascular pathologies [83], post stroke symptoms [84] or orthopedic injuries [85].

The data used in the present thesis have been acquired on healthy young adults (HYA), healthy older adults (HOA) and five cohorts of patients affected by different diseases (Parkinson's disease, multiple sclerosis, chronic obstructive pulmonary disease, congestive heart failure, proximal femoral fracture) within the Mobilise-D European project [16]. These cohorts of patients are characterized by diverse mobility impairments leading to specific disease patterns. For this reason, the gait-related outcomes used to describe them are very different from each other. As one of the goals of Mobilise-D project is to identify common mobility outcomes across multiple conditions, the choice of including a variety of cohorts was made to reach this aim according to a comprehensive approach. The following subparagraphs give details on the features and the gait impairments typically associated to each pathology.

2.2.1 Parkinson's disease

Parkinson's disease (PD) is a neurodegenerative disorder affecting around 10 million people worldwide [86]. The large majority of PD patients are over 60 (90%), with a higher percentage of men (ratio 2:1) than women affected [86]. PD is a fast-growing syndrome, which causes a broad spectrum of symptoms [87]. As regards effects on mobility, PD condition is characterized by bradykinesia (i.e., slowness of movements), which can be accompanied by tremor, rigidity, reduced gestures amplitude and smoothness [88]. In term of walking ability, this translates into reduced walking speed and stride length, increased rigidity and shuffling steps [88] – particularly evident during turning maneuvers, presence of obstacles and other changes in the path – and, in some cases, gait arrest episodes, better known as freezing of gait [89].

2.2.2 Multiple sclerosis

Multiple sclerosis (MS) is a chronic neurological disease which affects more than 2.8 million people worldwide [90]. MS commonly affects people in their young adulthood and it is three times more common in women [90]. As a progressive degenerative disease, it causes damages in the central nervous system which can lead to several motor impairments, balance loss and alterations in gait capacity

and performance [91]. In particular, MS patients show reduced walking speed, stride length and swing phase duration [92]. According to LaRocca [93], about 85% of people with MS indicate walking impairment as a major disability in their daily life.

2.2.3 Chronic obstructive pulmonary disease

Chronic obstructive pulmonary disease (COPD) is a chronic inflammatory disease that limits airflow in and out of the lungs [94]. It affects both men and women worldwide and can be caused by tobacco smoking or the exposure and inhalation of other toxic particles or gases [95]. Besides the evident respiratory symptoms, COPD patients can manifest abnormalities in skeletal muscle structure that underlie the decreased mobility [96]. The limited motor functions translate into postural control and balance issues, which cause frequent falls, especially during walking [97]. The deterioration of walking ability, associated with reduced walking speed, step length and cadence, represents the main risk of fall and it is strongly related to the risk of death [97].

2.2.4 Congestive heart failure

Congestive heart failure (CHF) is a clinical condition in which the heart blood pumping is reduced and inadequate to meet body requirements [98]. CHF can be the consequence of different diseases and it affects 26 million people in the world [98]. Fatigue symptoms, as also decreased exercise endurance and pulmonary function, have a huge impact on life quality and everyday activities [99]. Moreover, the insufficient blood flow results in a reduced lower limb muscle strength, that inevitably deteriorates gait function [99]. The most common impairments are associated with loss of balance, postural control, with a reduction of gait speed, stride length and stride duration [100].

2.2.5 Proximal femoral fracture

Proximal femoral fracture (PFF) consists in a break in the upper part of the femur, close to the hip joint [101]. PFF is quite common after a fall or a hip injury but, sometimes, can be caused by other conditions such as cancer [102]. Especially in elderly subjects, hip fracture represents an important risk factor of death (rate of 5-10% after one month) [103]; whereas in the majority of survivors it provokes pain and motor disabilities [101]. In particular, PFF can lead to a decrease in hip function and muscles strength, which can reflect negatively on the ability of

walking and result in evident gait asymmetry, both in temporal and spatial variables [104].

2.3 Parameters of gait

According to the quantitative description of gait phases reported in 2.1, this paragraph provides a detailed summary of the fundamental gait parameters. The parameters of gait are also called spatial-temporal parameters and can provide temporal information, spatial information or a combination of the two. It is worth mentioning that the gait parameters described in the following are those assessed and considered as relevant for the present study, but other primary and secondary parameters could be derived to describe human locomotion. Gait events timings, i.e. the instant at which each IC and FC occur, are not properly considered as gait parameters; however, the correct estimation of those events is fundamental to segment strides and define all the temporal variables.

Temporal parameters

- Stride duration: time interval between two consecutive ICs of the same foot.
- Step duration: time interval between the IC of one foot and the subsequent IC of the contralateral foot.
- Stance time: time interval between an IC and the subsequent FC of the same foot.
- Swing time: time interval between a FC and the subsequent IC of the same foot.
- Cadence: number of steps per minute, computed as a function of stride duration.

$$Cadence = \frac{\sum_{j=1}^{\#strides} \frac{60}{Stride\_Duration_j}}{\#strides} * 2$$

Spatial parameters

- Stride length: displacement covered within a stride.

- Stance length: displacement covered within a stance phase.
- Swing length: displacement covered within a swing phase.

Spatial - temporal parameters

- Stride speed: ratio between stride length and stride duration.
- Walking speed: average stride speed in a selected interval of gait.

$$Walking\ speed = \sum_{j=1}^{\#strides} \frac{Stride\_length_j}{Stride\_duration_j}$$

Additional parameters

Starting from the above-mentioned parameters, it is possible to define additional parameters, i.e. gait variability and symmetry:

- Gait variability: describes the stride-by-stride changes of a specific parameter, computed as the Coefficient of Variation (CoV) [105].

$$Gait\ variability = CoV = \frac{STD(P)}{mean(P)} * 100$$

- Gait symmetry: describes the differences between right and left side [106].

$$Gait\ symmetry = 2 * \left| \frac{mean(P_{left}) - mean(P_{right})}{mean(P_{left}) + mean(P_{right})} \right| * 100$$

Where P is a parameter of gait, P_{left} and P_{right} are the values of P computed from the left and right side, respectively.

2.4 Gait analysis in real-world

Gait-related parameters are commonly estimated and assessed in standard laboratory environments during basic tasks. Nevertheless, those conditions are quite far from what happens in the real-world, as they do not take into account all

the factors linked to the disease or, in general, to the specific individual condition (intrinsic) and to the ecological environment (extrinsic).

Gait has a fundamental role in everyday life, not only as an action end in itself but also as means of performing different types of activities independently. Real-world gait can be defined as free-living and unsupervised [107], in opposition to the standardized and controlled laboratory gait. For this reason, the study of real-world gait complements the traditional laboratory analysis providing a description of individual performances [10], [108]. In the last years, the interest of the scientific community in real-world gait analysis is increasingly growing thanks to the development of wearable technologies, which are described in detail in section 2.5.2. The description of gait in real-world conditions requires the definition of additional parameters or digital mobility outcomes (DMOs) [16], provided in the following, for an accurate assessment on different granularity levels.

Walking Bout

A Walking Bout (WB) or continuous walking period is defined by the combination of consecutive right and left strides that maintain the alternance [107]. For the purposes of this work, a specific definition of WB was adopted in accordance with the Mobilise-D consortium, which provides that the WB is a gait sequence including a minimum of two left and two right strides. Each WB can include rectilinear walking, curvilinear walking and incline walking (i.e., walking on stairs or along an inclined path), as also breaks and/or spurious movements with a duration < 3s (Figure 2). Moreover, some strides requirements, agreed within the Mobilise-D consortium, were imposed to discard spurious movements:

- Minimum stride duration equal to 0.2 s
- Maximum stride duration equal to 3 s
- Maximum stride height in case of level walking equal to 0.15 m
- Minimum stride length equal to 0.15 m
- Maximum stride length, defined as proposed by Zijlstra and Hof [109] and based on individual anthropometric features:

$$SL_{max,j} = 2 * \left(\sqrt{2\,L_j\,h_j - h_j^2}\right)$$

Where L_j is the leg length of the $j-th$ subject and h_j is the maximum displacement of the center of mass, defined in the following way, according to Miff et al. [110]:

$$h_j = 0.038 * v_{max,j}^2$$

Where $v_{max,j}$ is the maximum walking speed, described as a function of leg length [111], [112]:

$$v_{max,j} = \sqrt{Fr * g * L_j}$$

The leg length L_j, necessary to compute the above-mentioned variables, is defined with respect to the subject's height, according to what proposed by Winter [113]:

$$L_j = 0.53 * H_j$$

Stride level DMOs

In this thesis, Stride level DMOs include all the gait parameters extracted for each stride in a Walking Bout and validated according to a stride-by-stride matching with the corresponding reference values. Examples of Stride level DMOs are stride duration and stride length.

An additional class of DMOs is represented by the gait events (i.e., IC and FC timings) which can be analyzed with an aggregation strategy similar to that used for stride level DMOs, as we have multiple gait events values for each Walking Bout.

Walking Bout level DMOs

In this thesis, Walking Bout level DMOs include all the gait parameters extracted and validated at Walking Bout level. Examples of those DMOs are the walking speed and cadence but also the average stride length in a WB, obtained from the aggregation of individual stride lengths at WB level. For the Stride level DMOs we have multiple values associated to a WB, equal to the number of strides detected in the WB itself. Conversely, for Walking Bout level DMOs we have a

single value associated to the considered WB, as those parameters give a description of the entire gait sequence.

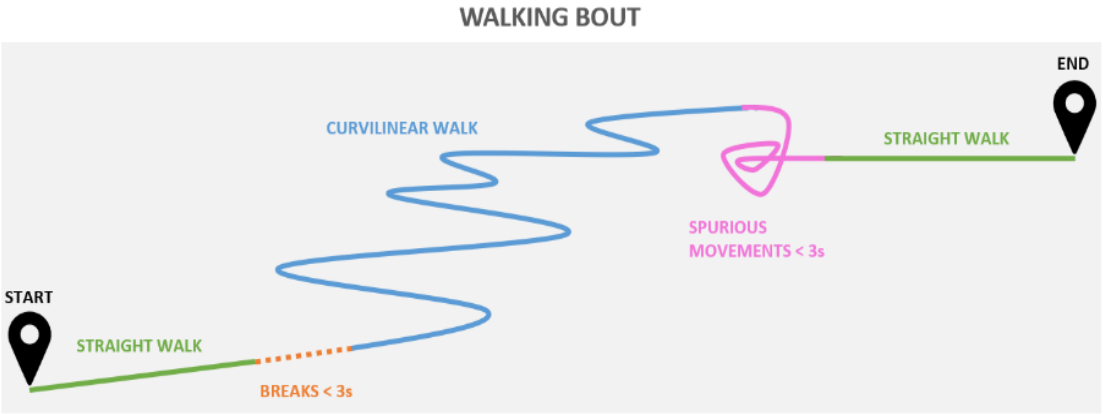

Figure 2: Example of Walking Bout that includes straight walk, curvilinear walk and breaks/spurious movements < 3s.

2.5 Technologies for instrumented gait analysis

The instrumented gait analysis entails the collection of quantitative data, allowing to estimate and assess specific parameters that cannot be explored with the conventional observational gait analysis [114], [115]. In fact, the latter is operator-dependent, resulting in an objective evaluation that can be only moderately reliable [116] and it is not sufficient, alone, to get a complete clinical picture [117]. In this sense, different technologies are used in clinical settings to better describe functional limitation and impairments, better understand the gait patterns associated to complex diseases, measure the efficacy of a medical treatment and help clinicians in the decision-making process [118]. For a better understanding, the following sections provide a description of the most used technologies for instrumented gait analysis both in laboratory settings and real-world conditions (i.e. wearable sensors). A representative picture is reported in Figure 3.

2.5.1 Laboratory technologies

Technologies used for laboratory gait analysis have a key role in the description of human mobility, as they have been widely used for the conventional assessment of motor capacity [119]–[122]. Those technologies include force platforms, instrumented walkways, optoelectronic stereophotogrammetric systems

and marker-less solutions. Details on the working principle, advantages and limitations of the above-mentioned solutions are provided in the following.

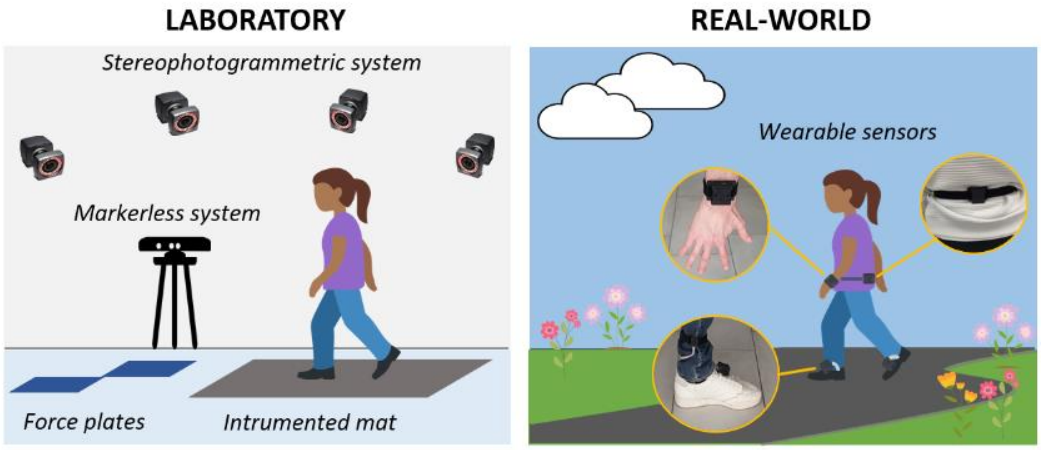

Figure 3: Representative picture of laboratory and real-world technologies. Laboratory technologies (left side) include all the traditional non-wearable devices that restrict the analysis to a confined setting (e.g., force plates, instrumented mats, stereophotogrammetric system and markerless system). Real-world technologies include wearable sensors of different types (e.g., footswitches, pressure insoles, IMUs) that can be used without any spatial restriction for analyzing gait both in supervised and unsupervised environments.

- Force platforms: force platforms are used to measure the ground reaction force resulting from the subject stepping above it [123]. They work thanks to the presence of load cells that, due to their structure, can measure the deformation caused by an external load in terms of force needed to produce such deformation [124]. The foot support during the stance is evaluated as a point-contact on the force platform surface, corresponding to the center of pressure. Force platforms are commonly employed in gait analysis to obtain accurate and reliable measures of gait events instants [125], [126], as well as the other temporal parameters. However, they do not allow for the estimation of spatial variables.

- Instrumented walkways: instrumented walkways include a high number of pressure sensors, organized in arrays, covering the entire mat surface [127]. This allows to obtain a full mapping of the foot-ground contact when the subject walks on it. The system is able to provide a large variety of temporal and spatial variables simply knowing which sensors have been activated or deactivated, the associated time instant and position on the mat [128]. Commercially available instrumented walkways include for example the GAITRite (CIR System, Inc., USA).

Both force platforms and instrumented walkways are considered a ground truth reference for the validation of other devices. However, the limited surface extension of both systems constraints the gait analysis to a limited number of consecutive strides on a rectilinear path [129]. Other technologies, such as optoelectronic stereophotogrammetric systems and markerless optical motion capture systems, can partially overcome this issue.

- Optoelectronic stereophotogrammetric systems: stereophotogrammetric (SP) systems base their operation on the so-called "stereoscopic vision", i.e. the perception of three-dimensionality of an object thanks to the combined action of both eyes [130]. This is because each eye can provide only a two-dimensional image of its surroundings, whereas the three-dimensional vision is given by the combination of the two. The SP system uses the same principle: it includes two or more cameras, operating in the visible or near-infrared region, and some retroreflective markers which are positioned on the subject. The position of each marker in the space is obtained thanks to the information provided by at least two cameras, that captured the same marker in the same instant from two different points of view. Basically, cameras work as human eyes. Marker trajectories can be used to obtain both temporal and spatial gait parameters. In particular, as trajectories are directly measured, the SP system represents the laboratory gold standard for spatial variables and it is often used for validating third party devices [131]. Among the commercial systems, the most used are the Vicon system and the Qualisys system. Despite their large use, SP systems are quite complex to use, as they require the positioning of a set of markers on the subject to reconstruct movement and the data acquisition needs to be managed by an expert operator.

- Markerless optical motion capture systems: markerless optical systems represent an affordable alternative to record human gait without the use of markers [132]. They are usually based on an RGB-camera used to track subject's movement minimizing efforts and complexity, but with a lower accuracy with respect to SP system in the estimation of temporal and spatial variables.

Compared to force platforms and instrumented walkways, SP systems allow to increase the number of strides and to set up more complex experimental protocols, for example including curvilinear walking and obstacles [133], as also markerless optical systems but with a lower accuracy. However, the assessment is

still limited to the capture volume, making all those technologies suitable only for laboratory measurements. Moreover, being all those technologies non-wearable and/or non-portable, they do not allow to move the analysis in real-world settings.

2.5.2 Wearable technologies

In the last decades, there is a growing interest in the use of wearable sensors for gait monitoring and health applications in general [134], [135]. Wearable sensors are low-cost devices, usually powered by an internal battery, which makes them fully portable [136]. For this reason, wearable technologies are suitable for moving gait analysis in real-world unconstrained conditions to evaluate motor performances [137]. Among the wearable technologies employed in gait assessment applications, there are foot switches, plantar pressure insoles and IMUs.

- Foot switches: foot switches are wearable devices, usually including two or three sensing elements positioned inside the shoe, between the foot and the internal insole [138]. The sensing elements can be compression closing or force sensitive resistors. Those devices allow the direct estimation of the foot-ground contacts and the other temporal parameters of gait through the measure of the impact force [56]. However, the presence of a reduced number of sensing elements limits the spatial resolution that, in turn, affects the correct foot contacts detection. In fact, the contacts can be detected only in correspondence of the sensing elements, that do not entirely cover foot surface. This can be even more difficult in case of pathological gait, where ground-foot contacts differ from the usual patterns [61].

- Plantar pressure insoles: plantar pressure insoles are instrumented insoles that integrate arrays of sensing elements covering the entire surface of the device. The insoles can be based on different technologies and the number of sensing elements usually varies from a hundred to a thousand [139]. The high resolution of pressure insoles with a high number of sensors makes them particularly suitable for foot pressure mapping applications without spatial resolution limitations [140]. However, such a high number of sensors greatly increases the cost and the amount of data and is not crucial for basic foot contacts identification.

- IMUs: inertial measurement units (IMUs) are one of the most widespread wearable solutions to monitor gait and mobility in general [141]. This because, compared to the previously mentioned wearable technologies, IMUs are able to provide not only temporal (indirectly derived) variables, but also a spatial description of gait [142]. They include an accelerometer and a gyroscope, but can also include a magnetometer and, in this case, are called magneto inertial measurement units (magneto-IMUs). Thanks to their small size and minimal invasiveness, they can be directly positioned on the body, integrated with clothing [136] or with other "smart" devices (telephones, watches or glasses) [143]–[145].

Chapter 3

State of the art

This chapter summarizes the state of the art of solutions proposed for the analysis of gait using wearable sensors, relevant for the objectives of the present thesis. The first part concerns the estimation of foot contacts (i.e. IC and FC) using wearable sensors, with an overview on the methods and technologies proposed in literature. The second part covers the state of the art on wearable solutions for gait assessment in real-world conditions and their technical validation. The third part gives an overview on the studies based on the evaluation of mobility during ADL, with a focus on MS population.

3.1 Gait events detection using wearable sensors

The estimation of gait events is crucial in the assessment of gait, as it allows to segment the strides and their phases. With the growing interest in moving gait analysis in real-word settings, several solutions have been proposed for the extraction of IC and FC using wearable sensors. The proposed methods vary depending on the number and type of sensors used, their working principle and the positioning.

The IMUs surely represent one of the most popular solutions employed for gait assessment to detect gait events, thanks to their low cost, reduced size and limited power consumption [146], in addition to the possibility of extending the analysis to spatial parameters (see Section 2.5.2 for further details). The algorithms for gait events detection using IMU data are commonly based on the study of signal morphology [147]–[150] or the application of machine learning

methods [151]–[153]. The characteristics of the developed method are strictly linked to sensor's positioning: in general, the further from the contact point with the ground, the more difficult the estimation of the gait-related variables becomes, as the signal pattern is more attenuated. The IMU-based approaches proposed in the literature typically use a single sensor or multiple sensor configuration. Usually, a single sensor, placed on the trunk, pelvis, or wrist, represents the most convenient solution in terms of usability and user-acceptance [39], [154] for long-term monitoring. In case of multiple IMUs, the preferred location is on feet or shanks, which is more suitable if a high accuracy in the estimation is required, especially in people with gait disorders [42], [155]–[157]. Despite their large use and suitability for real-world applications, IMU-based approaches for gait events detection are indirect methods and, therefore, they cannot be considered as a proper reference.

The validation of third-party devices in real-world settings requires the use of technologies which provide a direct measure of foot to ground contacts. Some works presented the use of body-worn cameras [51]–[53] for gait analysis applications, especially activity recognition. An example is the work from Hickey et al. [53], which proposed the use of a body worn camera, pointing on subject's feet, as reference for the validation of a 3D accelerometer mounted on the waist. Experiments were performed on ten healthy subjects and were carried out in real-world conditions, by recording the activity of the participants for one hour on two days. Videos were used to test the correct WBs detection and step count and the agreement between the two methods resulted to be excellent, as proved by the ICC values (0.941 for WB detection and 0.975 for step count).

Camera-based methods could be also used for gait events detection; however they rely on manual labelling, which is time-consuming and is strictly linked to camera resolution, in addition to potential privacy issues [158].

An adequate solution proposed in different studies is represented by footswitches [54], [56], [58]. Hausdorff and colleagues [56] presented a footswitch system for the estimation of IC and FC timings. The device included two footswitches connected in parallel, one placed under the anterior portion of the foot and the other under the heel. The algorithm was based on the initial identification of the local minima near the rising and falling edges. Then, each IC and FC was found by applying a threshold proportional to the value of the local minimum. Performance of the proposed method was validated against force platforms using data collected on ten healthy subjects with a sample frequency of

500 Hz. Participants were asked to walk stepping over the platforms ten times each at slow, comfortable and fast speed. Results from the comparison were computed in terms of mean errors showing a good accuracy both in ICs detection (0 ± 3ms) and FCs detection (-1 ± 8ms).

As already explained in Section 2.5.2, the footswitch technology includes two or three sensing elements, that are activated when the foot hits the ground and deactivated when it is lifted. Basically, IC and FC correspond to the instants of activation and deactivation of one or more switches, respectively, depending on how they have been positioned under the foot. Despite the accuracy of some footswitch-based methods, as that proposed by [56], the low spatial resolution can affect the correct gait events detection, especially in case of atypical or pathological foot support [61], thus limiting the validity of footswitches-based methods.

Another option is the use of plantar insoles for pressure mapping to detect temporal gait features by exploiting the variations in pressure values. As an example, the work from Catalfamo and colleagues [159] presented a method for the estimation of ICs and FCs, using the commercial pressure insoles F-scan Mobile Tekscan (sample frequency 200 Hz, 960 sensing elements). The proposed algorithm was based on the loaded area distribution during the gait cycle, that varies according to the foot portions in contact with the ground. An empirically set threshold was used for IC and FC detection to discard the insole areas that could be constantly loaded also during the swing phases. The method was validated using force platforms as reference. Ten healthy young subjects participated to the study and were asked to walk at their self-selected comfortable speed along a 10m path for six times, stepping over the platforms. Accuracy was evaluated in terms of mean absolute errors computed across all the observations (210 ICs and 210 FCs), which resulted to be quite low (22 ± 9 ms for IC, 10 ± 4 ms for FC). Nevertheless, the high cost of those devices prevents them for being the best available solution for reference gait events detection.

Some studies proposed the use of pressure insoles [62]–[65] with a number of sensors lower with respect to that of commercial devices specifically conceived for pressure mapping. However, the analysis was focused on temporal parameters other than gait events, in some cases without a proper reference [65].

The work from Braun et al. [62] suggested the use of a commercial pressure insole system including 13 capacitive sensors and a triaxial accelerometer

(Moticon GmbH, sampling frequency 50 Hz). Twelve healthy subjects were involved in the experiments and performed 30 steps with the dominant leg over a force platform, used as reference. The authors processed the data using the commercially available software, following a black box approach. Moreover, the analysis was focused on parameters other than gait events, such as the stance time.

Crea and colleagues [64] proposed a newly designed insole for foot pressure mapping during gait. The insole included 64 sensing elements and was validated against force platforms using data collected on two healthy subjects. Both participants were asked to walk along a straight path of about 10m without necessarily stepping on the force platform to avoid gait alterations. The task was repeated 15 times both at comfortable and fast speed. Validation focused on gait phases timings (e.g., stance and swing duration) but not on IC/FC detection.

Martini et al. [160] presented a new pressure insole based on optoelectronic technology, including a total 16 sensors, for measuring foot-to-ground reaction forces in lower limb robot applications. Ten healthy subjects participated in the experiments and were asked to walk on a 10m rectilinear path stepping over the force platforms, used as reference. ICs and FCs were obtained from the vertical ground reaction force given as output by the pressure insoles, applying a threshold of 3N. Algorithm performance was evaluated through the median absolute error computed across all the detected events for both ICs (60 ± 20 ms) and FCs (40 ± 20 ms).

An interesting work is that from Benocci and colleagues [161], as the authors provided a detailed description of the proposed method to detect gait events from pressure insoles data, but algorithms performance was not validated against a reference. Another study in which pressure insoles were used is that from Roth and colleagues [162], but the gait events were detected through a manual labelling and not with the application of a proper automatic method.

The current state of the art highlights the lack of a robust method based on an affordable wearable solution for gait events detection to be used as reference in the real-world, which is currently needed to move the validation of temporal parameters in unsupervised and unconstrained settings.

3.2 Gait assessment: from laboratory to real-world conditions

Recently, several studies have been published regarding the transition from laboratory to real-world conditions [12], [163]–[166] to capture the proper mobility performance of an individual, which cannot be observed during standardized assessments [165].

The transfer of gait assessment from standardized ambulatory or laboratory environments to unsupervised real-world settings requires the use of wearable technologies, which are low-cost, low-power and minimally obtrusive [136]. However, the availability of the suitable technology for real-world applications is not sufficient alone to make this transition. In fact, the proposed method should be validated in conditions similar to those of end use, to verify its applicability in ecological settings. However, this is not possible due to the lack of a wearable mobile gold standard to be used for the validation of wearable devices in real-world conditions. A system like that should be, in turn, validated against a gold standard system to assess its reliability as a reference. This requires the simulation of some of the most common circumstances encountered during everyday life. In addition, the method should be tested in real-world settings to establish its usability and the coherence of the estimated DMOs with those reported in the literature. As a further proof of reliability, the proposed solution should be tested on different populations, both healthy and pathological, to verify its applicability on different gait conditions.

3.2.1 Technical validation in standardized settings

In the last years, several wearable solutions were proposed and validated in standardized settings, with a focus on IMU-based approaches that exploit shanks/feet positioning. However, the large majority of the studies found in literature limits the assessment to basic motor tasks (i.e., straight walking patterns), which are quite far from what can be observed in real-world conditions.

Gastaldi and colleagues [41] proposed the assessment of a method based on two magneto-IMUs positioned on the shanks to estimate temporal gait parameters (i.e., stride duration, stance duration, swing duration, double support duration and cadence). These outcomes were compared with those obtained from a footswitch system (STEP32) using the proprietary software. The experiments were carried out on one healthy participant who walked along a 12m rectilinear path six times

back and forth, repeating the task three times. The authors reported that the error obtained for all the parameters was < 5% of the gait cycle.

Trojaniello et al. [42] presented a method for the estimation of gait spatial-temporal parameters based on two magneto IMUs attached above the ankles. Data were collected on four different cohorts (hemiparetic, choreic, PD and healthy elderly), each including ten subjects. Participants were asked to walk along a 12m straight path back and forth for one minute both at comfortable and fast speed. Performance of the proposed method was validated against an instrumented mat, used as reference, for the following parameters computed on each cohort: gait events, stride duration, step duration, stance duration, swing duration and stride length. Authors reported very good results for all the parameters, for example they reported mean absolute percentage errors of 1% for stride time and ≤ 3% for stride length.

The validation of the method proposed by [42] was further extended in the work from Bertoli and colleagues [43]. A total of 236 participants were involved (healthy older adults, older adults with mild cognitive impairment and PD) in the experiments, which followed the same experimental protocol illustrated for the above-mentioned study. Also in this case, the method was tested against the instrumented mat computing the errors on several spatial and temporal gait parameters. Results confirmed the accuracy of the method, with mean absolute errors ranging between 1% and 4% for the temporal parameters, around 2% for stride length and ≤ 3% for walking speed.

Zhou and colleagues [44] validated a method based on two IMUs mounted on the feet from Physiolog®5 system (GaitUp) using the OptoGait system as reference. The algorithm was based on a previous study [167] and allowed to compute a series of gait related parameters, including stride duration and stride length. Validation experiments involved five healthy participants who walked back and forth between the OptoGait bars for a total of 60m in three conditions (normal strides, short strides, long strides). The trials did not include gait initiation and termination as each participant was asked to start and stop walking outside the area delimited by the OptoGait bars. Results were reported in terms of root mean square errors for stride lengths (0.05m) and stride durations (0.04s) obtained over a total of 729 strides analyzed.

Jakob et al. [45] tested a wearable system (Portabiles-HCT GaitLab-System) made of two IMUs, each integrated in the midsole shoe, against a

stereophotogrammetric system. The experiments involved 33 PD patients who were asked to walk five times along a 10m path at self-selected speed. The algorithm used to extract gait related parameters from the wearable system signals was previously validated on different populations [168]–[170]. Agreement between the two system was computed using the Intraclass correlation coefficient (ICC) and showed excellent results for stride duration (0.966), stride length (0.985) and walking speed (0.986).

Although the results obtained in all studies were promising, the experimental protocols included only straight walk tasks, with a reduced number and variability of strides analyzed. The low complexity level does not reflect the heterogeneity of conditions that can be encountered in real-world environments, thus limiting the validity of the proposed methods. The limits linked to a standardized environment can be partially overcome including also curvilinear walking and dual-task conditions in the experimental protocol.

Romijnders et al. [46] stressed this necessity in their work, regarding the validation of an algorithm based on shank mounted IMUs for gait events detection. The method was tested on three populations (elderly subjects, PD patients and stroke patients) using the stereophotogrammetric system as reference. Each subject performed the following tests: 5m straight walk, 5m slalom walk, walk along an elliptical path while performing a numerical test (Stroop test). Performance was evaluated in terms of recall and precision obtaining very good results (recall from 84 to 100%, precision from 95 to 100%) in all cohorts.

Despite the higher complexity with respect to straight walking tasks, the introduction of curvilinear patterns and dual task walks in the experimental protocol is not sufficient, alone, to reproduce the heterogeneity and variability that characterizes daily-life environments. This further emphasizes the need for a greater effort in the validation of solutions specifically designed for real-world applications.

3.2.2 Technical validation in real-world settings

In the recent years, the scientific community highlighted the importance of moving the technical validation of gait analysis solutions in real world settings. Rochester and colleagues [15] stressed this point in their work, emphasizing the necessity of a proper validation in the same conditions of end use. This implies that solutions specifically conceived for real-world applications should be

validated in daily-life settings on the populations of interest to account for both intrinsic and extrinsic factors. Nevertheless, very few studies tried to address the challenge until now.

A possible solution is the use of methods based on global navigation satellite systems to obtain reference values. In their work, Soltani and colleagues [70] used this approach to validate the estimation of walking speed from a wrist mounted sensor. Despite the low positional errors that those systems can provide [171], their performance depends on environmental conditions, their use is limited to outdoor settings [172], the temporal resolution is low and a stride-by-stride description is not possible [47]. Moreover, they suffer from privacy issues as the participant's position can be detected [47].

Atrsaei and colleagues [47] used feet mounted IMUs as reference to validate the estimated of WBs detection and walking speed obtained from a lower back IMU. Data collection was performed on MS patients in three sessions: 10m test, repeated three times in a clinical setting; unsupervised 10m test performed at patient's home and repeated twelve times; real-world 6-hour recording in which the participant was asked to perform the usual daily living activities. The first session involved 35 patients, while the second and the third one was performed by a subset of participants (14 and 9, respectively). Compared with the reference, the algorithm for gait speed estimation showed mean errors of 0.00 m/s for both 10m test conditions and 0.02 for real-world acquisitions. The algorithm for WB detection, based on machine-learning techniques, reached an F1-score of 78.6%. It is important to recall that, as IMUs do not provide a direct measure of the quantities of interest, the solution adopted in this study as reference should be considered a silver standard, as also specified by the authors [47].

Storm and colleagues [48] proposed the use of pressure insoles for the validation of temporal parameters obtained from two different algorithms, one based on a single waist mounted IMU and the other on two IMUs positioned on the shanks. Experiments involved ten healthy participants that were asked to walk in four different conditions: indoor 20m walk at preferred speed, repeated eight times; outdoor 20m walk at preferred speed, repeated six times; indoor two minutes' walk inside a university building; outdoor real-world walk of fifteen minutes, avoiding stairs. The DMOs computed included gait events and temporal parameters such as stride duration and stance duration. Results were reported in terms of mean absolute error, obtaining good results (0.04s for the shank method and 0.03s for the waist methos in case of stance duration).

Roth et al. [49] published a relevant study regarding the validation of an algorithmic pipeline based on feet mounted IMUs for gait assessment. For this purpose, force sensitive resistor pressure insoles were used as reference. Data were collected on twenty healthy subjects while walking in supervised real-world conditions, including level walking, stairs ascending and stairs descending at different speed (i.e. slow, normal and fast). Performance in the estimation of temporal parameters was evaluated in term of mean absolute error, that ranged between 0.01s and 0.03s in all cases for gait events, stride time, swing time and stance time.

The present literature suggests the relevance of studies conducted in real-world conditions for the analysis of gait performance. Nevertheless, it also reveals that, in the large majority of cases, the solutions employed as reference suffer from some limitations. IMUs can be used to estimate both temporal and spatial parameters, providing a complete description of gait patterns; however, temporal parameters are obtained through indirect methods, thus limiting their use to a silver standard. Conversely, pressure insoles provide a direct measure of the gait events and the other temporal parameters, but do not allow the estimation of spatial variables. These considerations reinforce the need for a system combining different technologies to overcome those obstacles and provide an accurate reference.

3.2.3 Multi-sensor solutions for real-world gait analysis

The use of a multi-sensor approach has been proposed in some studies [71], [72], [173]–[176], but only a small subset addressed the systematic validation of the system with respect to a gold standard.

A preliminary work published by Li and colleagues [175] deals with the validation of a newly designed multi-sensor system including three force sensors, one IMU and four range sensors positioned on each foot. The proposed solution was tested against the stereophotogrammetric system using data acquired on four male healthy participants. The experiments were carried out indoor and included straight line walking along a 4m path. Among the parameters presented in the study, also stride length and walking speed were computed, obtaining percentage errors of 9.34% for stride length and 5.90% for walking speed.

Duong et al. [71] presented a multi-sensor solution (SportSole II) which consists of a pressure sensitive insole with eight force resistor elements and an

IMUs for each foot. The system was validated with respect to an instrumented mat using data collected on eleven HYA. In particular, the participants were asked to perform tasks including different activities (e.g., level walking, stair walking, sitting on a chair), both in a fixed order (structured) and self-selected order (unstructured). Then, portion of straight and curvilinear walking on the instrumented mat were selected and used for the validation. A support vector regression algorithm was used to extract gait parameters, obtaining good results in terms of mean absolute errors (Structured tests: 2.97% for stride length, 3.16% for stride speed; unstructured tests: 3.55% for stride length, 3.59% for stride velocity).

Although both studies show promising results, the validation should be extended to a larger sample of participants. Moreover, it should include different cohorts, both healthy and pathological, to establish the feasibility and robustness of the proposed solution on various gait patterns and walking speed ranges. In addition, a validation limited to straight and curvilinear walking portions is not sufficient, alone, to assess the applicability in real-world conditions. To this end, the experimental protocol should be designed ad hoc for stressing the system including a large variety of activities on different complexity levels, trying to mimic the conditions of end use.

3.3 Gait analysis during Activities of Daily Living

Despite the high relevance of gait analysis in unsupervised real-world settings, also the assessment during task-oriented acquisitions, including daily life activities, is of great interest. The first condition enables the evaluation of mobility performance, taking into account all the possible intrinsic/extrinsic factors linked to the individual environment; whereas the second condition can be useful to assess the performance during specific activities of interest, that are part of the protocol, and to study the effects of a treatment on the individual mobility through a direct comparison of two or more repetitions of the same activity. This can be beneficial in case of patients with neurological disorders to verify if a specific therapy has a significative impact on gait performance in terms DMOs changes and differences between right and left side [35], [164].

There are different ways to evaluate gait performance during ADL. Several studies base the evaluation on clinical scales, including the modified Barthel ADL Index [177], [178] and other disease-specific scales [179]. However, those evaluation are not sufficient alone to obtain an accurate assessment. Other studies

use various technologies for a more quantitative analysis, from the traditional SP systems [180], [181] to the most recent wearable technologies [182]–[189], that allow to overcome the spatial-temporal constraints. However, the large majority of them is focused on outcomes different from DMOs related to gait, e.g. activities recognition [182]–[184], kinematic analysis [185]–[187] or quantification of energy expenditure [188], [189]. In addition, most of them include patients with diseases other than MS or healthy elderly people.

A relevant but preliminary study is that from Chen and colleagues [38], that proposes a multi-sensor system for the assessment of gait during ADL, including a plantar pressure insole with 96 sensing elements and an IMU for each foot. The algorithmic pipeline, described in detail, provides up to 26 gait parameters comprising temporal parameters, but also gait variability and asymmetry. The algorithm is able to discriminate between different activities and provide the gait parameters for each of them. In fact, the authors highlight the importance of knowing the association between DMOs and activity for clinical purposes. Moreover, they stress the relevance of the above-mentioned parameters for an objective evaluation of the effectiveness of the therapy in patients with neurodegenerative diseases, as reported in previous studies [190]. However, the algorithm validation included only data acquired on healthy participants (one subject for temporal parameters block, ten subjects for ADL recognition block). Accuracy of temporal parameters block was evaluated on 20 steps using video recording as reference, obtaining low errors for gait events (IC 0.0 ± 14.1 ms, FC 5.2 ± 15.5 ms) and temporal parameters (1.2 ±14.9 ms for stride duration, −3.5 ± 15.6 ms for stance duration, 5.2 ± 8.0 ms for swing duration). ADL recognition block – based on a linear SVM classification model - was tested through five-fold cross validation including only the strides in the middle of the acquisition performed on the ten participants, resulting in an overall accuracy of 99.8%.

The above-cited studies propose the ADL monitoring as a one-time evaluation of mobility. To the best of my knowledge, there are not studies proposing the assessment of gait parameters during ADL to quantify potential changes after a physical rehabilitation treatment, as this type of analysis is usually performed through standard walking tests [27]–[31]. The current literature highlights the need for further investigation on the efficacy of medical treatments with the aid of validated technologies. In this perspective, the use of a reliable wearable system to obtain a quantitative mobility assessment could be beneficial to support the clinician in the decision-making process. This can be particularly relevant in case of patients with neurodegenerative diseases, such as MS, in which the

effectiveness of the treatment is fundamental to slow down the disease progression [19].

Chapter 4

Sensors overview

This chapter introduces the multi-sensor system used in the present thesis, called INDIP (INertial module with DIstance sensors and Pressure insoles). The first section regards the working principles of the different sensor technologies integrated in the system. The second part provides a detailed description of INDIP hardware, including not only the sensing units, but also the other components. The knowledge of this fundamentals is important to understand the limitations of the different technologies, as also to correctly process and analyze the measured signals.

4.1 Sensors working principle

The following section provides a description of the functioning principle for the different types of sensors employed for this thesis work. Three sensor technologies – IMUs, force sensitive resistors and time-of-flight infrared distance sensors – were integrated in the INDIP multi-sensor system for assessing gait in both standardized and real-world conditions.

4.1.1 Force sensitive resistors

Force sensitive resistors (FSRs) represent a possible solution for the measurement of foot pressure, which can be used for the estimation of IC and FC events and, as a result, of the temporal gait parameters. FSRs work thanks to the presence of a material whose resistance varies with the application of a force applied in normal

direction with respect to the surface [191]. In particular, the resistance is inversely proportional to the applied force, according to a non-linear trend [192], [193]. Basically, a FSR is made of a polymer matrix in which conductive particles are immersed; this material lies between two metal electrodes [194]. To better understand the working principle, the overall resistance across the FSR can be defined as reported in [194]:

$$R_{FSR} = R_{bulk} + 2R_C$$

Where R_{bulk} is the resistance of the conductive polymer deriving from the quantum tunneling conduction mechanism and R_C is the contact resistance between the electrodes and the conductive particles.

When no force is applied, the two electrodes are separated by a certain distance. The overall resistance is mainly due to the polymer resistance (R_{bulk}), while the contact resistance (R_C) gives a small contribution, as only few particles are in contact with the electrodes. Conversely, under an external force, the inter-particle distance diminishes, thus reducing the contribution of R_{bulk}; moreover, the deformation causes a reduction in the contact resistance R_C. This leads to a decrease in the overall resistance value (Figure 4).

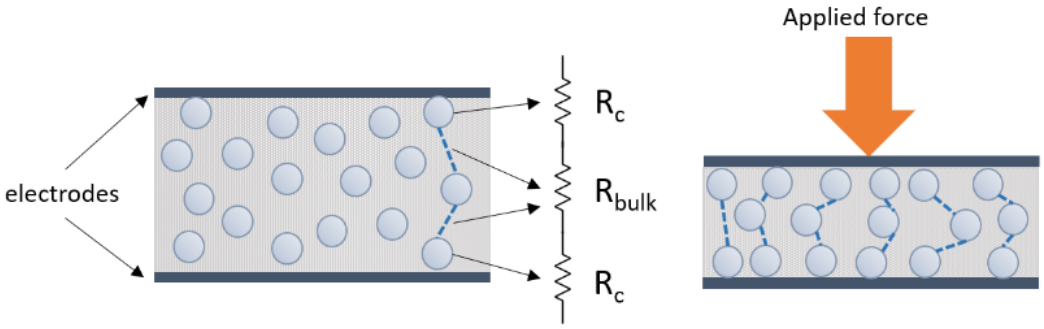

Figure 4: Force sensitive resistor working principle. The application of an external force causes a reduction of inter-particle distance, leading to a lower R_{bulk} value and to a decrease of the overall resistance.

Due to their thickness, FSRs are quite flexible and can be integrated into other devices, such as insoles or smart shoes for gait analysis application. To obtain a more linear trend, usually resistance is placed with conductance, for example using a transimpedance amplifier [195].

4.1.2 Inertial measurement units

In the recent years, the introduction of technologies like micro electromechanical systems (MEMS) and complementary metal oxide semiconductors (CMOS) enabled the development of low cost, miniaturized sensors for motion tracking [196]. Thanks to their characteristics, those sensors can be easily integrated with other electronic devices, e.g. smartphones, tablets and toys, and their use is widely spread in different fields, including the study of human mobility. Thanks to MEMS/CMOS technologies, a single silicon substrate can house various sensor types, thus allowing the construction of MEMS IMUs [196].

The working principle of an IMU is based on the mass/spring system. If the mass is subject to an external force, it undergoes a certain displacement [196]. According to the type of force applied, it can produce an acceleration or an angular rotation of the mass: the first one is well described by the principle of inertia, while the second one can be related to Coriolis effect. As a result, the IMU will measure the linear acceleration, sensed by the accelerometer [197], or the angular velocity of the mass, sensed by the gyroscope [198].

The term IMU is commonly used to indicate the entire device, where the sensors (i.e., accelerometer and gyroscope) are combined with a dedicated circuit that allows to convert the output signal from analog to digital. Moreover, it applies a preprocessing (including for example noise removal, filtering, sensor stabilization over temperature) that provides the desired signal for the specific application [196].

The number of measurement axis of the sensor can vary, leading to different degrees of freedom. Usually, IMUs combine a 3D accelerometer and a 3D gyroscope (6 DOF). However, they can also include a 3D magnetometer (9 DOF) and in this case they are called magneto inertial measurement units (magneto-IMUs). Even if the INDIP system includes magneto-IMUs, the magnetometer has not been used for the purpose of this thesis. For this reason, the following section will focus on accelerometer and gyroscope only.

Accelerometer

An accelerometer is a sensor that provides a measure of the linear acceleration. More precisely, it measures the proper acceleration [199], i.e. the physical acceleration felt by an object, which is defined as:

$$a_p = a_s - g$$

According to Mohammed and colleagues [200], an accelerometer can be described as a second order spring/mass/damper system, represented in Figure 5. If an external force (F_{ext}) is applied to the mass, it can be defined as:

$$F_{ext} = ma_{ext}$$

While the spring and damping forces correspond to:

$$F_{spring} = kx$$

$$F_{damper} = b\dot{x}$$

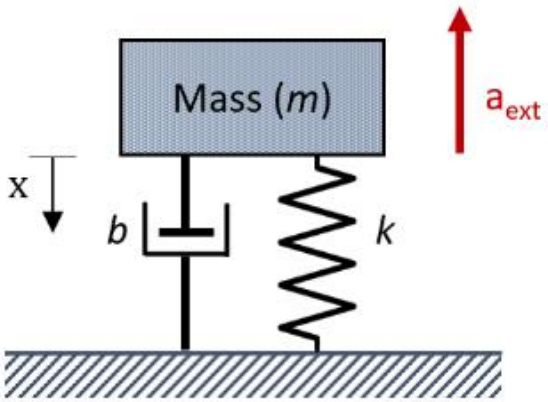

Figure 5: Second order spring/mass/damper system used as accelerometer model.

According to Newton's second law ($F = ma$), which describes the translational motion, the sum of the forces acting on the mass is directly proportional to the desired acceleration of the object. In this case we have:

$$F_{ext} - F_{spring} - F_{damper} = m\ddot{x}$$

$$F_{ext} = m\ddot{x} + b\dot{x} + kx = ma_{ext}$$

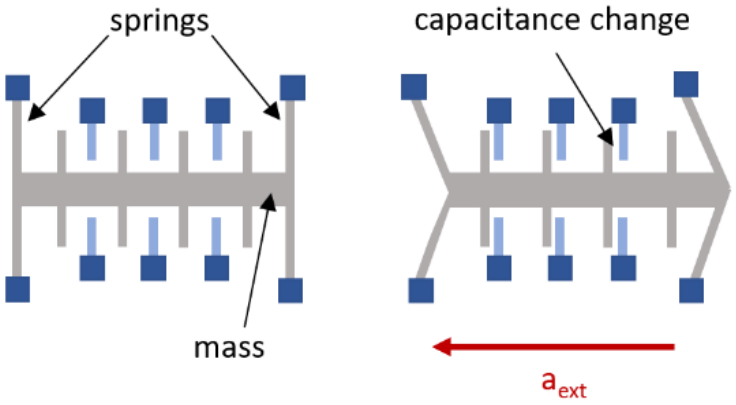

Figure 6: Working principle of a capacitive accelerometer. When an external force is applied, it causes a change in displacement that translates into a change in capacitance.

This means that the applied acceleration can be obtained as a function of the displacement. The accelerometers can be classified according to the mechanism of transduction of the displacement into a measurable electric signal. The most common technique is based on the use of a capacitor to measure the displacement [196], [200]. In practice, a change in displacement results in a proportional differential change in capacitance which is then converted in a voltage [196], [200]. A simplified illustration is reported in Figure 6.

Gyroscope

Gyroscope sensors are used to measure the angular velocity. Among the different working principles, gyroscopes designed according to the Coriolis effect are the most used in consumer-grade IMUs [201]. The Coriolis effect occurs when an object moves in a rotating reference frame: in this case the observer will see the object moving along a curvilinear trajectory, under the action of a transverse force (namely, Coriolis force [202]). Conversely, the same object observed from a stationary reference frame will result in a uniform linear motion. The Coriolis force is defined as:

$$F_{Coriolis} = -2m\Omega_z\dot{x}$$

Where Ω_z is the angular velocity around the vertical Z-axis.

Gyroscopes based on the Coriolis effect are also called vibrating gyroscopes and can be schematized as a spring-mass-damper system with two degreed of freedom [201], [203], as shown in Figure 7:

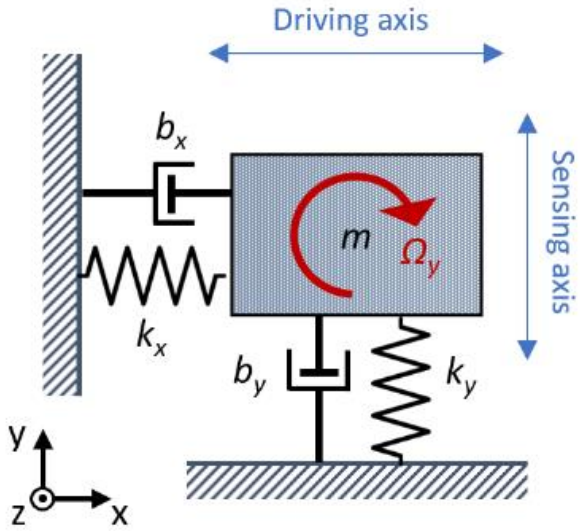

Figure 7: Spring/mass/damper system used to model the gyroscope.

Also in this case, the forces acting on the mass can be defined according to the Newton's second law in both drive and sense direction [203]:

$$F_x = m\ddot{x} + b_x\dot{x} + k_x x$$

$$F_y - 2m\Omega_z\dot{x} = m\ddot{y} + b_y\dot{y} + k_y y$$

This in turn means that the angular velocity can be obtained through the estimation of the mass displacement.

Although there are various constructional designs, the most popular solution is based on the use of capacitors which can be arranged in configurations of different complexity levels [204], [205]. The simplest gyroscope structure (Figure 8) comprises a proof mass attached to a substrate, driving electrodes (providing a constant momentum along the driving direction), sensing electrodes (providing the Coriolis force) and a suspension architecture made by four suspension pillars [201], [203]. Basically, the combined movement of driving and sensing electrodes causes a differential capacity change that is used to measure the Coriolis force and, in turn, the angular velocity.

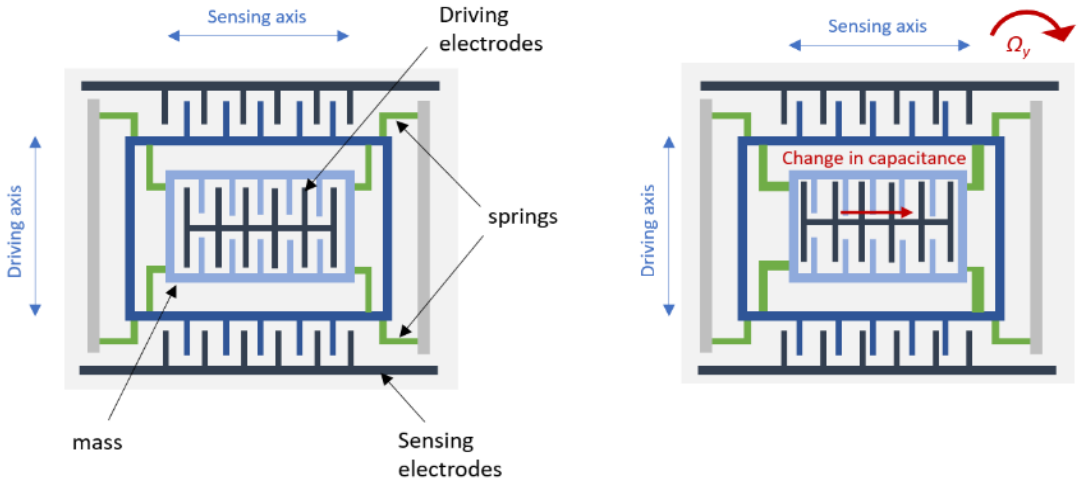

Figure 8: Simplified architecture of a capacitive vibrating gyroscope. The external force causes a displacement that results in a change in capacitance.

4.1.3 Time-of-Flight Infrared distance sensors

The Time-of-Flight Infrared (IR-ToF) distance sensors represent a recent solution for the estimation of inter-foot distance in the analysis of human movement [206]. The working principle (Figure 9) is based on the phase difference between the IR wave emitted by the sensor $s(t)$, directed to the target object, and the reflected IR wave detected by the sensor $r(t)$ [206], [207], defined as:

$$s(t) = \sin(2\pi f_M t)$$

$$r(t) = \mathrm{R} * \sin(2\pi f_M t - \varphi) = \mathrm{R} * \sin\left[2\pi f_M \left(t - \frac{2d}{c}\right)\right]$$

Where R is the reflection coefficient, f_M is the modulation frequency of the two signals and c is the speed of light [206].

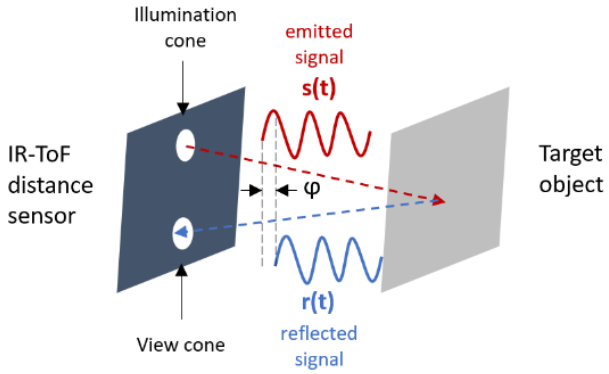

Figure 9: IR-ToF distance sensor working principle.

The distance between the sensor and the target object is then obtained as a function of the phase difference [206]–[208]:

$$d = \frac{c}{4\pi f_M}\varphi$$

This technology has several advantages, including the small size, the integration of transmitter and receiver in the same unit, the robustness to environmental conditions (e.g., ambient light) and the high output frequency (up to 50 Hz) [206]. Moreover, the low power consumption (2–5 mA) makes them particularly suitable for long monitoring applications.

4.2 The INDIP system

The INDIP (manufacturer (mfr.) 221e S.r.l. [209]) is a multi-sensor system including a magneto-IMU, which constitutes the motherboard, that can be enhanced by different sensing peripherals. Figure 10 shows a detailed picture of the system hardware architecture, the communication interfaces and the sensing peripherals (i.e., IR-ToF distance sensors and pressure insoles).

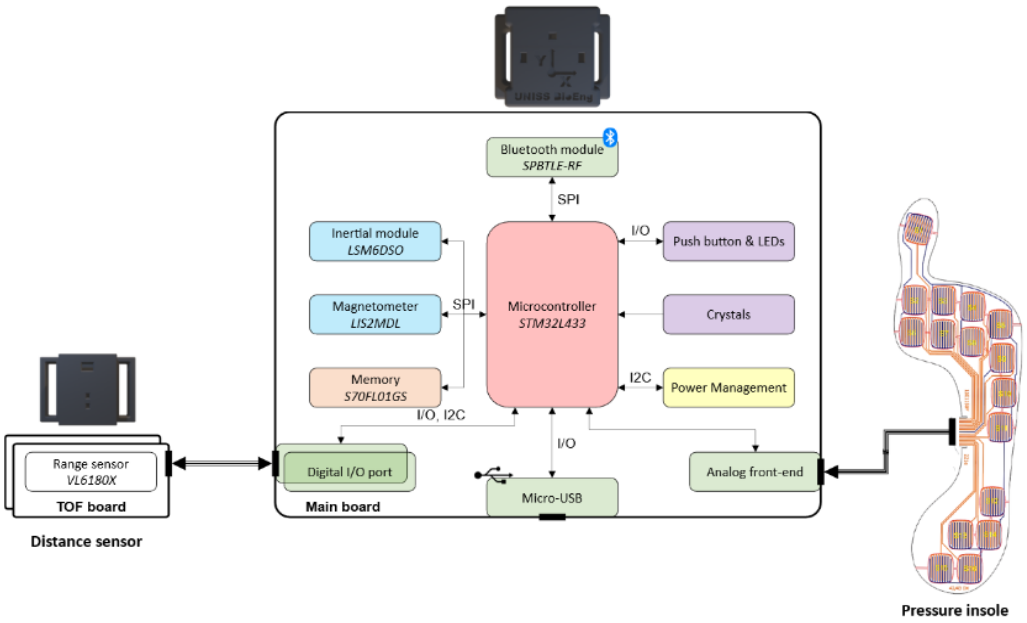

Figure 10: INDIP hardware's architecture.

4.2.1 Motherboard

The motherboard is the result of a design aimed at: (i) combining motion sensing and processing capabilities in a single system unit with a low power consumption; (ii) allowing data storage thanks to an on-board memory; (iii) ensuring wire/wireless transmission thanks to the presence of both USB connector and Bluetooth Low Energy module (BLE). The motherboard has a form factor of 31 L× 29 W× 7 H mm^3 (35 L × 47 W × 19 H mm^3 including case and battery, for a total weight of 16g). A detailed description of the architecture at the base of the core system functions is reported in the following.

Processing

The central unit of the motherboard is an ultra-low power microcontroller unit (STM32L433, mfr. STMicroelectronics). Based on the high-performance ARM® Cortex®-M4 32-bit architecture, it embeds high-speed memories (256 kB of flash memory and 64 kB of SRAM), a low-power real-time clock and an extensive range of enhanced inputs/outputs (I/Os) and peripherals. In addition, an external crystal (ASTMTXK, mfr. Abracon) has been connected to the microcontroller unit to generate time values with a higher accuracy and precision. This crystal

generates a clock signal of 32.768 kHz, with a frequency stability of ±5 ppm (parts per million) and a deviation of only ±18ms per hour.

Sensing

The sensing capabilities concern the motion measurement by means of two different sensors which allow to obtain both inertial and magnetic data. To work at higher baud rates both sensors were connected to the microcontroller via serial peripheral Interface (SPI).

The first sensor (LSM6DSO, mfr. STMicroelectronics) is a system-in-package with a 3D digital accelerometer (full scale ranges ±2/±4/±8/±16 g) and a 3D digital gyroscope (full scale ranges ±125/±245/±500/±1000/±2000 dps). The chip has a current draw of 0.55 mA when both sensors set to operate in high-performance mode, and it enables always-on low-power features.

The second sensor (LIS2MDL, mfr. STMicroelectronics) is an ultralow-power, high performance 3D digital magnetometer with a magnetic field dynamic range of ±50 gauss.

Storage

A Quad SPI NOR flash memory (S70FL01GS, mfr. Cypress) is used for storage purposes. The memory is connected to the microcontroller unit via SPI and allows data logging up to 13 hours.

Connectivity

The communication with external devices, such as laptops and smartphones/tablets, can be performed in two different ways: via Bluetooth or via USB. The Bluetooth connection is provided by an easy-to-use BLE master/slave network processor module (SPBTLE-RF, mfr. STMicroelectronics) compliant with Bluetooth v4.1. The USB connection is the micro-USB 2.0 high-speed port which is connected to the microcontroller unit. Both solutions allow data transfer in both directions (read/write).

Power management

The system is powered by a lithium polymers battery (nominal voltage: 3.7 V; capacity: 155 mAh, dimension: 24 L× 20 W× 3.8 H mm^3) scaled down to an operating volage of 3 V by means of a high efficiency step-down converter

(TPS62740, mfr. Texas Instruments). The battery can be recharged through the dedicated micro-USB connector and the process is managed by a constant current/voltage charger (STC4054, mfr. STMicroelectronics). Moreover, the micropower current fuel gauges for lithium-ion batteries (MAX17048, mfr. Maxim Integrated) was integrated into the board and connected to the microcontroller via the inter-integrated circuit protocol (I2C).

Analog front-end

The analog front-end comprises a negative feedback operational amplifier (gain equal to 6) where a voltage divider with two resistors works as voltage reference. Two identical amplifying stages, including an operation amplifier (AD8607, mfr. Analog Devices) and a multiplexer (74HC4051, NXP Semiconductors), were utilized to optimize the design and the management of the analog inputs (16 lines: one for each pressure insole sensing element). This allowed the connection of only 6 lines instead of 16 to the microcontroller (3 lines for each multiplexer allow to select up to 2^3 input signals).

I/O

The connection of external sensing peripherals is enabled by the presence of two communication interfaces. The first one is an 18-pin ZIF-connector mounted on the bottom of the motherboard, that allows the connection between the pressure insole and the microcontroller through an analog front-end. The second one consists of two 6-pin connectors that enable to manage every type of sensor supporting the I2C communication, in this case the IR-ToF distance sensor.

The motherboard supplies the required power, storage and connectivity capabilities: this allows to include only the strictly necessary components in the external sensing peripherals and to minimize their form factor.

External synchronization

The synchronization with third-party devices is supported through an external equipment and can be performed in two modes: (i) Output synchronization: when the motherboard starts recording, it sends a signal to the external equipment using the ID pin of the micro-USB; (ii) Input synchronization: the motherboard starts the recording when it receives a signal from the external equipment on the ID pin of the micro-USB.

4.2.2 Sensing peripherals

The sensing peripherals utilized in this thesis include IR-ToF distance sensor and FSR pressure insole.

IR-ToF distance sensor

The IR-ToF board integrates a sensor (VL6180X, mfr. STMicroelectronics) combining an IR emitter, a range sensor and an ambient light sensor. The range sensor can measure distances up to 0.2, 0.4 and 0.6 m at 50, 33, and 25Hz, respectively. A form factor, including the case, of 36.2 L × 25.2 W × 11 H mm^3 has been achieved, with a total weight of 4g. The sensor was fully characterized in [ref] taking into account different factors (e.g., target color, sensor-target distance, and sensor-target angle of incidence) in both static and dynamic conditions.

FSR pressure insole

The FSR pressure insole, with an overall thickness of 240μm includes 16 force sensing resistors covered with a polyester layer. Each force sensing resistor exhibits a resistance value which is inversely proportional to the amount of applied force. With the increasing applied force, the sensor resistance decreases. Pressure insoles are available in different sizes (EU 36-37 to 46-47) according to the user foot length.

4.2.3 Firmware

The firmware embedded on the motherboard has been implemented with the CubeMX hardware abstraction layer and the integrated development environment Atollic TrueSTUDIO® for STM32.

The application firmware is uploaded on the main board thanks to the presence of a bootloader, that allows to easily update it on the microcontroller via USB when a new version is available (e.g., new available features, bug fixed, etc.). After the application firmware has been correctly started, a general check of the main components of the main board (i.e., inertial module, magnetometer, memory, BLE, battery charger, fuel gauge) and of the connected sensing peripherals (i.e., IR-ToF distance sensor, pressure insole) is carried out. According to the result of the check, the system can move to different states: ERROR if the check fails (red light on), from INIT to IDLE if the check is successful. In this state all the components, except for the BLE module, are

switched off to reduce power consumption. From the IDLE state, the system can move to three different states depending on what happens:

1) LOG state: when the system receives the start LOG command via USB, BLE, or external trigger, then it starts logging data on the on-board memory. The data logging can be stopped through the STOP command either via USB, BLE, or external trigger and the system moves to IDLE.
2) TX state: when the system receives the TX command via BLE, it starts streaming data via BLE. Data streaming can be stopped via BLE through the STOP command. Streaming is not possible if the system is connected via USB.
3) READOUT state: when the system receives the READOUT command and the information about the recording to read, it starts transmitting the recorded data from the on-board memory. When all data have been sent or when the read timeout has expired, the system returns to the IDLE state.

Finally, the system moves to STANDBY when the button has been pressed and hold for at least 7s or the SHUTDOWN command has been sent by the user. Additional details on INDIP system firmware can be found in the supplementary material in [210].

4.2 INDIP system gold standard configuration

The INDIP system can be used in different configurations thanks to its modularity. For the purpose of this thesis, it was used in its gold standard configuration. In practice, it included:

- Three magneto-IMUs, with full range scale set to ± 16 g for the accelerometer and ± 2000 dps for the gyroscope.
- Two IR-ToF distance sensors with range set to 0.2 m at 50 Hz.
- Two FSR pressure insoles of appropriate size. For this study, one small size (EU 36–37) and one large size (EU 42–43) have been used.

Of the three magneto-IMUs, two were positioned over the instep and fixed to the shoelaces using custom-made clips. The third magneto-IMU was positioned on the lower back through an elastic Velcro belt. One IR-ToF distance sensor and one FSR pressure insole were connected to each of the feet magneto-IMUs via cable. The pressure insoles were selected according to subject's foot size and inserted between the insole and midsole of the shoes. The distance sensors were

fixed to the shanks using Velcro straps, both pointing medially. In particular, they were positioned asymmetrically (one just above the left ankle and the other about 3 cm higher on the right side) to avoid mutual interferences. Figure 11 shows the INDIP system gold standard configuration and its positioning.

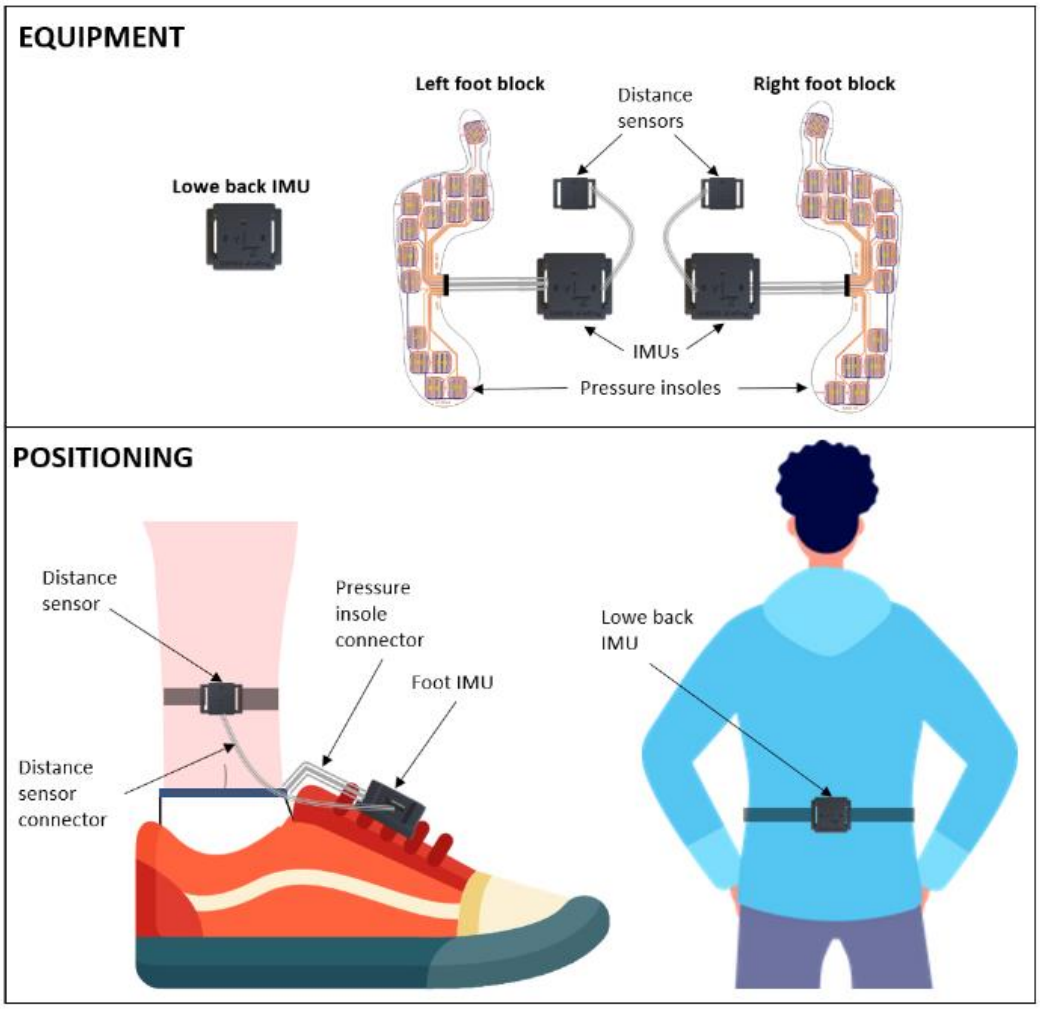

Figure 11: INDIP gold standard configuration and subject positioning

Chapter 5

Gait events detection from pressure insoles

This chapter reports the abstract of the contribution regarding the development of an algorithm for gait events detection based on pressure insoles data [211]. The full-length paper is reported in Appendix A.

5.1 A method for gait events detection based on low spatial resolution pressure insoles data

Salis, F. et al.: A method for gait events detection based on low spatial resolution pressure insoles data. In: Journal of Biomechanics, 127(2), 2021, p. 110687.

Abstract

The accurate identification of initial and final foot contacts is a crucial prerequisite for obtaining a reliable estimation of spatial-temporal parameters of gait. Well-accepted gold standard techniques in this field are force platforms and instrumented walkways, which provide a direct measure of the foot-ground reaction forces. Nonetheless, these tools are expensive, non-portable and restrict the analysis to laboratory settings. Instrumented insoles with a reduced number of pressure sensing elements might overcome these limitations, but a suitable method for gait events identification has not been adopted yet. The aim of this paper was to present and validate a method aiming at filling such void, as applied

to a system including two insoles with 16 pressure sensing elements (element area = 310 mm²), sampling at 100Hz. Gait events were identified exploiting the sensor redundancy and a cluster-based strategy. The method was tested in the laboratory against force platforms on nine healthy subjects for a total of 801 initial and final contacts. Initial and final contacts were detected with low average errors (about 20 ms and 10 ms, respectively). Similarly, the errors in estimating stance duration and step duration averaged 20 ms and less than 10 ms, respectively. By selecting appropriate thresholds, the method may be easily applied to other pressure insoles featuring similar requirements.

Chapter 6

Development and validation of a pipeline based on a multi-sensor system for real world gait analysis.

This chapter describes the work relative to the development and validation of a pipeline based on the use of a multi-sensor system (INDIP) for analyzing gait in real-world. The first part regards the design of the algorithmic pipeline, including the identification of the sensors suitable for the computation of each DMO and the project of algorithm workflow. The second part reports the abstract of the paper about the validation of INDIP-based algorithm on both healthy and pathological cohorts, with a focus on Walking bout level DMOs. The full-length paper is reported in Appendix B. The third section illustrates the results obtained from the validation of INDIP system considering stride level DMOs on the same dataset.

6.1 Design of the algorithm pipeline

The gait-related parameters of interest have been chosen by the Mobilise-D consortium in accordance with the granularity levels that can be exploited in a real-world context. The DMOs, including the most traditional spatial and temporal parameters but also the concept of Walking Bout, have been introduced in Section 2.4. Knowing the DMOs of interest allows to understand which variables are needed for their estimation, which is a fundamental prerequisite for the pipeline construction. In particular, a complete description of gait with the DMOs

previously describes, calls for the estimation of both temporal (i.e. feet contacts) and spatial (i.e. feet displacement) variables.

To establish how to extract the variables useful for DMOs estimation and how to integrate the information provided by the different INDIP sensors, the macro problem was divided into sub-problems, as depicted in Figure 12.

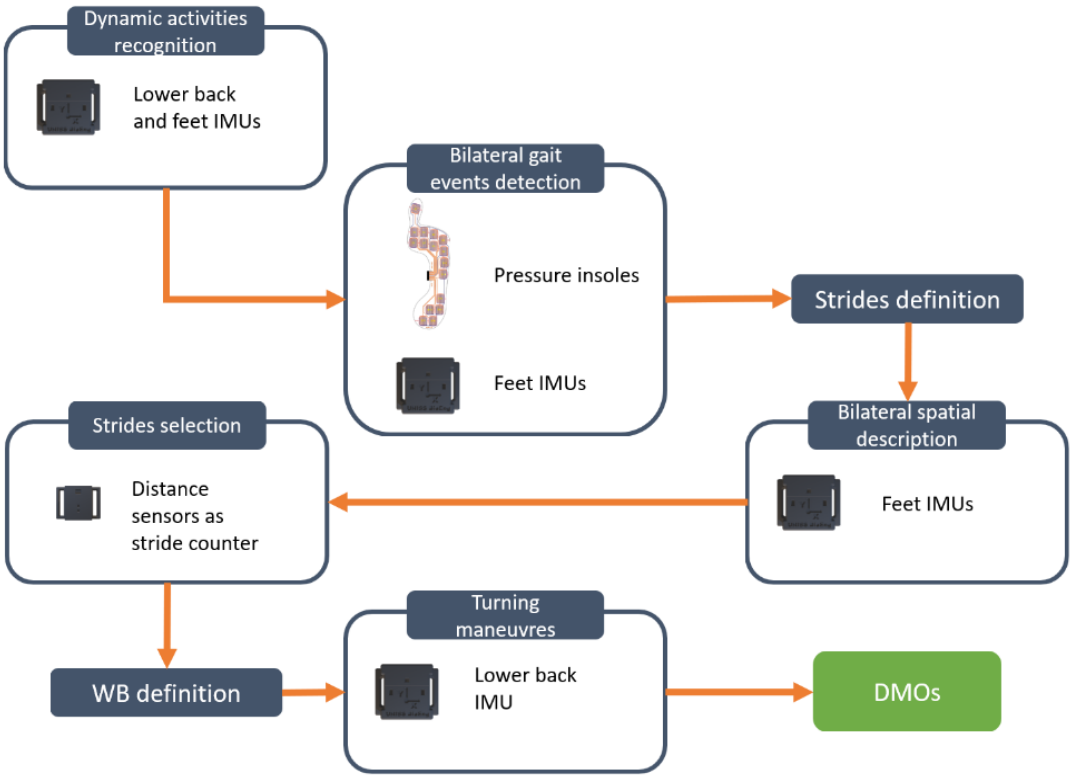

Figure 12: Workflow for the identification of the optimal sensor for each subproblem

The first step is the dynamic activities recognition, for which the lower back IMU is used together with the feet mounted IMUs. The second step is the identification of feet contacts: to do that, both PI and feet mounted IMUs are used, exploiting the redundancy of the system to minimize the number of missed events. The following step is the spatial description of both feet in terms of displacement; in this sense, the most reliable approach is based on the use of feet mounted IMUs. The steps computed till now allow the estimation of temporal and spatial variables that are used to define the strides. At this stage, distance sensors are employed as stride counters for an additional check on the correct strides detection. Having all the information, it is possible to construct the WB in

accordance with its definition. Turning maneuvers within a WB are identified through the use of the lower back IMU. Finally, all the relevant DMOs are extracted within each WB. Starting from the segmentation in subproblems, the algorithm flow for the estimation of spatial and temporal DMOs was defined. A detailed description of INDIP algorithm is reported in [210].

6.2 A multi-sensor wearable system for gait assessment in real-world conditions: performance in individuals with impaired mobility

Salis, F. et al.: A multi-sensor wearable system for gait assessment in real-world conditions: performance in individuals with impaired mobility. Submitted to: Frontiers in Bioengineering and Biotechnology.

Abstract

Accurately assessing people's gait, especially in real-world conditions and in case of impaired mobility, is still a challenge due to intrinsic and extrinsic factors resulting in gait complexity. To improve the estimation of gait-related digital mobility outcomes (DMOs) in real-world scenarios, this study presents a wearable multi-sensor system (INDIP), integrating complementary sensing approaches (two plantar pressure insoles, three inertial units and two distance sensors). The INDIP technical validity was assessed against stereophotogrammetry during a laboratory experimental protocol comprising structured tests (including continuous curvilinear and rectilinear walking and steps) and a simulation of daily-life activities (SDA, including intermittent gait and short walking bouts). To evaluate its performance on various gait patterns, data were collected on 128 participants from seven cohorts: healthy young and older adults, patients with Parkinson's disease, multiple sclerosis, chronic obstructive pulmonary disease, congestive heart failure, and proximal femur fracture. Moreover, INDIP usability was evaluated by recording 2.5-hours of real-world unsupervised activity. Excellent absolute agreement (ICC > 0.95) and very limited mean absolute errors were observed for all cohorts and DMOs (cadence ≤ 0.61 steps/min, stride length ≤ 0.02 m, walking speed ≤ 0.02 m/s) in the structured tests. Larger, but limited, errors were observed during the SDA (cadence 2.72-4.87 steps/min, stride length 0.04-0.06 m, walking speed 0.03-0.05 m/s). Neither major technical nor usability issues were declared during the 2.5-hours acquisitions. Therefore, the INDIP system can be considered a valid and feasible solution to collect reference data for analyzing gait in real-world conditions.

6.3 Validation of stride-level DMOs and gait events timings

An approach analogous to what described in [210] was adopted to perform a stride-level validation of INDIP system performances against the stereophotogrammetric system. In this context, the following DMOs were considered:

- Stride duration
- Swing duration
- Stance duration
- Stride length
- Swing length
- Stance length
- Stride speed

In addition, also IC and FC timings were included, since their validation follows an approach similar to that used for stride level DMOs. This section describes the procedure followed for stride-level DMOs and gait events validation, including the metrics description, the presentation of the results and their discussion. Further details about the experimental setup, protocol, participants and the algorithm pipeline can be found in [210].

Statistical analysis

The INDIP outputs obtained from the laboratory acquisitions were compared with those obtained from the SP system. Also in this case, the analysis was conducted separately for the structured tests and the simulated daily activities (SDA) test. While for the structured tests a 1:1 correspondence between WB and trial is expected, for simulated daily activities test a single trial can correspond to more WBs, as this type of test also includes pauses and other activities different from gait [212]. The here-presented analysis takes into account only the WBs detected by both the systems (*matching WBs*). For each *matching WB*, the IC and FC identified by both the systems were selected by applying a tolerance window of ±

0.25 s around the INDIP event and by selecting the closest SP event within that interval. A similar approach was adopted to match the strides but, in this case, a necessary condition to find the correspondence was the matching of the ICs defining the start and stop timings of the considered stride.

The analysis was performed by aggregating the DMOs values, computed for each stride (or for each gait event, in case of IC and FC timings) of the considered WB, at cohort level. For sake of brevity, the aggregation procedure will be explained only for stride level DMOs, but it is performed in the same way for gait events. For example, considering a cohort composed by N subjects, the *i-th* subject performs several trials corresponding to a number of WB equal to m_i and for the *j-th* WB the number of strides is equal to s_j. The total number of stride-level DMOs for the cohort of interest is then:

$$S = \sum_{i=1}^{N} \sum_{j=1}^{m_i} s_j$$

For each DMO, mean and standard deviation (STD) values were computed for both INDIP and SP measures over the S observations, equal to the total number of strides obtained for a given population ($\overline{DMO}_{SP}$, $\overline{DMO}_{INDIP}$, STD(DMO_{SP}), STD(DMO_{INDIP}).

Moreover, for each DMO, errors (E_k) and relative errors ($E\%_k$) for the *k-th* stride were computed as:

$$E_k = DMO_{INDIP,k} - DMO_{SP,k}$$

$$E\%_k = \frac{DMO_{INDIP,k} - DMO_{SP,k}}{DMO_{SP,k}}$$

Were $DMO_{SP,k}$ and $DMO_{INDIP,k}$ are the DMO values obtained for the INDIP system and the SP system, respectively, for the *k-th* stride with $k = 1{:}S$.

Median value, median absolute value and interquartile range value of the errors were computed over the S observations obtained for the relevant cohort to describe performance in terms of bias, accuracy and precision. Mean value and mean absolute value were also computed to allow the comparison with previous studies.

Results

For the stride-level analysis, 119/128 participants were taken into account, applying the same exclusion criteria explained in the INDIP validation paper [210]. As in the WB analysis, also in this case it was necessary to check the trials having gaps longer than 0.5 s in a foot marker trajectory from the SP data. Those gaps affected 44 subjects in at least one trial, for a total of 129 *trials with gaps* to be checked. In particular, the strategy for gaps check was based on the error distribution obtained from the trials without gaps. The 75th percentile of that distribution was considered as a threshold *T* to discard potential outliers, i.e. DMOs with errors higher than *T*, belonging to the distribution of errors obtained from the trials without gaps. This procedure allowed to minimize the number of strides/gait events discarded, as it considers the single values separately and not at the entire trial. In total, 335 strides, 278 IC, 201 FC were discarded from structured tests; while 211 strides, 277 IC, 182 FC were discarded from the SDA test. Overall, 12773 strides, 14989 IC, 12787 FC were analyzed for the structured tests and 3225 strides, 4180 IC, 3114 FC for the SDA test. These values are reported in detail in Table 1.

Table 1: Number of analyzed strides, IC and FC in laboratory (Structured tests and SDA test)

Cohort	Laboratory					
	Structured tests			SDA test		
	Strides (n)	IC (n)	FC (n)	Strides (n)	IC (n)	FC (n)
HYA	2011	2394	2031	670	889	646
HOA	1747	2077	1736	433	582	390
PD	2198	2538	2191	580	741	573
MS	2002	2357	2034	449	542	429
COPD	1804	2079	1808	546	741	545
CHF	1025	1225	979	219	270	210
PFF	1986	2319	2008	328	415	321
Total	12773	14989	12787	3225	4180	3114

The results obtained from the comparison of INDIP and stereophotogrammetric systems are reported in Table 2 for the structured tests and in Table 3 for the SDA test. For each cohort and relevant DMO, descriptive statistics (M and STD) of the relevant stride-level DMOs values obtained from INDIP and stereophotogrammetric system are reported. In addition, the following metrics were reported: mean error, mean absolute error and relative percentage values (ME, MAE, ME%, and MAE%); median error, median absolute error and relative percentage values (MDE, MDAE, MDE%, and MDAE%); interquartile range error and relative percentage value (IQRE and IQRE%).

Structured tests

Considering the results obtained from all cohorts, the structured tests show *MDE%* between -4.25% and 2.08% and *ME%* between -4.40% and 3.71% for all DMOs except for stance length, were small biases (*MDE* -0.01 and *ME* 0.01) lead to high percentage errors (*MDE%* up to -11.14% in MS, *ME%* up to 14.28% in HOA). In case of IC, FC and temporal parameters, both mean and median absolute errors show low values in all cohorts (*MAE* and *MDAE* ≤ 0.04s for IC and FC timings, stride duration, swing duration and stance duration). Also for spatial parameters the errors are limited (*MDAE* ≤ 0.04m for stride length and swing length, ≤ 0.03m for stance length; *MAE* ≤ 0.05m for stride length, swing length and stance length). A similar trend can be noticed for walking speed, with slightly larger, but still limited *MAE* (≤ 0.05 m/s) compared to *MDAE* (≤ 0.04 m/s) for all cohorts. Percentage errors are enough content for all DMOs (*MDAE%* ≤ 1.23% for stride duration, lower or around 4% for stance duration, stride length and walking speed, ≤ 4.43% for swing length) except for swing duration (up to 7.32% in PFF) and stance length (up to 24.60% in MS).

SDA test

Also the SDA test shows good results across the different cohorts. The *MDE%* is between -5.26% and 2.51%, while the *ME%* -1.09% and 5.68%. Only for stance length we reach higher percentage values with biases between -0.01 m and 0.01 m for both *MDE* and *ME* (*MDE%* up to -8.43% in PFF, *ME%* up to 34.35% in HOA). The median absolute error shows low values in all cohorts for the temporal DMOs and IC/FC timings (*MDAE* ≤ 0.03s for IC and FC, ≤ 0.02s for stride duration, ≤ 0.04s for swing duration and stance duration; *MAE* ≤ 0.03s for IC and stride duration). Slightly larger errors were observed in case of *MAE* for stance duration and swing duration (≤ 0.08s) as also for FC timings (≤ 0.06s). Also errors

in spatial parameters and walking speed are limited for the SDA test (*MDAE* ≤ 0.04m for swing length and stance length; ≤ 0.05m for stride length; ≤ 0.03 m/s for walking speed). As for the temporal parameters, also in this case *MAE* are slightly higher (≤ 0.07m for stride length, ≤ 0.05m for swing length, ≤ 0.05m/s for walking speed, ≤ 0.04m for stance length). Percentage errors are ≤ 6% for almost all DMOs and cohorts, except for swing duration (up to 10.00% for PFF) and stance length (up to 30.68% for HOA) which show higher values.

Table 2: Comparison between INDIP and SP system for IC, FC and relevant stride-level DMOs (structured tests)

DMO	Cohort	Mean±STD (INDIP)	Mean±STD (SP)	ME (ME%)	MDE (MDE%)	MAE (MAE%)	MDAE (MDAE%)	IQRE (IQRE%)
IC (s)	YHA	-	-	0.00 (0.02%)	0.00 (0.00%)	0.02 (0.39%)	0.02 (0.20%)	0.04 (0.41%)
	HOA	-	-	-0.01 (-0.14%)	-0.01 (-0.14%)	0.03 (0.33%)	0.02 (0.20%)	0.03 (0.34%)
	PD	-	-	-0.01 (-0.11%)	-0.01 (-0.11%)	0.03 (0.31%)	0.02 (0.20%)	0.04 (0.33%)
	MS	-	-	0.00 (0.04%)	-0.01 (-0.05%)	0.03 (0.39%)	0.02 (0.20%)	0.03 (0.40%)
	COPD	-	-	-0.01 (-0.09%)	-0.01 (-0.10%)	0.02 (0.27%)	0.02 (0.17%)	0.03 (0.27%)
	CHF	-	-	-0.01 (-0.05%)	-0.01 (0.10%)	0.03 (0.37%)	0.02 (0.23%)	0.04 (0.41%)
	PFF	-	-	-0.02 (-0.17%)	-0.02 (-0.16%)	0.03 (0.37%)	0.03 (0.23%)	0.04 (0.40%)
FC (s)	YHA	-	-	0.00 (0.05%)	0.01 (0.04%)	0.02 (0.30%)	0.02 (0.18%)	0.03 (0.37%)
	HOA	-	-	0.00 (0.02%)	0.00 (0.00%)	0.03 (0.31%)	0.02 (0.18%)	0.04 (0.36%)
	PD	-	-	-0.01 (-0.08%)	-0.01 (-0.08%)	0.03 (0.31%)	0.02 (0.19%)	0.04 (0.37%)
	MS	-	-	-0.00 (-0.06%)	0.00 (0.00%)	0.03 (0.32%)	0.02 (0.16%)	0.03 (0.33%)
	COPD	-	-	-0.01 (-0.13%)	-0.01 (-0.11%)	0.02 (0.23%)	0.02 (0.16%)	0.03 (0.26%)
	CHF	-	-	-0.00 (-0.05%)	0.00 (0.00%)	0.03 (0.38%)	0.02 (0.18%)	0.03 (0.36%)
	PFF	-	-	-0.02 (-0.18%)	-0.01 (-0.12%)	0.04 (0.42%)	0.02 (0.20%)	0.04 (0.36%)
Stride duration (s)	YHA	1.20±0.19	1.20±0.18	-0.00 (-0.27%)	0.00 (0.00%)	0.02 (1.96%)	0.01 (0.93%)	0.02 (2.05%)
	HOA	1.18±0.19	1.18±0.19	-0.00 (-0.09%)	0.00 (0.00%)	0.02 (1.90%)	0.01 (0.98%)	0.02 (1.98%)
	PD	1.31±0.24	1.31±0.24	-0.00 (-0.07%)	0.00 (0.00%)	0.02 (1.60%)	0.01 (0.91%)	0.02 (1.85%)
	MS	1.33±0.29	1.33±0.28	-0.00 (-0.16%)	0.00 (0.00%)	0.03 (1.91%)	0.02 (1.03%)	0.03 (2.22%)
	COPD	1.22±0.18	1.22±0.18	0.00 (-0.04%)	0.00 (0.00%)	0.02 (1.52%)	0.01 (0.93%)	0.02 (1.85%)
	CHF	1.31±0.26	1.31±0.25	0.00 (-0.06%)	0.00 (0.00%)	0.02 (1.81%)	0.02 (1.23%)	0.03 (2.37%)
	PFF	1.30±0.28	1.30±0.28	0.00 (-0.07%)	0.00 (0.00%)	0.02 (1.61%)	0.01 (0.97%)	0.02 (1.98%)
Swing duration (s)	YHA	0.41±0.08	0.41±0.05	0.00 (-1.00%)	-0.01 (-2.08%)	0.03 (7.35%)	0.02 (5.00%)	0.04 (9.29%)
	HOA	0.39±0.08	0.40±0.06	-0.02 (-4.33%)	-0.02 (-4.25%)	0.03 (8.69%)	0.02 (5.71%)	0.04 (10.00%)
	PD	0.43±0.09	0.43±0.08	-0.00 (-0.11%)	0.00 (-0.00%)	0.03 (9.01%)	0.03 (6.25%)	0.05 (12.08%)
	MS	0.43±0.10	0.43±0.07	0.00 (0.91%)	0.00 (0.00%)	0.04 (9.46%)	0.03 (6.67%)	0.06 (13.33%)
	COPD	0.41±0.08	0.41±0.06	0.00 (0.38%)	0.00 (0.00%)	0.03 (6.16%)	0.02 (4.76%)	0.04 (9.32%)
	CHF	0.43±0.10	0.43±0.08	0.00 (-1.32%)	-0.01 (-2.22%)	0.03 (8.43%)	0.02 (5.55%)	0.05 (10.99%)
	PFF	0.41±0.10	0.41±0.07	0.00 (-0.58%)	-0.01 (-1.92%)	0.04 (10.07%)	0.03 (7.32%)	0.06 (14.45%)
Stance duration (s)	YHA	0.79±0.14	0.79±0.14	0.00 (0.18%)	0.00 (0.00%)	0.03 (4.18%)	0.02 (2.67%)	0.04 (5.34%)
	HOA	0.79±0.15	0.77±0.14	0.02 (2.32%)	0.01 (1.59%)	0.03 (4.74%)	0.02 (2.94%)	0.04 (5.13%)
	PD	0.88±0.19	0.88±0.20	0.00 (0.63%)	0.00 (0.00%)	0.04 (4.13%)	0.03 (2.98%)	0.05 (6.16%)
	MS	0.90±0.24	0.91±0.24	-0.01 (-0.56%)	0.00 (0.00%)	0.04 (4.94%)	0.03 (3.23%)	0.06 (6.46%)
	COPD	0.81±0.13	0.81±0.13	0.00 (-0.17%)	0.00 (0.00%)	0.03 (3.20%)	0.02 (2.38%)	0.04 (4.68%)
	CHF	0.88±0.21	0.88±0.21	0.00 (0.70%)	0.01 (1.11%)	0.03 (4.28%)	0.02 (2.90%)	0.05 (5.60%)
	PFF	0.90±0.24	0.89±0.24	0.00 (0.42%)	0.00 (0.00%)	0.04 (4.70%)	0.03 (3.45%)	0.06 (6.97%)
Stride length (m)	YHA	1.29±0.22	1.27±0.21	0.01 (1.05%)	0.01 (1.06%)	0.05 (4.57%)	0.04 (3.27%)	0.08 (6.58%)
	HOA	1.10±0.24	1.09±0.22	0.00 (0.24%)	0.01 (0.82%)	0.05 (5.32%)	0.04 (3.85%)	0.08 (7.60%)
	PD	0.98±0.30	0.97±0.29	0.01 (0.27%)	0.01 (0.76%)	0.05 (6.01%)	0.04 (4.14%)	0.08 (8.07%)
	MS	1.01±0.26	1.00±0.25	0.01 (0.63%)	0.01 (0.83%)	0.05 (5.74%)	0.04 (3.86%)	0.08 (7.64%)
	COPD	1.11±0.22	1.11±0.21	0.01 (0.55%)	0.01 (0.98%)	0.05 (4.43%)	0.04 (3.39%)	0.07 (6.49%)
	CHF	1.05±0.30	1.05±0.28	0.00 (-0.41%)	0.00 (-0.27%)	0.05 (5.04%)	0.04 (3.60%)	0.07 (7.27%)
	PFF	0.79±0.29	0.79±0.28	0.00 (-0.42%)	0.00 (0.21%)	0.04 (5.11%)	0.03 (3.74%)	0.06 (7.47%)
Swing length (m)	YHA	1.20±0.20	1.19±0.19	0.01 (0.76%)	0.01 (1.39%)	0.05 (4.74%)	0.04 (3.69%)	0.07 (6.80%)
	HOA	0.93±0.22	0.95±0.20	-0.01 (-1.24%)	0.00 (-0.37%)	0.05 (5.74%)	0.04 (4.15%)	0.08 (8.40%)
	PD	0.85±0.27	0.84±0.26	0.01 (3.71%)	0.02 (1.97%)	0.05 (8.09%)	0.04 (4.43%)	0.07 (8.01%)
	MS	0.88±0.24	0.87±0.23	0.02 (1.82%)	0.02 (2.08%)	0.05 (5.50%)	0.03 (4.27%)	0.07 (7.90%)
	COPD	0.95±0.19	0.94±0.18	0.01 (1.08%)	0.01 (1.50%)	0.04 (4.42%)	0.03 (3.43%)	0.06 (6.22%)
	CHF	0.89±0.26	0.89±0.24	0.00 (0.00%)	0.00 (0.28%)	0.04 (5.09%)	0.03 (3.80%)	0.06 (7.39%)
	PFF	0.68±0.25	0.67±0.25	0.00 (0.79%)	0.01 (1.61%)	0.04 (5.76%)	0.03 (4.30%)	0.05 (7.72%)
Stance length (m)	YHA	0.19±0.07	0.20±0.04	-0.01 (-1.77%)	-0.01 (-5.23)	0.05 (24.95%)	0.03 (18.10%)	0.06 (34.84%)
	HOA	0.16±0.07	0.15±0.05	0.01 (14.28%)	0.00 (3.20%)	0.05 (34.28%)	0.03 (22.25%)	0.06 (46.14%)
	PD	0.13±0.07	0.13±0.04	-0.01 (-4.40%)	-0.01 (-10.23%)	0.04 (30.61%)	0.03 (23.98%)	0.06 (44.33%)
	MS	0.12±0.06	0.14±0.05	-0.01 (-3.42%)	-0.01 (-11.14%)	0.04 (32.71%)	0.03 (24.60%)	0.06 (44.08%)
	COPD	0.16±0.05	0.17±0.04	-0.01 (-2.33)	-0.01 (-4.01%)	0.03 (21.76%)	0.03 (16.73%)	0.05 (32.35%)
	CHF	0.15±0.07	0.16±0.05	0.00 (0.43%)	-0.01 (-7.98%)	0.04 (30.36%)	0.03 (20.93%)	0.06 (37.65%)
	PFF	0.11±0.07	0.12±0.04	0.00 (-0.99%)	0.00 (-4.29%)	0.04 (31.85%)	0.02 (22.61%)	0.05 (44.08%)
Stride speed (m/s)	YHA	1.10±0.28	1.09±0.27	0.01 (1.42%)	0.01 (1.22%)	0.05 (4.73%)	0.03 (3.35%)	0.07 (6.57%)
	HOA	0.95±0.27	0.95±0.25	0.01 (0.46%)	0.01 (0.99%)	0.05 (5.39%)	0.04 (3.90%)	0.07 (7.67%)
	PD	0.78±0.30	0.77±0.29	0.01 (0.40%)	0.01 (0.93%)	0.04 (6.14%)	0.03 (4.15%)	0.06 (8.02%)
	MS	0.80±0.29	0.79±0.28	0.01 (0.86%)	0.01 (1.13%)	0.04 (5.96%)	0.03 (4.05%)	0.06 (7.86%)
	COPD	0.93±0.25	0.93±0.24	0.01 (0.64%)	0.01 (1.12%)	0.04 (4.62%)	0.03 (3.48%)	0.06 (6.60%)
	CHF	0.85±0.34	0.84±0.32	0.00 (-0.31%)	0.00 (-0.06)	0.04 (5.17%)	0.03 (3.93%)	0.06 (7.85%)
	PFF	0.64±0.29	0.64±0.28	0.00 (-0.24%)	0.00 (0.49%)	0.03 (5.16%)	0.02 (3.70%)	0.04 (7.39%)

Table 3: Comparison between INDIP and SP system for IC, FC and relevant stride-level DMOs (SDA test)

DMO	Cohort	Mean±STD (INDIP)	Mean±STD (SP)	ME (ME%)	MDE (MDE%)	MAE (MAE%)	MDAE (MDAE%)	IQRE (IQRE%)
IC (s)	YHA	-	-	-0.01 (-0.02%)	-0.01 (-0.01%)	0.03 (0.08%)	0.03 (0.02%)	0.05 (0.03%)
	HOA	-	-	-0.01 (-0.02%)	-0.02 (-0.01%)	0.03 (0.07%)	0.03 (0.02%)	0.04 (0.03)
	PD	-	-	-0.01 (-0.03%)	-0.02 (-0.02%)	0.03 (0.06%)	0.03 (0.02%)	0.04 (0.04%)
	MS	-	-	-0.01 (-0.04%)	-0.01 (-0.01%)	0.03 (0.10%)	0.02 (0.02%)	0.04 (0.05%)
	COPD	-	-	-0.01 (-0.01%)	-0.01 (-0.01%)	0.03 (0.07%)	0.03 (0.02%)	0.04 (0.03%)
	CHF	-	-	-0.01 (-0.03%)	-0.01 (-0.01%)	0.02 (0.08%)	0.02 (0.02%)	0.04 (0.05%)
	PFF	-	-	-0.02 (-0.06%)	-0.03 (-0.02%)	0.03 (0.13%)	0.03 (0.03%)	0.04 (0.06%)
FC (s)	YHA	-	-	0.01 (0.01%)	0.01 (0.01%)	0.03 (0.07%)	0.02 (0.02%)	0.04 (0.03%)
	HOA	-	-	0.00 (0.01%)	0.00 (0.00%)	0.04 (0.09%)	0.02 (0.02%)	0.05 (0.04%)
	PD	-	-	-0.01 (-0.02%)	-0.01 (-0.01%)	0.05 (0.10%)	0.03 (0.03%)	0.06 (0.06%)
	MS	-	-	0.00 (0.01%)	0.00 (0.00%)	0.05 (0.11%)	0.02 (0.025)	0.03 (0.04%)
	COPD	-	-	-0.01 (-0.02%)	-0.01 (-0.01%)	0.05 (0.08%)	0.02 (0.01%)	0.04 (0.03%)
	CHF	-	-	-0.01 (-0.05%)	-0.01 (-0.01%)	0.06 (0.16%)	0.03 (0.03%)	0.06 (0.07%)
	PFF	-	-	-0.02 (-0.04%)	-0.02 (-0.01%)	0.05 (0.19%)	0.03 (0.03%)	0.07 (0.06%)
Stride duration (s)	YHA	1.52±0.45	1.52±0.45	0.00 (-0.32%)	0.00 (0.00%)	0.03 (2.44%)	0.02 (1.54%)	0.04 (2.99%)
	HOA	1.36±0.43	1.37±0.43	0.00 (-0.43%)	0.00 (0.00%)	0.03 (2.58%)	0.02 (1.67%)	0.05 (3.13%)
	PD	1.48±0.43	1.49±0.43	0.00 (-0.25%)	0.00 (0.00%)	0.03 (2.36%)	0.02 (1.58%)	0.05 (3.06%)
	MS	1.39±0.37	1.40±0.38	0.00 (-0.29%)	0.00 (0.00%)	0.03 (2.20%)	0.02 (1.48%)	0.04 (2.93%)
	COPD	1.46±0.45	1.47±0.44	0.00 (-0.14%)	0.00 (0.00%)	0.03 (2.42%)	0.02 (1.45%)	0.04 (2.71%)
	CHF	1.49±0.45	1.47±0.43	0.00 (0.10%)	0.00 (0.00%)	0.02 (1.80%)	0.02 (1.28%)	0.04 (2.30%)
	PFF	1.36±0.39	1.37±0.40	-0.01 (-0.53%)	0.00 (0.00%)	0.03 (2.23%)	0.02 (0.96%)	0.03 (2.25%)
Swing duration (s)	YHA	0.47±0.23	0.46±0.13	0.01 (3.38%)	-0.02 (-4.86%)	0.08 (19.38%)	0.04 (7.95%)	0.06 (13.07%)
	HOA	0.41±0.19	0.40±0.12	0.00 (3.56%)	-0.02 (-5.26%)	0.07 (21.37%)	0.04 (8.89%)	0.05 (13.66%)
	PD	0.45±0.23	0.43±0.11	0.01 (2.24%)	-0.01 (-3.03%)	0.07 (16.43%)	0.04 (8.89%)	0.06 (15.02%)
	MS	0.40±0.15	0.41±0.09	0.00 (1.96%)	-0.02 (-5.00%)	0.06 (18.78%)	0.04 (9.52%)	0.06 (14.88%)
	COPD	0.44±0.19	0.42±0.12	0.02 (5.13%)	0.01 (-2.22%)	0.06 (14.72%)	0.03 (6.67%)	0.05 (12.24%)
	CHF	0.45±0.20	0.43±0.13	0.02 (5.68%)	-0.01 (-2.13%)	0.06 (15.50%)	0.03 (7.14%)	0.06 (13.93%)
	PFF	0.40±0.16	0.38±0.10	0.00 (0.84%)	-0.01 (-2.13%)	0.05 (14.03%)	0.04 (10.00%)	0.07 (19.71%)
Stance duration (s)	YHA	1.05±0.38	1.06±0.41	-0.01 (1.67%)	0.02 (1.47%)	0.08 (8.08%)	0.04 (3.86%)	0.07 (7.17%)
	HOA	0.96±0.37	0.95±0.38	0.00 (1.28%)	0.02 (2.51%)	0.07 (7.19%)	0.04 (4.17%)	0.06 (7.08%)
	PD	1.03±0.37	1.05±0.38	-0.02 (-0.14%)	0.01 (1.24%)	0.07 (6.07%)	0.03 (3.66%)	0.07 (6.82%)
	MS	0.99±0.35	0.99±0.37	0.00 (1.40%)	0.02 (2.30%)	0.07 (6.83%)	0.04 (4.17%)	0.07 (7.04%)
	COPD	1.03±0.40	1.05±0.43	-0.02 (-0.30%)	0.00 (0.00%)	0.06 (5.53%)	0.03 (3.17%)	0.05 (5.97%)
	CHF	1.04±0.41	1.04±0.40	-0.02 (-0.45%)	0.00 (0.00%)	0.06 (4.84%)	0.03 (3.19%)	0.06 (6.15%)
	PFF	0.96±0.35	0.96±0.33	-0.01 (-0.60%)	0.00 (0.00%)	0.06 (5.64%)	0.04 (4.69%)	0.08 (9.22%)
Stride length (m)	YHA	0.96±0.33	0.94±0.34	0.01 (3.01%)	0.01 (1.12%)	0.06 (8.68%)	0.05 (4.84%)	0.09 (9.47%)
	HOA	0.81±0.34	0.79±0.34	0.01 (3.06%)	0.01 (0.61%)	0.06 (11.14%)	0.04 (5.75%)	0.09 (11.85%)
	PD	0.77±0.32	0.74±0.32	0.02 (4.75%)	0.01 (1.43%)	0.07 (12.08%)	0.04 (6.05%)	0.09 (12.94%)
	MS	0.83±0.30	0.80±0.30	0.02 (3.90%)	0.02 (1.90%)	0.05 (9.12%)	0.04 (4.31%)	0.07 (8.53%)
	COPD	0.84±0.34	0.82±0.34	0.02 (4.50%)	0.01 (1.59%)	0.05 (9.65%)	0.04 (4.62%)	0.07 (8.70%)
	CHF	0.88±0.28	0.86±0.30	0.01 (1.98%)	0.00 (0.09%)	0.05 (7.99%)	0.03 (4.25%)	0.07 (9.06%)
	PFF	0.61±0.26	0.60±0.25	-0.01 (-1.09%)	-0.01 (-1.07%)	0.04 (8.61%)	0.03 (4.50%)	0.06 (10.21%)
Swing length (m)	YHA	0.83±0.30	0.84±0.29	0.00 (0.44%)	0.00 (0.09%)	0.04 (7.85%)	0.03 (4.20%)	0.07 (8.41%)
	HOA	0.69±0.30	0.72±0.30	-0.01 (1.74%)	-0.01 (-1.56%)	0.05 (12.65%)	0.04 (5.81%)	0.07 (11.67%)
	PD	0.67±0.29	0.67±0.28	0.00 (1.05%)	0.00 (0.40%)	0.04 (8.41%)	0.03 (5.31%)	0.07 (10.50%)
	MS	0.71±0.27	0.71±0.26	0.00 (3.46%)	0.00 (-0.33%)	0.04 (11.72%)	0.03 (4.86%)	0.06 (9.73%)
	COPD	0.72±0.30	0.72±0.29	0.00 (0.31%)	0.00 (0.68%)	0.04 (6.13%)	0.03 (4.37%)	0.06 (8.52%)
	CHF	0.76±0.25	0.78±0.24	0.00 (1.25%)	0.01 (1.17%)	0.04 (5.98%)	0.03 (4.66%)	0.06 (8.22%)
	PFF	0.53±0.24	0.52±0.22	0.00 (-0.66%)	0.00 (0.60%)	0.03 (6.84%)	0.02 (5.26%)	0.05 (10.52%)
Stance length (m)	YHA	0.13±0.07	0.13±0.06	0.00 (22.23%)	0.00 (-0.02%)	0.04 (53.83%)	0.03 (23.32%)	0.06 (46.69%)
	HOA	0.12±0.07	0.11±0.07	0.01 (34.35%)	0.00 (5.91%)	0.04 (63.93%)	0.03 (30.68%)	0.06 (65.77%)
	PD	0.10±0.07	0.10±0.05	0.00 (27.93%)	0.00 (-3.89%)	0.04 (66.04%)	0.03 (29.14%)	0.05 (57.82%)
	MS	0.11±0.06	0.11±0.05	0.01 (25.29%)	0.01 (5.99%)	0.04 (52.90%)	0.04 (27.59%)	0.06 (56.07%)
	COPD	0.12±0.06	0.12±0.05	0.00 (13.71%)	0.00 (2.75%)	0.03 (44.00%)	0.02 (21.94%)	0.05 (43.67%)
	CHF	0.12±0.06	0.12±0.04	-0.01 (-5.86%)	-0.01 (-7.68%)	0.03 (32.22%)	0.03 (23.14%)	0.06 (46.71%)
	PFF	0.08±0.05	0.09±0.04	-0.01 (5.98%)	-0.01 (-8.43%)	0.03 (52.14%)	0.03 (28.26%)	0.05 (61.99%)
Stride speed (m/s)	YHA	0.69±0.31	0.68±0.31	0.01 (3.33%)	0.01 (1.77%)	0.04 (8.71%)	0.03 (5.02%)	0.06 (928%)
	HOA	0.64±0.30	0.63±0.30	0.01 (3.55%)	0.01 (0.97%)	0.05 (11.23%)	0.03 (6.33%)	0.07 (11.31%)
	PD	0.56±0.28	0.54±0.28	0.01 (5.07%)	0.01 (1.82%)	0.04 (12.12%)	0.03 (5.72%)	0.06 (12.73%)
	MS	0.63±0.26	0.61±0.27	0.01 (4.34%)	0.01 (2.07%)	0.04 (9.73%)	0.03 (4.66%)	0.05 (8.80%)
	COPD	0.63±0.31	0.62±0.31	0.01 (4.82%)	0.01 (2.00%)	0.04 (10.20%)	0.03 (4.76%)	0.05 (9.30%)
	CHF	0.64±0.25	0.63±0.26	0.00 (1.96%)	0.00 (0.17%)	0.04 (8.18%)	0.02 (4.31%)	0.05 (8.99%)
	PFF	0.47±0.21	0.47±0.21	0.00 (-0.39%)	0.00 (-0.62%)	0.03 (8.79%)	0.02 (4.63%)	0.05 (9.90%)

Discussion

Results obtained on stride-level parameters confirm the reliability of the INDIP system in assessing gait, as already established in [210]. As expected, stride-by-stride errors are slightly larger with respect to those computed at WB level, as also with respect to previous studies [42], [43] from which INDIP algorithms were derived and optimized. For example, *MAE* for average stride length was 0.03m for structured tests and 0.05m for SDA test; while in this case we have a *MAE* on stride length of 0.05m for structured tests and 0.07m for SDA test due to the different type of aggregation. Despite this, results are very encouraging, also considering the higher complexity level reached in the experimental protocol and the good performance on all cohorts. This can be easily noticed comparing the INDIP results with those obtained in previous studies.

The work from Storms and colleagues [48] reported an average absolute error of 0.04 s on stance duration obtained from two shank mounted IMU using data collected on ten healthy participants while performing straight and curvilinear walking. The INDIP system showed a *MAE* of 0.03s in healthy cohorts (YHA and HOA), as also in COPD and CHF, and 0.04s in the remaining cohorts (PD, MS, PFF) for stance duration computed from structured tests. On the other side, the work from Roth et al. [49] showed a low *MAE* for stance duration (0.02s level walking, 0.03s ascending stairs, 0.02s descending stairs) during supervised real-world conditions on healthy participants. This result is comparable to what obtained for the INDIP system during structured tests (0.03s in YHA and HOA).

Li and colleagues [175] presented the results obtained on healthy participants in terms of stride length and stride speed on straight walk (MAE% 9.34% and 5.90%, respectively). Looking at the structured tests, the INDIP showed better performance (MAE% 4.57% for stride length, 4.73% for stride speed in YHA). Lower errors were reported by Duong et al. [71] (MAE% structured session: 2.97% for stride length and 3.16% for stride velocity; MAE% unstructured session: 3.55% for stride length and 3.59% for stride velocity) but performance was validated only on selected gait portions (i.e., when the subject was walking on the instrumented walkway) and not on the entire task.

In general, the INDIP method shows promising results for what concerns the stride-level analysis, bearing in mind the complexity of the designed protocol [212] [213], both in terms of tasks and participants included.

Chapter 7

Quantification of gait changes after physical rehabilitation in people with multiple sclerosis during Activities of Daily Living

This chapter regards the use of INDIP system to extract gait-related variables and quantify gait changes in patients with MS during ADL, performed before and after physical rehabilitation. First, the experimental setup and protocol are described, together with the population participating in the study. Then, results obtained from the explorative analysis on INDIP system outcomes are presented and commented.

7.1 Materials and methods

Experimental setup

Each participant was equipped with the INDIP system in its gold standard configuration (described in Section 4.2). In addition, three INDIP magneto-IMUs were positioned on head, left wrist and right wrist, respectively. Only the sensors belonging to the gold standard configuration were used for the purposes of the present study; however, the additional INDIP magneto-IMUs were used in other works.

Experimental protocol

Experiments were conducted at the Department of Biomedical Sciences of the University of Sassari (Italy) as part of a project financed by the FISM (Federazione Italiana Sclerosi Multipla) society. The protocol included a supervised ADL acquisition comprising the following tasks:

- Wash the floor: typical housework simulation.
    i. Starting from the sitting position, stand up and take the bucket filled with water and put the detergent inside;
    ii. Dip the floor rag into the bucket and put it under the scrubber to wash the floor;
    iii. Dip again the floor rag into the bucket to clean it;
    iv. Wring out the floor rag and put it under the scrubber to dry the floor;
    v. Put the floor rag into the bucket and go to the sitting position.
- Transfer light: move from one room to another on the same floor.
    i. Starting from the sitting position, stand up and walk from room A to room B along a 20m distance;
    ii. Go back from room B to room A and return in sitting position.
- Do the laundry: laundry progress simulation.
    i. Starting from the sitting position, stand up and select garments from the washing basket;
    ii. Put the garments inside the washing machine;
    iii. Remove the garments from the washing machine at the end of the wash cycle;
    iv. Spread the garments on the clothes horse to let them dry;
    v. Go to the sitting position.
- Meal management: from table setting to meal consumption.
    i. Starting from the sitting position, stand up and set the table with the necessary crockeries (1 plate, 1 knife, 1 fork, 1 spoon, 1 glass);
    ii. Serve the sandwich on a plate on the table; take the bottle and fill the glass with water;
    iii. Sit down and eat;
    iv. Stand up, remove all the items and clear the table;
    v. Go back to sitting position.

- Clean surfaces: housework simulation.
    i. Starting from the sitting position, stand up and take the rag and the detergent;
    ii. Spray the detergent on the surface of the table and clean it, moving around the table;
    iii. Spray the detergent on the other surface of the kitchen floor and clean it, moving all the stuff upon the floor;
    iv. Go back to sitting position.
- Climb stairs: move from one place to another doing stairs.
    i. Starting from the sitting position, stand up and go to the stairs;
    ii. Walk up the stairs (two floors) at self-selected speed;
    iii. Turn on the landing and go back downstairs at self-selected speed;
    iv. Return to sitting position.

Each participant was asked to execute the ADL in two sessions: the first one performed before the physical rehabilitation treatment and the second one performed after the treatment.

Participants

The experiments involved 20 patients affected by MS (inclusion criteria: EDSS ≤ 6.5, no cognitive impairments) and are still in progress. All participants provided written informed consent before taking part to the study. A subset of 9 participants was included in the present study (1 male/8 females, 48.89±11.36 years old, EDSS 3.33±1.90).

7.2 Data processing and analysis

Data collected on the MS participants were manually segmented in the different ADL activities thanks to the annotations provided by the operators regarding the start and end of each activity. Then, each activity interval was processed with the INDIP system pipeline [210] to extract gait related variables (see Chapter 6 for more details). In particular, the following DMOs were computed for each subject and every ADL activity:

- Stride duration
- Stance duration
- Swing duration

- Stride length
- Stance length
- Swing length
- Stride speed

In addition, two secondary outcomes were computed for each of the above-listed DMOs, i.e. gait variability and gait symmetry. Mean and standard deviation values were computed, for each primary DMO and activity, at group level, aggregating the values obtained from all the subjects. Also the secondary outcomes were reported in terms of mean and standard deviation obtained from the aggregation of the same DMO (e.g. gait variability or gait symmetry) across subjects.

Statistical analysis was performed for each DMO and activity: after verifying the normality of each distribution using Shapiro-Wilk test, either paired t-test or Wilcoxon signed rank test was performed to assess the presence of statistically meaningful differences between the two sessions, before and after the treatment.

7.3 Results

Table 4 reports the mean and standard deviation for the primary and secondary DMOs in each ADL activity for both experimental sessions. Table 5 shows the results of the statistical analysis in terms of p-values obtained from the comparison of the two sessions for each DMO and activity.

7.4 Discussion

As reported in Table 5, no meaningful statistical differences were observed in gait symmetry for all the DMOs and activity; whereas a significant difference was observed in stride speed gait variability for transfer light task. Concerning the primary DMOs, meaningful differences from the statistical point of view were observed in stride duration for the laundry task, stride length and swing length (laundry and clean surface tasks) and stride speed (wash floor, laundry and clean surface tasks). Looking at the values of those DMOs (Table 4), in the cases reporting a statistical difference, it is possible to notice a decrease in stride duration (change of -0.09s on average) and an increase in stride length (change of 0.10-0.17m on average), swing length (change 0.10-0.16m on average) and stride

(change of 0.07-0.17 m/s on average) from the first ADL session (before treatment) to the second ADL session (after treatment). The here obtained results are in line with those presented in previous studies, in which the effectiveness of a physical treatment was evaluated looking at the variation of gait parameters during standard straight walking trials [31]–[33]. This suggests the suitability of the proposed system for detecting changes in DMOs related to gait. However, the statistical significance of the differences is not sufficient, alone, to consider the changes as clinically meaningful for patients, as it is necessary to look also at the magnitude of changes [31]. For example, Learmonth and colleagues [214] reported that a change of 20% in stride speed in the six-minute walk test can be clinically meaningful. In this study, percentage changes > 20% were obtained for the cases reporting a statistical difference (changes in stride speed 21-50% on average for Laundry, Clean Surface and Wash Floor). Conversely, no values for clinically meaningful change are reported in literature for the other DMOs (i.e., stride length, stride duration and swing length). The stride speed gait variability in the transfer light task shows values which are higher for the session after the treatment with respect to the first session. Some studies suggest a directly proportional relation between the gait variability and the severity of the impairment [190], [215], meaning that an effective medical treatment should lead to a decrease of the gait variability. However, other studies highlighted the difficulty in interpreting gait variability [37], which can assume both low and high values in elderly or diseased people depending on factors such as age, gender and walking speed. Therefore, those results should be further explored through the comparison with a control group to provide reference values for the extracted DMOs, which is currently missing.

An important limit of the present study is the low number of participants involved: this number should be increased to improve the robustness of the analysis and to test the effective outcomes relevance. It is also relevant to notice that the subjects involved had a relatively low impairment (EDSS 3.33 on average) and the increase in the number of participants would allow to perform an analysis stratification by disease severity.

Table 4: Mean and standard deviation (STD) values obtained for primary DMOs (Value) and secondary DMOs (gait variability and gait symmetry) for each ADL activity performed in the two sessions.

DMOs (Mean ± STD)		ADL tasks											
		Wash Floor		Transfer Light		Laundry		Meal Management		Clean Surface		Climb Stairs	
		Before	After	Before	After	Before	After	Before	After	Before	After	Before	After
Stride duration (s)	Value	1.70±0.49	1.68±0.51	1.60±0.44	1.70±0.48	1.51±0.51	1.42±0.49	1.48±0.49	1.46±0.51	1.66±0.51	1.54±0.50	1.68±0.51	1.62±0.49
	Gait variability	27.24±3.40	29.13±3.54	28.85±5.26	30.12±9.69	29.75±5.03	30.33±5.72	30.07±5.12	32.47±4.62	27.22±4.04	30.08±5.32	26.14±4.56	28.53±4.99
	Gait symmetry	5.40±5.39	6.09±5.85	19.79±17.73	14.77±12.92	5.38±9.01	7.76±8.13	3.41±2.83	5.31±9.57	6.34±9.24	6.67±10.30	7.31±5.70	14.08±10.28
Stance duration (s)	Value	1.24±0.49	1.25±0.49	1.10±0.45	1.23±0.47	1.06±0.47	1.01±0.45	1.04±0.47	1.04±0.47	1.20±0.51	1.09±0.46	1.21±0.53	1.16±0.47
	Gait variability	35.68±8.38	37.67±3.74	36.93±10.86	39.69±10.89	37.53±8.40	39.49±7.88	39.67±8.61	41.68±4.96	35.26±9.01	38.67±5.43	33.77±9.74	38.44±7.36
	Gait symmetry	14.97±25.36	10.07±8.34	27.35±25.40	18.47±13.58	11.77±17.08	13.56±8.56	10.68±17.98	9.66±6.50	15.86±18.18	9.26±6.68	16.35±24.79	19.84±9.38
Swing duration (s)	Value	0.46±0.24	0.44±0.23	0.49±0.26	0.47±0.25	0.46±0.25	0.41±0.20	0.44±0.20	0.42±0.21	0.47±0.24	0.45±0.23	0.47±0.26	0.47±0.26
	Gait variability	42.82±15.23	47.05±13.64	39.78±15.21	44.94±15.89	48.64±18.38	42.99±23.38	40.73±16.88	46.14±13.68	44.60±16.51	48.23±15.68	43.04±19.32	45.27±22.67
	Gait symmetry	15.87±19.65	20.86±13.30	37.86±22.48	24.37±16.03	17.92±19.65	17.15±14.07	12.33±19.15	15.71±10.86	18.46±16.91	18.86±10.10	28.79±26.51	26.51±14.12
Stride length (m)	Value	0.48±0.29	0.52±0.32	0.48±0.29	0.52±0.33	0.70±0.43	0.80±0.47	0.74±0.45	0.79±0.47	0.52±0.35	0.69±0.41	0.47±0.28	0.54±0.34
	Gait variability	56.18±10.96	58.44±10.60	49.55±15.08	57.60±16.40	53.82±12.71	49.16±13.27	52.08±13.16	55.36±10.10	56.22±14.06	56.99±14.80	50.59±14.91	53.42±16.31
	Gait symmetry	9.70±9.67	9.63±10.01	21.54±21.27	14.98±18.85	14.69±19.56	3.37±1.88	14.41±18.61	9.33±15.34	16.91±19.59	11.00±18.30	16.72±20.06	13.46±17.66
Stance length (m)	Value	0.07±0.10	0.07±0.08	0.06±0.07	0.07±0.07	0.11±0.11	0.12±0.10	0.12±0.12	0.12±0.10	0.09±0.12	0.10±0.10	0.08±0.12	0.07±0.07
	Gait variability	105.71±32.99	99.23±33.41	67.56±28.48	80.09±31.66	82.44±22.31	64.93±20.25	87.98±29.75	85.03±21.10	107.88±35.83	98.23±36.77	95.83±33.92	79.18±30.26
	Gait symmetry	34.20±18.16	49.96±23.24	47.48±43.05	33.43±22.57	25.83±20.74	24.69±27.3	25.79±22.56	39.14±26.71	35.95±21.16	45.69±23.21	34.02±17.86	25.19±25.11
Swing length (m)	Value	0.41±0.26	0.45±0.28	0.42±0.27	0.46±0.29	0.59±0.38	0.69±0.40	0.62±0.39	0.68±0.40	0.43±0.31	0.59±0.36	0.40±0.25	0.47±0.30
	Gait variability	57.24±11.60	58.82±10.04	53.28±18.52	59.02±17.67	54.08±16.82	50.37±12.68	53.04±16.39	56.35±10.86	57.05±17.12	57.54±14.13	52.98±16.37	54.12±16.29
	Gait symmetry	12.10±12.72	9.07±8.53	26.22±19.78	18.56±18.49	17.03±29.01	6.28±6.38	18.55±28.79	10.41±17.21	19.54±29.22	13.58±18.78	19.84±21.44	17.91±17.49
Stride speed (m/s)	Value	0.33±0.26	0.37±0.33	0.33±0.24	0.37±0.32	0.55±0.42	0.69±0.50	0.60±0.44	0.67±0.51	0.37±0.33	0.54±0.42	0.32±0.23	0.41±0.35
	Gait variability	74.29±19.41	80.42±18.45	51.36±15.53	78.41±26.42	68.91±17.57	58.55±19.47	63.10±15.85	70.21±15.38	75.00±21.34	76.92±24.82	57.40±21.89	72.04±27.92
	Gait symmetry	9.26±10.62	11.90±16.16	28.68±22.77	19.13±25.71	17.79±21.26	6.66±4.96	14.39±18.90	10.78±20.33	18.47±22.80	15.16±24.33	15.82±15.07	16.34±24.45

Table 5: P-values obtained from the statistical analysis for primary DMOs (Value) and secondary DMOs (gait variability and gait symmetry) for each ADL activity. Significant p-values are indicated in bold.

DMOs (p-value)		ADL tasks					
		Wash Floor	Transfer Light	Laundry	Meal Management	Clean Surface	Climb Stairs
Stride duration (s)	Value	0.931	0.189	**0.011**	0.652	0.111	0.496
	Gait variability	0.267	0.796	1.000	0.310	0.217	0.305
	Gait symmetry	0.652	0.502	0.359	0.820	0.910	0.090
Stance duration (s)	Value	0.690	0.153	0.054	0.910	0.211	0.490
	Gait variability	0.062	0.340	0.618	0.552	0.161	0.161
	Gait symmetry	0.570	0.734	0.359	0.426	0.910	0.129
Swing duration (s)	Value	0.769	0.775	0.129	0.661	0.682	0.792
	Gait variability	0.543	0.491	0.576	0.466	0.640	0.823
	Gait symmetry	0.301	0.223	0.924	0.570	0.910	0.910
Stride length (m)	Value	0.110	0.124	**0.022**	0.098	**0.034**	0.074
	Gait variability	0.663	0.136	0.457	0.561	0.911	0.489
	Gait symmetry	0.734	0.652	0.129	0.301	0.426	0.910
Stance length (m)	Value	0.767	0.173	0.077	0.727	0.334	0.310
	Gait variability	0.546	0.390	0.100	0.811	0.581	0.288
	Gait symmetry	0.096	0.652	0.496	0.317	0.402	0.362
Swing length (m)	Value	0.205	0.219	**0.019**	0.426	**0.033**	0.080
	Gait variability	0.931	0.510	0.604	0.546	0.863	0.884
	Gait symmetry	0.098	0.359	0.496	0.098	0.300	1.000
Stride speed (m/s)	Value	**0.039**	0.145	**0.020**	0.235	**0.030**	0.094
	Gait variability	0.502	**0.017**	0.254	0.348	0.862	0.234
	Gait symmetry	0.652	0.496	0.203	0.734	0.910	0.910

Chapter 8

Conclusion

The present thesis aims at making new advances in the field of gait analysis in real-world conditions. New solutions based on wearable technologies to be used as reference and extract technically valid DMOs for the validation of third-party devices were proposed. In addition, the same solutions were adopted as a mobile gait laboratory to enable a complete assessment of gait during supervised ADL in people with MS and try to evaluate the efficacy of a rehabilitation treatment without the limitations imposed by the most traditional technologies.

For this purpose, three main works were presented. The first one regards the development and validation of a new algorithm for accurate gait events detection based on wearable low-cost pressure insoles data [211]. The proposed method was tested on nine healthy participants against force platforms in a laboratory setting. The low errors obtained in IC and FC detection demonstrated that the combination of low-cost PI and a specifically developed algorithmic pipeline are a valid wearable solution for the estimation of reference gait events and temporal DMOs. In addition, the proposed method represents a good compromise between more complex and expensive solutions (e.g. pressure mapping insoles) and foot-switch systems. Thanks to the cluster-based approach, the algorithm can be easily adapted to different PIs with a sufficient number of sensing elements. This study has some limitations regarding the validation of the proposed method on healthy subjects and straight walk only, that require further investigation to be overcome.

The above-mentioned low-cost PIs were then integrated in a multi-sensor wearable system (INDIP) in combination with three IMUs positioned on feet and

lower back plus two distance sensors to enable a complete gait assessment in real-world conditions. To this end, a specific pipeline based on state-of-the-art algorithms that exploits sensors redundancy was designed to extract relevant DMOs. The INDIP system was validated against the SP system on seven cohorts of participants, including healthy (HYA, HOA) and pathological (PD, MS, CHF, COPD, PFF) subjects, while performing a complex experimental protocol. The same system was employed in 2.5h real-world acquisitions. The second contribution entails the INDIP system validation and reports the good results obtained for WB-level DMOs [210] In addition, results obtained for the stride-level DMOs were reported and discussed in the present thesis. The validation proved that the INDIP system is a reliable wearable solution that can be used as reference and enables an exhaustive gait assessment in ecological settings.

The use of the INDIP system as a mobile gait laboratory was further explored within the third work, where the system was employed to extract useful gait DMOs in people affected by MS. Participants to the experiments were asked to wear the sensors while performing supervised ADL before and after a rehabilitation treatment. For both sessions, temporal and spatial parameters of gait were extracted, together with two secondary parameters to quantify variability and symmetry of the primary DMOs. Differences in the estimates before and after the treatment were assessed through a statistical analysis aiming at identifying statistically meaningful differences. Results showed that some gait parameters, including stride duration, stride length, swing length and stride speed report significant differences which might be linked to the physical rehabilitation treatment. However, this work should be extended to a larger number of participants to confirm these preliminary results and a control group should be involved to have reference data and correctly interpret DMOs variation. Despite those limitations, the INDIP system proved to be a suitable solution for this kind of applications.

In conclusion, the work presented in this thesis demonstrated the enforceability of wearable solutions for the characterization of gait in real-world conditions. The proposed methods were validated against a laboratory reference to assess their accuracy both in healthy and pathological participants according to a structured experimental protocol. In addition, the same methods were exploited in a different application to investigate the clinical utility of the extracted DMOs and try to provide a concrete support to clinicians.

Appendix

A. A method for gait events detection based on low spatial resolution pressure insoles data.

Journal of Biomechanics 127 (2021) 110687

Contents lists available at ScienceDirect

Journal of Biomechanics

journal homepage: www.elsevier.com/locate/jbiomech

Short communication

A method for gait events detection based on low spatial resolution pressure insoles data

F. Salis [a,b,*], S. Bertuletti [a,b], T. Bonci [c], U. Della Croce [a,b], C. Mazzà [c], A. Cereatti [b,d]

[a] Department of Biomedical Sciences, University of Sassari, Sassari, Italy
[b] Interuniversity Centre of Bioengineering of the Human Neuromusculoskeletal System, Sassari, Italy
[c] Insigneo Institute and Department of Mechanical Engineering, University of Sheffield, Sheffield, UK
[d] Department of Electronics and Telecommunications, Politecnico di Torino, Torino, Italy

ARTICLE INFO

Keywords:
Gait analysis
Wearable sensors
Pressure insoles
Locomotion
Gait events

ABSTRACT

The accurate identification of initial and final foot contacts is a crucial prerequisite for obtaining a reliable estimation of spatio-temporal parameters of gait. Well-accepted gold standard techniques in this field are force platforms and instrumented walkways, which provide a direct measure of the foot–ground reaction forces. Nonetheless, these tools are expensive, non-portable and restrict the analysis to laboratory settings. Instrumented insoles with a reduced number of pressure sensing elements might overcome these limitations, but a suitable method for gait events identification has not been adopted yet. The aim of this paper was to present and validate a method aiming at filling such void, as applied to a system including two insoles with 16 pressure sensing elements (element area = 310 mm^2), sampling at 100 Hz. Gait events were identified exploiting the sensor redundancy and a cluster-based strategy. The method was tested in the laboratory against force platforms on nine healthy subjects for a total of 801 initial and final contacts. Initial and final contacts were detected with low average errors of (about 20 ms and 10 ms, respectively). Similarly, the errors in estimating stance duration and step duration averaged 20 ms and <10 ms, respectively. By selecting appropriate thresholds, the method may be easily applied to other pressure insoles featuring similar requirements.

1. Introduction

The gait cycle represents the functional element of walking, traditionally identified by the initial contact (IC) of the foot with the ground and the following IC of the same foot (Della Croce et al., 2018; Whittle, 1993). A direct approach to detect these gait events (GEs) is by using force platforms (FPs) and instrumented walkways. These provide a direct measure of forces resulting from the foot–ground interaction, thus representing a gold standard for GEs detection. However, both devices are non-portable, expensive and require an appropriate laboratory environment, therefore constraining the analysis to few strides and/or straight walks (Adkin et al., 2000). Moreover, laboratory analysis only allows for the assessment of walking capacity, which should ideally be complemented with continuous daily living measures of mobility performance to obtain a thorough assessment (World Health Organization, 2007; Rochester et al., 2020). In this perspective, wearable inertial measurement units (IMUs) are the key to enable gait analysis in real-world scenarios as GEs can be identified from the accelerations and angular velocities signals recorded by two units attached to the ankles/feet (Mariani et al., 2012; Trojaniello et al., 2014). However, being the latter an indirect method, processing algorithms performance may be affected by errors, and it should, therefore, be regarded as a silver standard solution.

Foot switches are an effective alternative to estimate GEs and their use has been explored in several studies over the last decades (Agostini et al., 2013; Bae et al., 2011; Hausdorff et al., 1995; Kong et al., 2009; Skelly et al., 2001). The foot switch technology, however, generally includes only two or three sensing elements, which require a proper positioning under the foot. Due its low spatial sensor resolution, the approach does not allow to identify the specific area of the sole-ground contact and, in turn, it may also affect the GEs temporal resolution. This is even more true in case of pathological gait (i.e., pronation, supination, equine gait, foot drop, shuffling children with cerebral palsy), for which few sensors are not sufficient (Smith et al., 2016). Another attractive

* Corresponding author at: Department of Biomedical Sciences, University of Sassari, Sassari, Italy.
E-mail addresses: fsalis1@uniss.it (F. Salis), sbertuletti@uniss.it (S. Bertuletti), t.bonci@sheffield.ac.uk (T. Bonci), dellacro@uniss.it (U. Della Croce), c.mazza@sheffield.ac.uk (C. Mazzà), andrea.cereatti@polito.it (A. Cereatti).

https://doi.org/10.1016/j.jbiomech.2021.110687
Accepted 9 August 2021
Available online 13 August 2021

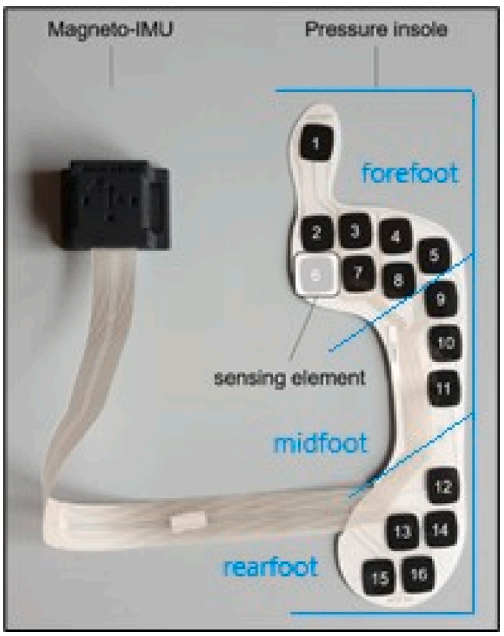

Fig. 1. Magneto-IMU and pressure insole used for the right foot.

option is represented by plantar pressure insoles, based on different technologies and sensors configurations (e.g., Tekscan® F-Scan® System; Novel® Pedar® System, etc.). However, these devices are specifically conceived for high-resolution pressure mapping applications and generally include a dense grid of sensors (from 99 to 960 sensing elements) which inevitably lead to higher costs and complexity in terms of data management and reading, but which are not strictly necessary for simple GEs estimations.

In this study we propose an original method for GEs detection, based on the use of instrumented insoles, each including only sixteen force-sensing resistor elements (pressure insoles, PIs). The implemented algorithm exploits the number of sensors by using a cluster-based approach to describe foot–ground contacts in a finer way and avoid missed and extra GEs, providing information about foot positioning. The method was tested against FPs in the laboratory using data collected on healthy subjects.

2. Methods

A. System Description and GEs algorithm

Two plantar PIs (mod. YETI, 221e S.r.l., Padua, Italy; 16 sensing elements; element area = 310 mm^2; fs = 100 Hz; ground reaction force threshold = 5 N) were used in this study, with a design similar to that adopted by Ciniglio et al. 2021. Each sensing element is constituted by a force sensing resistor, exhibiting a resistance value inversely proportional to the applied force. The output is expressed as voltage (full-scale voltage value V_{FS} = 2.8 V). Each pressure insole is connected to a central processing unit, which also includes a magneto-IMU (Fig. 1) that is not used for this study. Data is recorded by an ultra-low-power microcontroller and stored in an on-board flash storage.

The PI signals processing algorithm is described by the following steps (Fig. 2):

(i) Pre-processing.

PI signals are normalised with respect to V_{FS}, expressed in normalised units (nu), and then filtered using a 5-points non-linear median filter to have a smoothing effect while enhancing edges (Stork et al., 2003);

(ii) Detection and selection of instants of rising and falling edges.

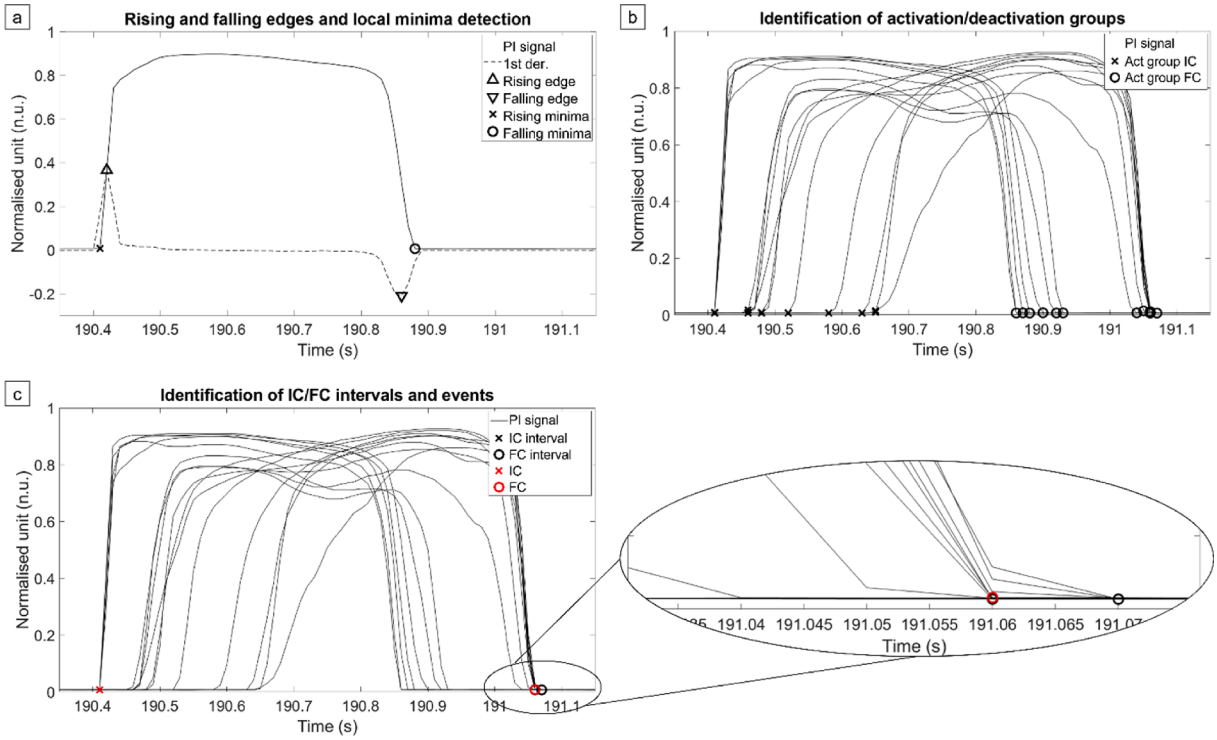

Fig. 2. Principal steps of the algorithm shown for one stance. a) Detection and selection of rising and falling edges and local minima (rising and falling minima) for each PI signal; b) Identification of one activation/deactivation cluster on PI signals; c) Identification of IC/FC intervals and definition of IC and FC events on PI signals.

Fig. 3. a) PI positioning inside the shoe; b) Clip attached to shoe laces; c) Final sensors positioning with magneto-IMU fixed to the clip.

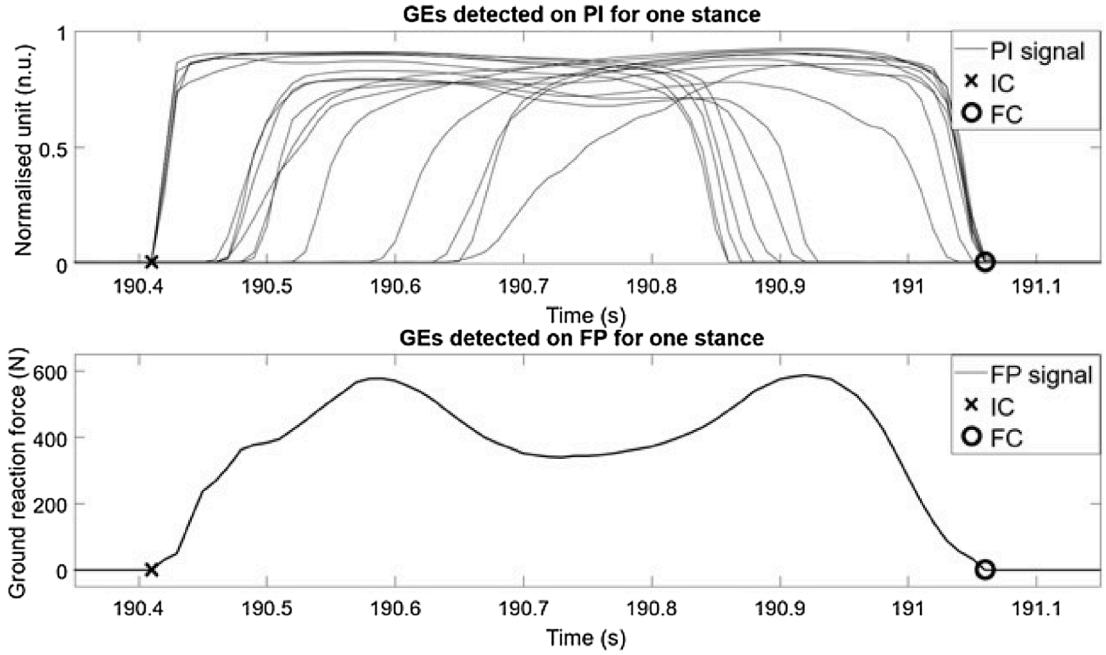

Fig. 4. Gait events (GEs) detection from both pressure insole (PI) and force plate (FP).

Table 1
RMS error, bias, and SD error.

Variable	Average RMS Error (ms; frames)	Average Bias (ms; frames)	Average SD Error (ms; frames)
IC	22; 2	−21; −2	7; <1
FC	18; <2	3; <1	12; 1
Stance duration	18; <2	23; 2	7; <1
Step duration	10; 1	0; <1	10; 1

For each of the filtered PI signals $X_i(t)$, where i = 1,..,16 represents the i-th PI signal, a first derivative approach (Hopkins, 2001) is applied to detect rising and falling edges. Edges are identified from $\dot{X}_i(t)$ using a peak detection approach (Benocci et al., 2009) with an amplitude threshold defined as $Th_1 = 5n$, being n the signal noise amplitude as computed in static conditions (in this study, we used $Th_1 = 0.05$ nu). For each PI signal, rising edges are identified as positive peaks $> Th_1$ and the corresponding time instants are organized in a vector $t_{RE,i}$. Similarly, falling edges are identified as negative peaks $< -Th_1$ and the corresponding time instants are organized in a vector $t_{FE,i}$. Rising and falling edges are automatically checked, in terms of time distance and amplitude of the PI signal, to discard false positives. Fig. 2a shows an example of detection of a rising edge and a falling edge;

(iii) Detection and selection of local minima (instants of rising and falling minima).

The identification of the instants of rising and falling minima is performed by applying to $X_i(t)$ a threshold $Th_2 = 0.02$ nu, using rising and falling edges as reference points (Hausdorff et al., 1995). In particular, each rising minima is identified as the first point with $X_i(t) < Th_2$ preceding the considered rising edge instant, while each falling minima is identified as the first point with $X_i(t) < Th_2$ after the considered falling edge instant. Rising minima instants and falling minima instants were organised in vectors, $t_{RM,i}$ and $t_{FM,i}$ respectively. Fig. 2a shows an example of detection of one rising minimum and one falling minimum;

(iv) Identification of activation/deactivation clusters.

Once the rising and falling minima instants are detected for all the PI signals, they are organised in chronological order in a unique vector (t_{RM} and t_{FM} respectively), also noting the corresponding sensing element number in another vector (s_{RM} and s_{FM}). This step is needed to group the instants of rising/falling minima corresponding to the same foot contact, i.e. the PI sensing elements which activate/deactivate together when the foot hits the ground. An activation cluster is identified imposing that the time distance between consecutive instants of t_{RM} is lower than $Th_3 = 0.4$ s. Then, a deactivation cluster includes the instants of t_{FM} between

two consecutive activation clusters. For each cluster, the minima instants and the sensing elements numbers are saved (A_cluster$_j$ /D_cluster$_j$, where j = j-th activation/deactivation cluster).

Fig. 2b shows an example of one activation cluster and one deactivation cluster.

(v) Identification of IC/FC (final contact) intervals and definition of IC/FC events.

A foot–ground contact interval is defined when at least three sensing elements of the PI belonging to the same spatial neighbourhood are consecutively activated and deactivated, i.e. correspond to three consecutive minima belonging to the same cluster (A_cluster for ICs and D_cluster for FCs). For each PI's sensing element, the neighbourhood consists of those sensing elements which are spatially close to the considered unit (Fig. 1) (e.g. for the sensing element no. 12, the neighbourhood includes sensing elements 11, 13, 14, 15, 16; further details are reported in *Appendix B*). In fact, it is reasonable to assume that, when an IC or FC occurs, the sensing elements which refer to the same anatomically functional area of foot sole are activated or deactivated, respectively.

Each IC interval is identified starting from the first rising minima of an activation cluster; while each FC interval is identified starting from the last falling minima of a deactivation cluster.

Finally, each IC is assumed to coincide with the rising minimum instant corresponding to the third sequentially activated sensing elements within the considered IC interval. Likewise, each FC is assumed to coincide with the falling minimum instant corresponding to the third sequentially deactivated sensing elements within the considered FC interval. Fig. 2c shows an example of one IC interval and one FC interval. A workflow of the algorithm can be found in *Appendix A*.

B. Experimental setup

The validation experiments involved nine healthy participants (5 females and 4 males; age 25.4 ± 1.3 years, shoe size 40.5 ± 4.1 EU) and took place at the University of Sassari (Italy). All participants signed an informed consent approved by the IRB before taking part to the study. PIs were inserted in participants' shoes and central processing units were clipped over the instep (Fig. 3). The only specific requirement for the shoes was to avoid knee-high boots. Data from two FPs (AMTI, Massachusetts, USA; fs = 1000 Hz) were acquired through a motion capture system also including video recordings (Vicon Vue, fs = 50 Hz). Data from PIs and FPs were synchronized using an additional central processing unit as external trigger, connected to the motion capture system via cable. Each participant was asked to walk for six minutes back and forth at comfortable speed, stepping on the FPs as many times as possible.

C. Data processing

For each subject, a preliminary visual inspection of the "good strides" (entire foot on the FP during stance phase) was performed using video recordings. Then, FP data were down-sampled to 100 Hz. A pre-processing procedure was applied for the synchronisation of PIs measurements (started via BLE protocol, v. 4.1) with the FP data, using the time vector provided by the trigger to interpolate the data.

The GEs detection algorithm results were compared with those obtained from the FPs (ground reaction force threshold = 25 N) in terms of average root mean square (RMS) error, bias and standard deviation (SD) error computed over the stances of all participants. An example of IC and FC detection from both PI and FP is shown in Fig. 4.

3. Results

RMS error, bias and SD error obtained from the comparison are reported in Table 1. A total of 801 ICs and 801 FCs were analysed (89 ICs and FCs on average for each participant), while errors on step duration were computed considering 315 steps in total. Average errors were lower than 10 ms for FCs, 20 ms for ICs, 20 ms for stance duration, <1 ms for step duration.

4. Discussion

GEs and temporal parameters obtained from the PIs showed a 100% correspondence with those estimated from the FPs. Low average RMS errors were obtained for stance duration (<20 ms) and for both IC and FC events, (22 ms and 17 ms, respectively). IC events, as detected by the proposed method were, on average, anticipated with respect to those detected by the FP (average bias = 21 ms), while FC events were marginally delayed. A bias of 23 ms was obtained for stance duration. Very low values were obtained for the average SD error (7 ms for ICs, 12 ms for FCs and 7 ms for stance duration). For step duration, both RMS error and SD error were around one sample, while the average bias was zero.

Similar but slightly larger errors were reported by Catalfamo and colleagues (2008) using a F-Scan Mobile Tekscan pressure insole (22 ± 9 ms for ICs and 10 ± 4 ms for FCs). However, it should be noted that the proposed algorithm was successful in obtaining lower errors using a pressure insole with a much smaller number of sensing elements (16 vs 960) and using a lower sample-frequency (100 Hz vs 200 Hz), with clear advantages in terms of cost and efficiency.

In general, the majority of the methodological studies analysing the performance of different pressure insoles, focused on gait parameters other than ICs and FCs and reported larger errors (Agarwal et al., 2020; Braun et al., 2015; Carbonaro et al., 2016; Crea et al., 2014). For instance, the average error reported in Carbonaro et al. (2016) by comparing a commercial smart shoe including two force sensors (FootMov) against a motion capture system was 39 ± 65 ms for stance duration. Often, a direct comparison with the results in the literature was not possible due to the lack of a gold standard (Benocci et al., 2009), adoption of manual labelling of the GE detection (Roth et al., 2018) or different research objectives (i.e., PI signals used only for activity recognition).

The low errors found for both ICs and FCs demonstrated that the combined use of low-cost PI and specific algorithms for signal processing are a good compromise between more complex solutions, such as high-resolution pressure mapping technology, and foot-switch systems with a low number of sensors. A notable feature of the proposed method is that it can be applied to other PIs having a sufficient number of sensing elements. The minimum sensor number and area would clearly depend on the shoe size of the subjects to analyse (e.g. children), however, we found that an activated/deactivated area of about 900 mm^2 (area of three sensing unit of the PI) guaranteed for good results for both male and female adults. Having a sufficiently high number of sensors allows to describe the foot–ground contact in a comprehensive way and virtually recognise all the possible strategies of foot-floor contact. Last but not least, the PIs here used can be easily combined with IMUs as part of a multi-sensor wearable system, which could provide accurate temporal estimates and a for a more extensive gait assessment also in a free-living context. Further studies will focus on overcoming the limitations of having tested the proposed method only on healthy subjects and on straight walking.

Declaration of Competing Interest

The authors declare that they have no known competing financial interests or personal relationships that could have appeared to influence the work reported in this paper.

Acknowledgement

The work was supported by the MOBILISE-D (EU H2020, EFPIA, and IMI 2 Joint Undertaking; Grant no. 820820), the UK EPSRC (K03877X/1 and S032940/1) and the NIHR Sheffield BRC. The study sponsors were not involved in the study phases, in the writing of the manuscript and in the decision about its submission.

Appendix A

In Fig. A1 a detailed description of the algorithm workflow is illustrated.
Definitions:

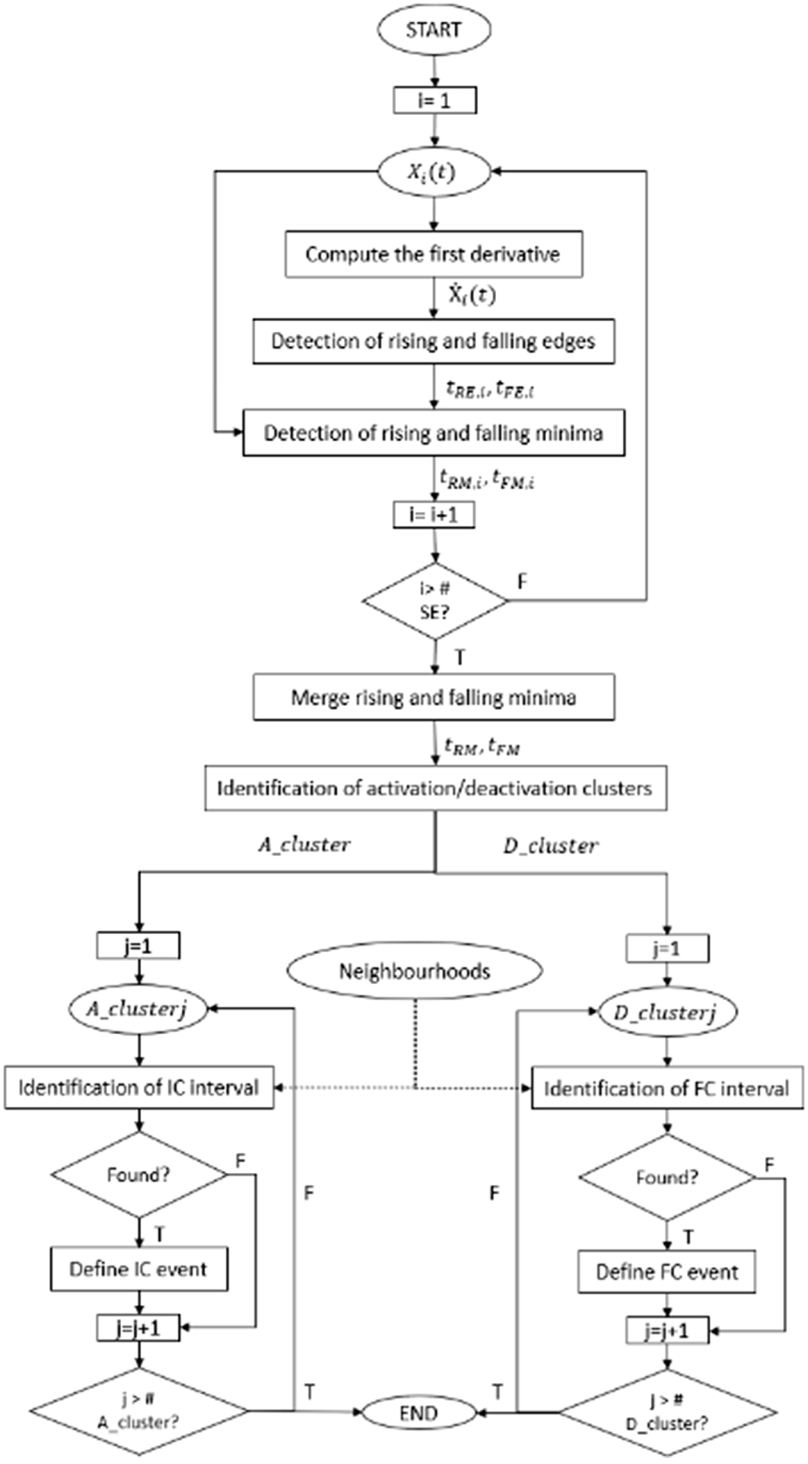

Fig. A1. Algorithm workflow.

$X_i(t)$ = pre-processed signal from the i-th sensing element
#SE = number of sensing elements of the pressure insole
$\dot{X}_i(t)$ = first derivative of $Xp_i[n]$
$t_{RE,i}$ = rising edges instants
$t_{FE,i}$ = falling edges instants
$t_{RM,i}$ = rising minima instants
$t_{FM,i}$ = falling minima instants
t_{RE} = rising minima instants of all the sensing units
t_{FE} = falling minima instants of all the sensing units
A_cluster = activation clusters
D_cluster = deactivation clusters
Checks on rising and falling edges instants:

- Check on temporal distance. This is performed applying a threshold $Th_d = 0.6$ s. If the distance between consecutive events is lower than Th_d, the second event is discarded in case of rising edges, while the first event is discarded for the falling edges.
- Check on the amplitude reached by $x_i(t)$ after each rising edge instant and before each falling edge instant. The amplitude reached in the considered window (10 samples after a rising edge instant or 10 samples before a falling edge instant) must be at least 0.3 nu, otherwise the event is discarded.

Appendix B

The neighbourhood of each sensing element of the PI is defined as reported in the following table:

Sensing unit number	Neighbourhood
1	2,3,4,6,7
2	1,3,4,6,7
3	1,2,4,6,7,8,5
4	1,2,3,5,7,8,6,9
5	1,2,3,5,7,8,6,9
6	1,2,3,4,7,8
7	1,2,3,4,5,6,8,9
8	3,4,5,6,7,9,10
9	5,8,4,7,10,11
10	9,11,8,5,12
11	9,10,12,14,13,15,16
12	10,11,13,14,15,16
13	11,12,14,15,16
14	11,12,13,15,16
15	12,13,14,16,11
16	12,13,14,15,11

References

Adkin, A.L., Frank, J.S., Carpenter, M.G., Peysar, G.W., 2000. Postural control is scaled to level of postural threat. Gait & Posture 12 (2), 87–93.

Agarwal, R., Aggarwal, A., Gupta, R., 2020. A Wireless Sensorized Insole Design for Spatio-Temporal Gait Analysis. Neurophysiology 52 (3), 212–221.

Agostini, V., Balestra, G., Knaflitz, M., 2013. Segmentation and classification of gait cycles. Proceedings of IEEE Transactions on Neural Systems and Rehabilitation Engineering 22 (5), 946–952.

Bae, J., Tomizuka, M., 2011. Gait phase analysis based on a Hidden Markov Model. Mechatronics 21 (6), 961–970.

Benocci, M., Rocchi, L., Farella, E., Chiari, L., Benini, L., 2009. A Wireless System for Gait and Posture Analysis Based on Pressure Insoles and Inertial Measurement Units. In: In Proceedings of the 3rd International Conference on Pervasive Computing Technologies for Healthcare, pp. 1–6.

Braun, B.J., Veith, N.T., Hell, R., Döbele, S., Roland, M., Rollmann, M., Pohlemann, T., 2015. Validation and reliability testing of a new, fully integrated gait analysis insole. Journal of foot and ankle research 8 (1), 1–7.

Carbonaro, N., Lorussi, F., Tognetti, A., 2016. Assessment of a smart sensing shoe for gait phase detection in level walking. Electronics 5 (4), 78.

Catalfamo, P., Moser, D., Ghoussayni, S., Ewins, D., 2008. Detection of gait events using an F-Scan in-shoe pressure measurement system. Gait & posture 28 (3), 420–426.

Ciniglio, A., Guiotto, A., Spolaor, F., Sawacha, Z., 2021. The design and simulation of a 16-sensors plantar pressure insole layout for different applications: From sports to clinics, a pilot study. Sensors 21 (4), 1450.

Crea, S., Donati, M., De Rossi, S.M.M., Oddo, C.M., Vitiello, N., 2014. A wireless flexible sensorized insole for gait analysis. Sensors 14 (1), 1073–1093.

Della Croce, U., Cereatti, A., Mancini, M., 2018. Gait parameters estimated using inertial measurement units. In: Müller, B., Wolf, S.I., Brüggemann, G.P., Deng, Z., McIntosh, A.S., Miller, F., Selbie, W.S. (Eds.), Handbook of human motion. Springer International Publishing, pp. 245–265.

Hausdorff, J.M., Ladin, Z., Wei, J.Y., 1995. Footswitch system for measurement of the temporal parameters of gait. Journal of biomechanics 28 (3), 347–351.

Hopkins, D.W., 2001. What is a Norris derivative? NIR news 12 (3), 3–5.

Kong, K., Tomizuka, M., 2009. A gait monitoring system based on air pressure sensors embedded in a shoe. Proceedings of IEEE/ASME Transactions on mechatronics 14 (3), 358–370.

Mariani, B., Rochat, S., Büla, C.J., Aminian, K., 2012. Heel and toe clearance estimation for gait analysis using wireless inertial sensors. Proceedings of the IEEE transactions on bio-medical engineering 59 (11), 3162–3168.

Novel® Pedar® System Web Page. Url: http://www.novel.de.

Rochester, L., Mazzà, C., Mueller, A., Caulfield, B., McCarthy, M., Becker, C., Mobilise-D Consortium, 2020. A roadmap to inform development, validation and approval of digital mobility outcomes: the Mobilise-D approach. Digital Biomarkers 4 (1), 13–27.

Roth, N., Martindale, C.F., Eskofier, B.M., Gaßner, H., Kohl, Z., Klucken, J., 2018. Synchronized sensor insoles for clinical gait analysis in home-monitoring applications. Current Directions in Biomedical Engineering 4 (1), 433–437.

Skelly, M.M., Chizeck, H.J., 2001. Real-time gait event detection for paraplegic FES walking. Proceedings of IEEE Transactions on neural systems and rehabilitation engineering 9 (1), 59–68.

Smith, B.T., Coiro, D.J., Finson, R., Betz, R.R., McCarthy, J., 2002. Evaluation of force-sensing resistors for gait event detection to trigger electrical stimulation to improve walking in the child with cerebral palsy. Proceedings of IEEE Transactions on Neural Systems and Rehabilitation Engineering 10 (1), 22–29.

Stork, M., 2003. Median filters theory and applications. In: In Proceedings of the third International Conference on Electrical and Electronics Engineering Papers-Chamber of Electrical Engineering, pp. 1–5.

Tekscan® F-Scan® System Web Page. Url: http://www.tekscan.com.

Trojaniello, D., Cereatti, A., Pelosin, E., Avanzino, L., Mirelman, A., Hausdorff, J.M., Della Croce, U., 2014. Estimation of step-by-step spatio-temporal parameters of normal and impaired gait using shank-mounted magneto-inertial sensors: application to elderly, hemiparetic, parkinsonian and choreic gait. Journal of neuroengineering and rehabilitation 11 (1), 1–12.

Whittle, Michael W., 1993. Gait analysis. In: Butterworth-Heinemann (Eds), The soft tissues., 187-199.

World Health Organization, 2007. International Classification of Functioning, Disability, and Health: Children & Youth Version: ICF-CY. World Health. Organization.

B. A multi-sensor wearable system for gait assessment in real-world conditions: performance in individuals with impaired mobility.

frontiers | Frontiers in Bioengineering and Biotechnology

TYPE Original Research
PUBLISHED 21 April 2023
DOI 10.3389/fbioe.2023.1143248

OPEN ACCESS

EDITED BY
Simone Carozzo,
Sant'Anna Crotone Institute, Italy

REVIEWED BY
Guoru Zhao,
Shenzhen Institute of Advanced Technology (CAS), China
Stephen Matthew Cain,
University of Michigan, United States

*CORRESPONDENCE
Francesca Salis,
fsalis1@uniss.it

SPECIALTY SECTION
This article was submitted to Biomechanics, a section of the journal Frontiers in Biofabrication

RECEIVED 13 January 2023
ACCEPTED 30 March 2023
PUBLISHED 21 April 2023

CITATION
Salis F, Bertuletti S, Bonci T, Caruso M, Scott K, Alcock L, Buckley E, Gazit E, Hansen C, Schwickert L, Aminian K, Becker C, Brown P, Carsin A-E, Caulfield B, Chiari L, D'Ascanio I, Del Din S, Eskofier BM, Garcia-Aymerich J, Hausdorff JM, Hume EC, Kirk C, Kluge F, Koch S, Kuederle A, Maetzler W, Micó-Amigo EM, Mueller A, Neatrour I, Paraschiv-Ionescu A, Palmerini L, Yarnall AJ, Rochester L, Sharrack B, Singleton D, Vereijken B, Vogiatzis I, Della Croce U, Mazzà C, Cereatti A, for the Mobilise-D consortium (2023), A multi-sensor wearable system for the assessment of diseased gait in real-world conditions.
Front. Bioeng. Biotechnol. 11:1143248.
doi: 10.3389/fbioe.2023.1143248

A multi-sensor wearable system for the assessment of diseased gait in real-world conditions

Francesca Salis[1,2]*, Stefano Bertuletti[1,2], Tecla Bonci[3], Marco Caruso[2,4], Kirsty Scott[3], Lisa Alcock[5,6], Ellen Buckley[3], Eran Gazit[7], Clint Hansen[8], Lars Schwickert[9], Kamiar Aminian[10], Clemens Becker[9], Philip Brown[11], Anne-Elie Carsin[12,13,14], Brian Caulfield[15], Lorenzo Chiari[16,17], Ilaria D'Ascanio[16], Silvia Del Din[5,6], Bjoern M. Eskofier[18], Judith Garcia-Aymerich[12,13,14], Jeffrey M. Hausdorff[7], Emily C. Hume[19], Cameron Kirk[5], Felix Kluge[18,20], Sarah Koch[12,13,14], Arne Kuederle[18], Walter Maetzler[8], Encarna M. Micó-Amigo[5], Arne Mueller[20], Isabel Neatrour[5], Anisoara Paraschiv-Ionescu[10], Luca Palmerini[16,17], Alison J. Yarnall[5,6,11], Lynn Rochester[5,6,11], Basil Sharrack[21], David Singleton[15], Beatrix Vereijken[22], Ioannis Vogiatzis[19], Ugo Della Croce[1,2], Claudia Mazzà[3], Andrea Cereatti[2,4] and for the Mobilise-D consortium

[1]Department of Biomedical Sciences, University of Sassari, Sassari, Italy, [2]Interuniversity Centre of Bioengineering of the Human Neuromusculoskeletal System (IuC BoHNes), Sassari, Italy, [3]Department of Mechanical Engineering, Insigneo Institute for In Silico Medicine, The University of Sheffield, Sheffield, United Kingdom, [4]Department of Electronics and Telecommunications, Politecnico Di Torino, Torino, Italy, [5]Translational and Clinical Research Institute, Faculty of Medical Sciences, Newcastle University, Newcastle Upon Tyne, United Kingdom, [6]National Institute for Health and Care Research (NIHR) Newcastle Biomedical Research Centre (BRC), Newcastle University, Newcastle Upon Tyne, United Kingdom, [7]Centre for the Study of Movement, Cognition and Mobility, Neurological Institute, Tel Aviv Sourasky Medical Centre, Tel Aviv, Israel, [8]Department of Neurology, University Medical Centre Schleswig-Holstein Campus Kiel and Kiel University, Kiel, Germany, [9]Department for Geriatric Rehabilitation, Robert-Bosch-Hospital, Stuttgart, Germany, [10]Laboratory of Movement Analysis and Measurement, Ecole Polytechnique Federale de Lausanne, Lausanne, Switzerland, [11]Newcastle upon Tyne Hospitals NHS Foundation Trust, Newcastle Upon Tyne, United Kingdom, [12]Instituto de Salud Global Barcelona, Barcelona Institute for Global Health (ISGlobal), Barcelona, Spain, [13]Faculty of Health and Life Sciences, Universitat Pompeu Fabra, Barcelona, Spain, [14]CIBER Epidemiología y Salud Pública, Madrid, Spain, [15]Insight Centre for Data Analytics, University College Dublin, Dublin, Ireland, [16]Department of Electrical, Electronic and Information Engineering "Guglielmo Marconi", University of Bologna, Bologna, Italy, [17]Health Sciences and Technologies-Interdepartmental Centre for Industrial Research (CIRI-SDV), University of Bologna, Bologna, Italy, [18]Machine Learning and Data Analytics Lab, Department Artificial Intelligence in Biomedical Engineering, Friedrich-Alexander-Universität Erlangen-Nürnberg, Erlangen, Germany, [19]Department of Sport, Exercise and Rehabilitation, Faculty of Health and Life Sciences, Northumbria University, Northumbia, United Kingdom, [20]Novartis Institutes of Biomedical Research, Novartis Pharma AG, Basel, Switzerland, [21]Department of Neuroscience and Sheffield NIHR Translational Neuroscience BRC, Sheffield Teaching Hospitals NHS Foundation Trust, Sheffield, United Kingdom, [22]Department of Neuromedicine and Movement Science, Norwegian University of Science and Technology, Trondheim, Norway

Introduction: Accurately assessing people's gait, especially in real-world conditions and in case of impaired mobility, is still a challenge due to intrinsic and extrinsic factors resulting in gait complexity. To improve the estimation of gait-related digital mobility outcomes (DMOs) in real-world scenarios, this study

presents a wearable multi-sensor system (INDIP), integrating complementary sensing approaches (two plantar pressure insoles, three inertial units and two distance sensors).

Methods: The INDIP technical validity was assessed against stereophotogrammetry during a laboratory experimental protocol comprising structured tests (including continuous curvilinear and rectilinear walking and steps) and a simulation of daily-life activities (including intermittent gait and short walking bouts). To evaluate its performance on various gait patterns, data were collected on 128 participants from seven cohorts: healthy young and older adults, patients with Parkinson's disease, multiple sclerosis, chronic obstructive pulmonary disease, congestive heart failure, and proximal femur fracture. Moreover, INDIP usability was evaluated by recording 2.5-h of real-world unsupervised activity.

Results and discussion: Excellent absolute agreement (ICC >0.95) and very limited mean absolute errors were observed for all cohorts and digital mobility outcomes (cadence ≤0.61 steps/min, stride length ≤0.02 m, walking speed ≤0.02 m/s) in the structured tests. Larger, but limited, errors were observed during the daily-life simulation (cadence 2.72–4.87 steps/min, stride length 0.04–0.06 m, walking speed 0.03–0.05 m/s). Neither major technical nor usability issues were declared during the 2.5-h acquisitions. Therefore, the INDIP system can be considered a valid and feasible solution to collect reference data for analyzing gait in real-world conditions.

KEYWORDS

gait analysis, IMU, wearable sensors, ecological conditions, pressure insoles, distance sensors, spatial-temporal gait parameters

1 Introduction

It is well established that gait impairments affect one's functional status and overall health, (Laudani et al., 2013; Polhemus et al., 2021), and that a holistic model of functioning and disability should not rely only on a conventional laboratory assessment. Rather, it should also include a quantitative description of a person's mobility in its own ecological environment to include social and personal factors (World Health Organization, 2001; Giannouli et al., 2016; Galperin et al., 2019; Hillel et al., 2019). Nonetheless, the description of gait in real-world conditions is still a major challenge in people with impaired mobility due to the increased gait complexity associated with changes in speed and direction of progression, slow walking and use of walking aids, presence of breaks, short walking bouts, and confounding factors such as non-walking activities (Mobilise-D 2019). Several technologies and algorithms have been proposed to extract clinically meaningful spatial-temporal digital mobility outcomes (DMOs) across a large spectrum of gait disorders, but technical validity was in most of the cases assessed in a supervised laboratory setting evaluating basic gait tasks (Zijlstra and Hof, 2003; Wang et al., 2016; Pacini et al., 2018; Bertuletti et al., 2019). Further efforts are hence required to generalize results under real-world conditions.

One of the most promising solutions for mobility assessment in ecological conditions is the use of wearable inertial measurement units (IMUs). A single-IMU approach is preferred when maximizing user acceptance is key (Bonci et al., 2020; Mobbs et al., 2022). Conversely, a bilateral lower extremities positioning (i.e., IMUs attached to the shanks or feet) is suggested to obtain a more accurate gait description in people with severe gait disorders (Yang et al., 2013; Bourgeois et al., 2014; Hundza et al., 2014; Trojaniello et al., 2014). However, when using these devices, the identification of gait events (i.e., initial and final foot contact timings), which is a prerequisite for the estimation of the temporal and spatial parameters, is indirectly derived from the linear acceleration and angular velocity signals which vary their morphology, amplitude, and repeatability, depending on specific walking patterns. This implies that the technical validity of the DMOs provided by IMU-based methods should be tested against reference data under the same conditions of end-use. Furthermore, the availability of reliable reference gait data is also essential for the development, optimization, and testing of newly proposed IMU-based machine learning methods (Martindale et al., 2019; Roth et al., 2021a).

A commonly employed solution to obtain a reference for gait detection and activity discrimination is the use of body-worn cameras pointing to the subjects feet (Buso et al., 2015; Full et al., 2015; Hickey et al., 2016). However, besides potential privacy issues, the temporal resolution of this approach depends on camera frame rate. Furthermore, it requires extensive manual intervention for labeling gait events, and it doesn't provide information on spatial gait parameters nor on turning maneuvers. Conversely, methods based on the use of global navigation satellite systems can potentially provide low positional errors (Terrier et al., 2000), but their performance greatly depends on environmental conditions (Reggi et al., 2022), they aren't reliable indoor, are characterized by a low temporal resolution, and don't allow for a stride-by-stride gait description (Atrsaei et al., 2021). An accurate and reliable solution for gait events detection is to use plantar pressure insoles (Hausdorff et al., 1995; Storm, Buckley, and

Mazzà, 2016; Roth et al., 2018) as this technology provides a direct sensing of the foot-ground forces (Salis et al., 2021a). When using these systems, however, no spatial information is provided.

To overcome the intrinsic technological limitations of the aforementioned systems, the simultaneous integration of complementary sensing approaches and the exploitation of data redundancy to improve methods employed and optimize performance may be beneficial. In this regard, several research and consumer-grade systems integrating pressure insoles with IMUs attached to the feet have been proposed (Salis et al., 2021b; Duong et al., 2022; Refai et al., 2018; Feetme Devices, 2022b; NURVV, 2022). Based on this sensor configuration, Duong and colleagues (Duong et al., 2022) have proposed a machine learning model for spatial-temporal gait analysis (SportSole II). The method's accuracy was validated in terms of mean absolute percentage errors on eleven healthy young adults during simple straight and curvilinear walking, whereas ecological validation was performed in terms of DMOs agreement between spatial-temporal parameters estimated in laboratory and real-world conditions. Although the results of this study were promising, with errors of stride length ~3.5%, the restriction of including only healthy young adults does not support applicability of the systems use within pathological cohorts with potentially impaired gait. In the latest years, several consumer grade systems such as FeetMe® and NURVV® have been made available for healthcare applications (Feetme Devices, 2022b; NURVV, 2022). In general, these commercial systems were designed to improve user-friendliness and provide a full gait report, however, they operate as a black box system whereby the algorithms employed are not described in detail, and their validation procedures are limited to basic gait tasks such as straight walking (Feetme Devices, 2022a).

The aim of this study is thus to present and characterize the performance of a novel multi-sensor system for gait assessment to be employed as reference in people with impaired mobility in real-world. The INDIP system (INertial module with DIstance sensors and Pressure insoles) integrates two plantar pressure insoles for a direct measure of foot-to-ground contacts, three IMUs attached to both feet and lower back for activity recognition, turning detection, and displacement estimation, two time-of-flight infrared distance sensors to detect the alternating movements of the lower extremities.

To meet the emerging demands associated with reproducibility and replicability in biomedical research and regulatory qualification (Viceconti et al., 2020), a complete description of INDIP system hardware specifications and of the algorithms used for DMOs estimation based on standardized operational definitions (Kluge et al., 2021) is provided here. Furthermore, to assess the INDIP performances under testing conditions resembling those likely to be encountered in real life, a multi-task experimental protocol in a lab setting, which included speed and trajectory changes, surfaces and inclinations, obstacles, breaks, and even cognitive demand levels (Mazzà et al., 2021; Scott et al., 2022), was implemented. To evaluate the potential influence of different gait types on the accuracy of the estimated DMOs, gait data of 128 participants were analyzed, including healthy young and older adults, people with Parkinson's disease (PD), multiple sclerosis (MS), chronic obstructive pulmonary disease (COPD), congestive heart failure (CHF) and proximal femoral fracture (PFF). Finally, INDIP usability was evaluated by recording 2.5 h of unsupervised activity performed in the participants habitual environment in five different clinical centers participating in the IMI2-JU-funded Mobilise-D project (Number 820820) (Mobilise-D 2019; Mazzà et al., 2021).

2 Materials and methods

2.1 The INDIP system

The central unit of the INDIP system (manufacturer (mfr.) 221e S.r.l. (221 e S.r.l, 2020) is a state-of-the-art magneto-IMU that can be connected to various sensing peripherals. The overall system hardware architecture, as well as the communication interfaces used, is shown in Figure 1. A description of the firmware's architecture, together with some additional details on the hardware, are reported in Appendix A.

2.1.1 Main board

The main board has been designed to sense motion and process relevant data with a low power consumption, to store recorded data on-board and to offer a wired/wireless transmission. Motion data include both inertial and magnetic data. The inertial module is a system-in-package featuring a 3D digital accelerometer and a 3D digital gyroscope (full-scale ranges set to ±16 g and ±2,000 dps respectively for this study). The magnetic module is an ultra-low-power, high performance 3-axis digital magnetic sensor (magnetic field dynamic range of ±50 G).

One 18-pin (i.e., analog front end) and two 6-pin connectors (i.e., digital I/O port) are mounted on the bottom and right/left side of the main board, respectively (Figure 1). The 18-pin ZIF-connector enables the connection between the pressure insoles and the microcontroller unit through the analog front-end, while the two 6-pin connectors allow the main board to manage any digital sensor that supports the I2C communication protocol (e.g., the distance sensor). The main board acts as a "motherboard," i.e., supplying the required power and providing storage and connectivity capabilities. Therefore, any external sensing peripheral (e.g., distance sensor, pressure insole) could be designed with the strictly necessary components, thus minimizing its form factor.

An external crystal with a frequency stability of ±5 ppm (parts per million) has been selected to generate more accurate and precise time values. The main board also supports the synchronization with an external equipment in two modes:

- output synchronization: when the main board starts recording data, it outputs a signal to external equipment by exploiting the ID pin of the micro-USB;
- input synchronization: when the main board receives a signal from external equipment on the ID pin of the micro-USB, it starts recording. Input and output signals can be either rising edge or level triggered.

2.1.2 Sensing peripherals

- The Time-of-Flight infrared distance sensor includes an infrared emitter, a range sensor (range set to 0.2 m at 50 Hz for this study), and an ambient light sensor in a three-in-one package. A fully comprehensive characterization while considering different factors, such as target color, sensor-target distance, and sensor-target angle of

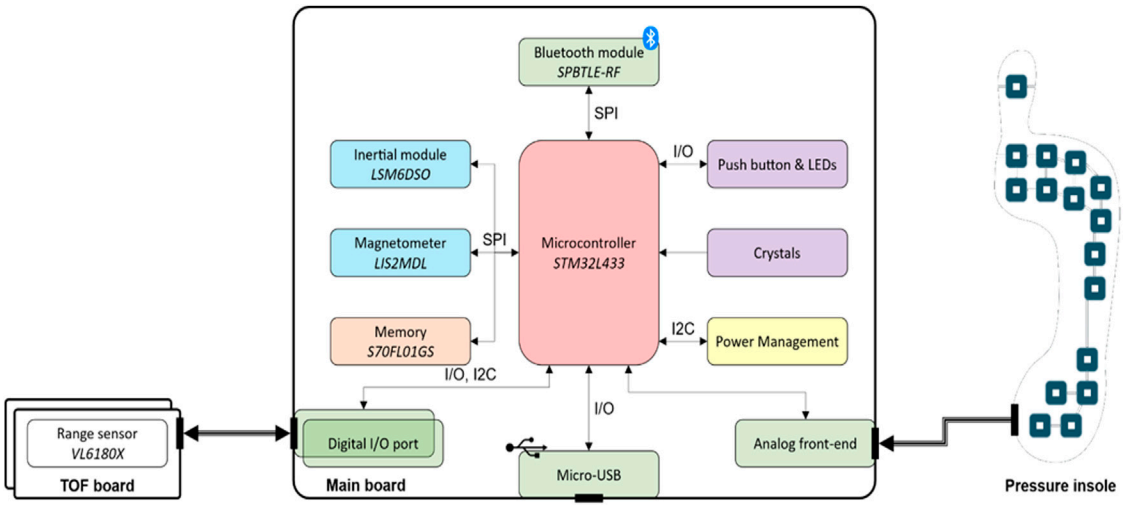

FIGURE 1
INDIP system architecture which includes the following components: Bluetooth Low Energy module SPBTLE-RF (mfr. STMicroelectronics), inertial module LSM6DSO (mfr. STMicroelectronics), magnetic module LIS2MDL (mfr. STMicroelectronics), memory (S70FL01GS, mfr. Infineon; up to 13 h of data logging), microcontroller STM32L433 (mfr. STMicroelectronics, ARM® Cortex®-M4 32-bit architecture), range sensor VL6180X sensor (mfr. STMicroelectronics).

incidence in both static and dynamic conditions, can be found in (Bertuletti et al., 2017).

- The force sensitive resistor pressure insole (PI) consists of 16 force sensing resistors, with an overall thickness of 240 µm, covered with a polyester layer. Each force sensing resistor exhibits a resistance value which is inversely proportional to the amount of the applied force and, when no force is applied, the sensor features an infinite resistance. As the applied force increases, the equivalent resistance of the sensor decreases. In this study, two different sizes have been used, one small (EU 36–37) and one large (EU 42–43).

2.2 Calibration refinement and characterization of the inertial sensor noise level

As sensor performance may deteriorate over time, regular refinements of the accelerometer and gyroscope calibration coefficients are recommended to compensate for residual cross-axis sensitivity and misalignments (Ferraris et al., 1995) (systematic errors). This is beneficial for ensuring good quality of the measurements and facilitating results comparability in multi-center validations. The calibration refinement of both accelerometers (Ferraris et al., 1995) and gyroscopes (Stančin and Tomažič, 2014) was carried out for each of the 72 INDIP IMUs deployed in this study, before their first use. Furthermore, each INDIP IMU was characterized in terms of noise level (random errors). This information was relevant for the optimal tuning of algorithm parameters to estimate orientation and displacement (Caruso et al., 2021a; Rossanigo et al., 2021). Moreover, the characterization of the magnitude of residual random and systematic errors for each signal allowed the setting of specific reference values to be used to identify poorly performing IMUs that need to be recalibrated or discarded. The characterization of the accelerometers and gyroscopes random errors was performed in accordance with *IEEE 2700–2017 Standard for Sensor Performance Parameter Definitions* (IEEE, 2017). In particular, the accelerometer and gyroscope standard deviation (STD) was computed during a 100 s static acquisition, while the gyroscope bias instability (i.e., slow fluctuations of the measurement offset described as a Gauss-Markov process with zero-mean (Unsal and Demirbas, 2012)) was quantified using the Allan variance during an 8-h static acquisition (El-Sheimy, Hou, and Niu, 2008).

2.3 Experimental measurement set-up

A pair of PIs were selected, according to the subject's foot size, and inserted between the insole and midsole of the shoes. Two magneto-IMUs were positioned over the instep and fixed to the shoelaces using custom-made clips, and a third magneto-IMU was attached to the lower back using an elastic belt with Velcro. To avoid mutual infrared interferences, distance sensors were positioned asymmetrically using Velcro straps (one just above the left ankle and the other about 3 cm higher on the right side), both pointing medially. Both PIs and distance sensors were connected *via* cable to the magneto-IMU of the corresponding foot (Figure 2).

To validate INDIP system, stereophotogrammetric technology was used, as it allows to accurately reconstruct the human movement also under complex motor tasks. In each laboratory, marker trajectories were recorded using the stereophotogrammetric system locally installed (Newcastle: 14-camera Vicon Bonita, Sheffield: 10-camera Vicon MX T160 Vicon Vero, Tel Aviv: 8-camera Vicon T10, Kiel: 12-camera Qualisys Miqus, Stuttgart: 8-

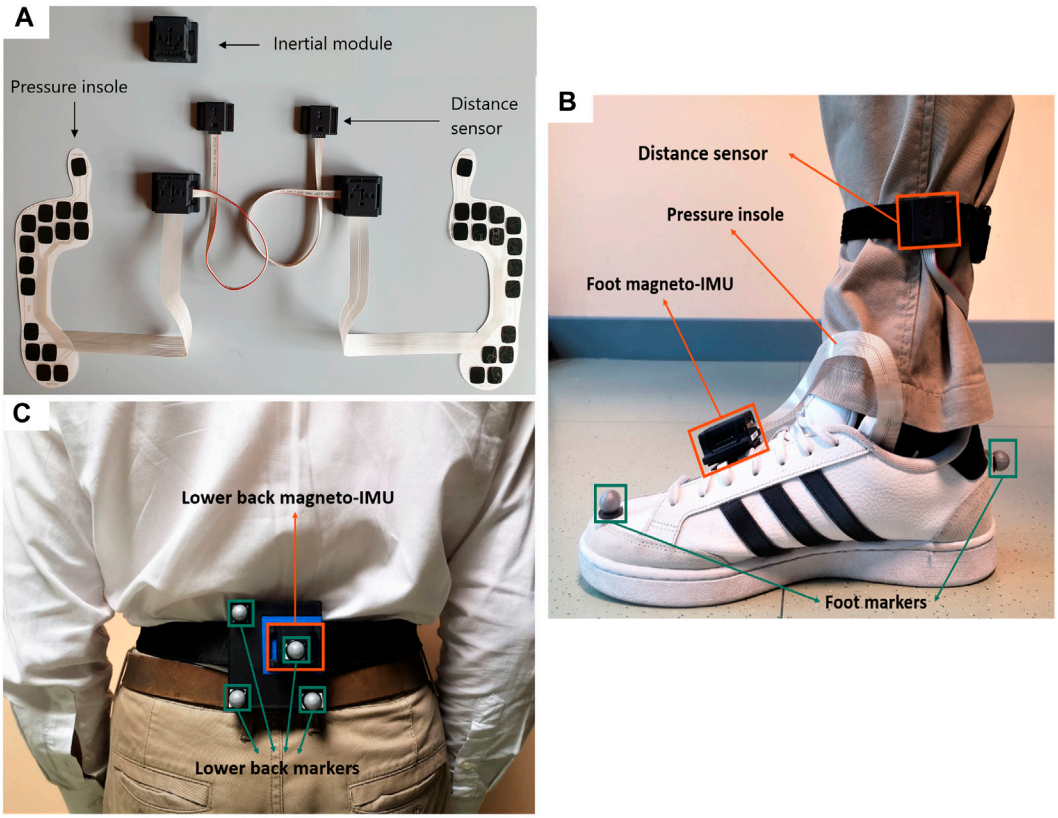

FIGURE 2
(A) Picture of INDIP system hardware. **(B)** Foot positioning, example on right foot (INDIP and stereophotogrammetric system markers). **(C)** Lower back positioning (INDIP and stereophotogrammetric system markers).

camera Vicon T10). A total of eight reflective markers were used: two markers on each foot (heel and toe), and four markers placed on a rigid cluster used as support for the lower back magneto-IMU (Figure 2). For each marker acquisition, a quality control procedure was followed to estimate random and systematic errors of the different stereophotogrammetric systems as described in (Della Croce and Cappozzo, 2000; Scott et al., 2021). The stereophotogrammetric and the INDIP systems, both acquiring at 100 Hz, were synchronized using an additional INDIP magneto-IMU as external trigger, connected to the stereophotogrammetric system *via* USB cable. To this end, the clock of each INDIP magneto-IMU, including the one adopted as external trigger, was set on the same timestamp before each experimental session.

2.4 Experimental protocol

The experimental protocol for the validation comprised eight different motor tasks for a total of eleven trials with an increasing level of complexity (Scott et al., 2022). These included simulated daily activities test and seven structured walking tests: Timed-Up and Go, straight walk at comfortable, slow, and fast speed (each repeated twice), L-test, Surface test, and Hallway test. The simulated daily activities test is the most complex and challenging task and was used to capture various daily activities expected in the real-world simulated in a lab environment (i.e., setting the table for dinner, sitting down for a short break, clearing the table etc.). The INDIP was also used during 2.5-h real-world acquisitions to test the usability of the system and the consistency of the extracted DMOs values with those found in literature. In this case, all participants were asked to continue with their daily routine, including some recommended activities such as: walking outside; walking along an inclined path; walking up and down stairs; moving from one room to another, etc. Further details about the experimental protocol can be found in (Mazzà et al., 2021; Scott et al., 2022).

Before any experimental session, each magneto-IMU underwent a preliminary 60 s short static spot-check to compute the gyroscope bias and verify that all the sensors (i.e., accelerometer, gyroscope) were working properly (Picerno, Cereatti, and Cappozzo, 2011). Quality of the PIs signals was checked by applying a direct finger pressure on each sensing unit separately.

2.5 Participants

The validation experiments involved two groups of healthy participants—young adults (HYA) and older adults (HOA)—and

TABLE 1 Cohorts descriptors and clinical parameters of the patient groups.

Cohort	Parameters						
	Participants recruited n)	Gender (M/F)	Age (years, mean ± STD)	Height (m, mean ± STD)	Body mass (kg, mean ± STD)	Walking aid users (n, general use, lab)	Clinical scale
HYA	20	11/9	29.4 ± 9.4	1.74 ± 0.09	70.2 ± 10.1	—	—
HOA	20	11/9	71.7 ± 5.8	1.66 ± 0.10	75.1 ± 11.8	1, 0	—
PD	20	16/4	69.8 ± 7.2	1.73 ± 0.07	78.2 ± 14.4	6, 1	UPDRS III* (mean ± STD, 28.4 ± 13.6)
							H&Y Scale* (I n = 4, II n = 11, III n = 5)
MS	20	11/9	48.7 ± 9.7	1.71 ± 0.13	84.0 ± 22.9	5, 3	EDSS* (mean ± STD, 3.5 ± 1.7)
COPD	17	9/8	69.4 ± 9.1	1.69 ± 0.07	73.7 ± 14.2	1, 0	CAT* (mean ± STD, 16.6 ± 8.9)
							FEV_{1*} (mean ± STD, 1.6 ± 0.6)
CHF	12	8/4	69.1 ± 11.7	1.74 ± 0.10	84.5 ± 16.8	4, 4	KCCQ* (mean ± STD 80.5 ± 20.2)
PFF	19	8/11	80.0 ± 8.5	1.69 ± 0.08	68.4 ± 16.0	13, 6	SPPB* (mean ± STD, 6.2 ± 3.9)

* CAT, COPD assessment test; EDSS, expanded disability status scale; FEV_1, forced expiratory volume; H&Y, hoehn and yahr scale; KCCQ, kansas city cardiomyopathy questionnaire; MDS-UPDRS, Movement Disorder Society-sponsored Unified Parkinson's Disease Rating Scale; SPPB, short physical performance battery.

five cohorts of patients with different diseases that impact mobility (PD, MS, COPD, CHF, PFF), totaling 128 participants (Table 1). All participants provided written informed consent before participating to the study (Ethics approval for the HYA: University of Sheffield Research Ethics Committee, Application number 029143; Ethics approvals for HOA and the cohorts of patients are reported in (Scott et al., 2022).

For the lab-based validation, each participant was equipped with the INDIP system and the reflective markers for the stereophotogrammetric system as depicted in Figure 2. For the real-world acquisitions, each participant was equipped with the INDIP system only. In addition, the HYA participating in the real-world experiment (n = 11/20) were asked to fill out a questionnaire regarding the INDIP system usability (Comfort Rating Scale, see Appendix B for more details). Patients were not asked to fill out the questionnaire since this was not the principal aim of the validation study.

2.6 Data cleaning, quality check, and processing

Data acquired with the INDIP system, both in laboratory and real-world acquisitions, underwent a quality check procedure and were discarded in case of technical issues associated with 1) partial data loss or synchronization failure due to trigger functioning or to timestamp setting procedure, and/or 2) deteriorated PI data quality. Moreover, stereophotogrammetric recordings were checked in case of gaps longer than 0.5 s due to occlusions (trials with gaps). In particular, trials with gaps were double checked to verify if the identification of the number of strides based on the stereophotogrammetric system was affected by the presence of gaps, in which case they were definitively discarded. Further details are reported in the Results section.

A pre-processing procedure was applied to refine the data synchronization among the INDIP IMUs and the stereophotogrammetric system over each data recording to prevent potential inaccuracy in the sample frequency or differences in clock stability. In particular, the recordings of the three mounted INDIP IMUs (started *via* Bluetooth at the beginning of each trial) were cut and interpolated using a common time vector provided by the external trigger with a synchronization error of ±10 ms (±1 frame).

2.7 INDIP algorithms for DMOs estimation

The estimation of the relevant spatial-temporal parameters from INDIP data consisted of the following steps, reported as a workflow in Figure 3:

- *Static/dynamic activity periods recognition*: this step was performed to identify dynamic activity intervals potentially including walking. The participant was considered "active" if the standard deviation of the total acceleration of both lower back and at least one foot were above thresholds, empirically chosen (0.7 and 2.1 m/s^2, respectively) (Lyons et al., 2005; Hickey et al., 2016).
- *Initial contact (IC) and final contact (FC) events detection*: temporal events were detected separately using the

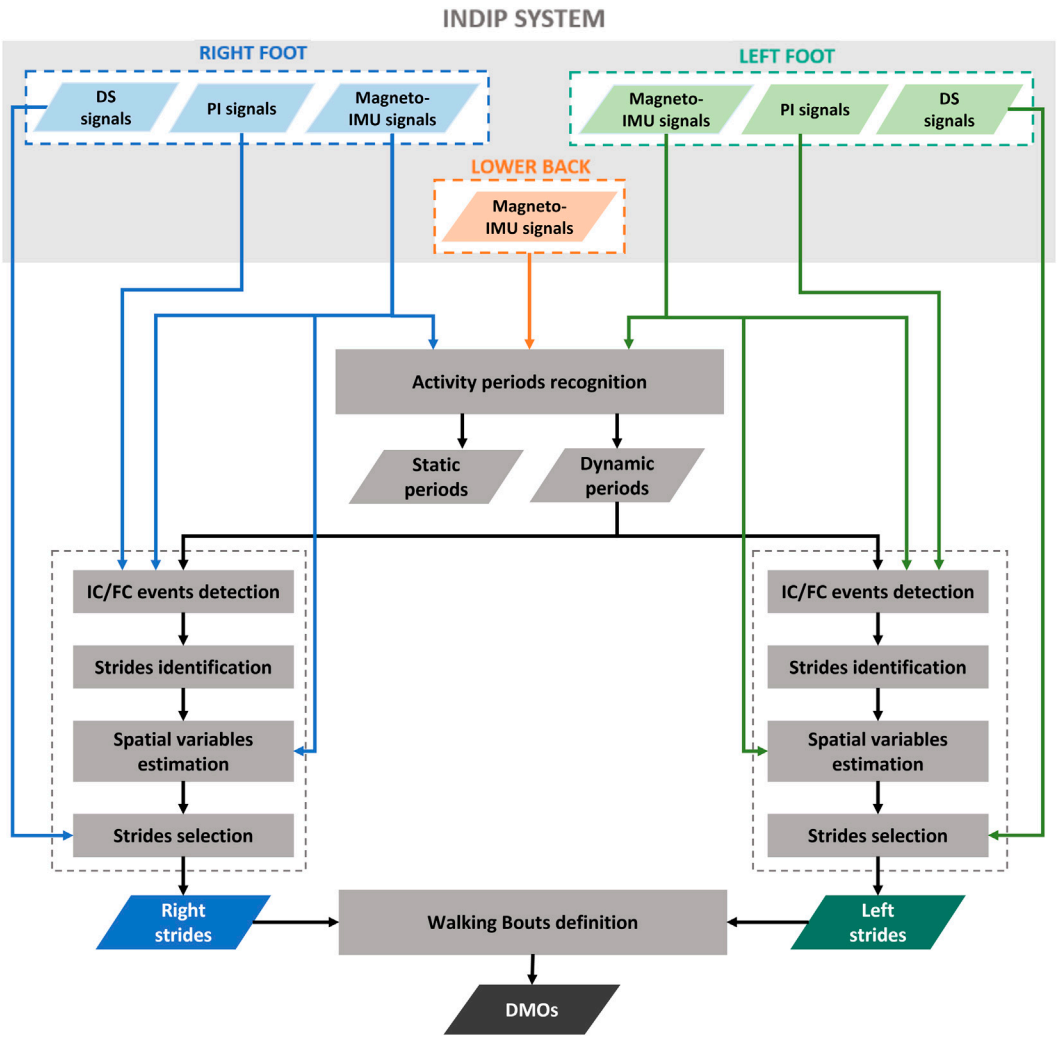

FIGURE 3
Workflow that shows the principal steps of INDIP algorithm.

information obtained from PIs signals and from magneto-IMUs on the subject's feet. The PI-method is based on the identification of activation/deactivation clusters of PI sensing elements belonging to the same neighborhood under the hypothesis that, when an IC or FC occurs, the sensing elements referring to the same anatomical region of the foot are activated or deactivated, respectively. A detailed description of the method is provided in (Salis et al., 2021a). The algorithm used to detect gait events from IMU signals is a modified version, adapted for foot mounted IMUs, of that proposed by Trojaniello and colleagues for shank positioning, which exploits invariant kinematic constraints to optimize the IC and FC search (Trojaniello et al., 2014).

Each event obtained from the PIs was associated with the closest event obtained from the feet magneto-IMUs within a tolerance interval of ±0.25 s. An event detected by both magneto-IMUs and PIs, or by the PIs only, was considered as a true event, and the value obtained from the PIs was assigned. The events detected by the feet magneto-IMUs only were included after verifying that the time interval identified between IC and FC corresponded to a stance phase. This was done by applying additional checks based on two detectors typically used for Zero velocity update technique (ZUPT) (Skog et al., 2010): 1) A threshold on the Angular Rate Energy detector signal (0.5 normalized unit). If the values of the angular rate energy were below the threshold for less than 100 ms, the corresponding IC and FC were discarded; 2) A threshold on the Moving Variance detector signal (0.005 normalized unit). If the values of the variance were below the threshold for less than 100 ms, the corresponding IC and FC were discarded.

- *Strides identification*: based on the detected temporal gait events, right and left strides were defined as the interval between two consecutive ICs of the same foot.
- *Spatial variables estimation*: stride velocity and displacement were computed from the linear acceleration recorded by feet

magneto-IMUs. First, a Madgwick filter was applied to obtain an accurate orientation estimate for each foot magneto-IMU (Madgwick, Harrison, and Vaidyanathan, 2011). This filter was chosen for its simplicity, as it requires the tuning of only one parameter (Caruso et al., 2020; Caruso et al., 2021b), and low computational burden (Caruso et al., 2021a). The parameter value was optimized by minimizing the error obtained on stride length estimates (Rossanigo et al., 2021). The drift associated to the acceleration signal was then reduced taking advantage of the cyclic nature of gait. ZUPT was applied, specifically using the Angular Rate Energy detector to identify the integration intervals, under the hypothesis that foot velocity is negligible during the mid-stance phase (Skog et al., 2010; Skog, Nilsson, and Peter, 2010; Peruzzi, Croce, and Cereatti, 2011). Finally, velocity and displacement were obtained with a direct and reverse integration approach (Zok, Mazzà, and Della Croce, 2004; Trojaniello et al., 2014). In particular, the procedure reported in (Trojaniello et al., 2014), well described in (Zok, Mazzà, and Della Croce, 2004), was adapted to feet positioning, according to what described in (Rossanigo et al., 2021), by exploiting the information obtained from ZUPT to: 1) define each integration instant as the time point in the middle of the corresponding ZUPT interval; 2) correct the velocity estimation in correspondence of the ZUPT intervals before integrating to obtain the displacement.

- *Strides selection*: based on temporal and spatial variables, a selection of right and left strides was performed by applying thresholds on specific stride relevant parameters agreed within the Mobilise-D consortium, including minimum (≥0.2 s) and maximum duration (≤3 s), and minimum length (≥0.15 m). Finally, for each selected stride, measures of the inter-leg distance obtained from the distance sensors were used as a further verification element of the correct stride identification procedure (Bertuletti et al., 2018).
- *Definition of Walking Bouts*: each walking bout was defined starting from the identification of left and right stride sequences separately. Two consecutive ipsilateral strides separated by a time interval lower than 3 s (short break) were considered as belonging to the same stride sequence. Left and right stride sequences were then combined to obtain the walking bouts, according to the matching of the corresponding time sequences. Initial and terminal phases of gait were discarded by removing the first and last stride of each walking bout, since the first and last IC are part of the transition from the previous and following activity, respectively. At this point, eligible walking bouts were selected according to the number of strides they included (minimum two left and two right strides) (Mazzà et al., 2021). An example of walking bout is shown in Figure 4.
- *Calculation of Digital Mobility Outcomes (DMOs)*: a complete set of primary and secondary DMOs were computed for each walking bout (Mazzà et al., 2021). For practical reasons, only a selected DMOs subset is reported:
  - o Walking bout duration (WB duration, s), walking bout length (WB length, m), and number of strides, all being informative of the general walking bout characteristics.
  - o Cadence (steps/min), being associated with the reliability of ICs identification, and computed as follows:

$$Cadence = \frac{\sum_{j=1}^{\#strides}\left(\frac{60}{Stride\_Duration_j}\right)}{\#strides} \times 2 \quad (1)$$

  - o Average stance duration (s) at walking bout level, associated with the reliability of both FCs and ICs identification (swing duration was not reported as it provides similar information).
  - o Average stride length (m) at walking bout level, being associated with the capability of accurately estimating displacement.
  - o Walking speed (m/s), informative of the correct estimate of both ICs and displacement, computed as:

$$Walking\ speed = \sum_{j=1}^{\#strides} \frac{Stride\_Length_j}{Stride\_Duration_j} \quad (2)$$

2.8 Description of the stereophotogrammetry algorithms for DMOs estimation

For the stereophotogrammetry-based method, relevant DMOs were quantified from pelvic and foot marker trajectories according to the method proposed by (Bonci et al., 2022). Briefly, foot

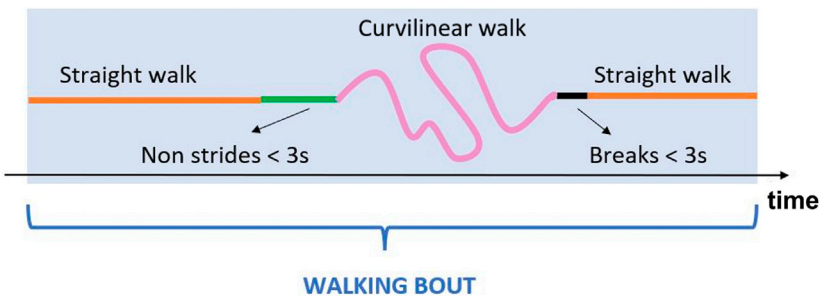

FIGURE 4
Example of a generic walking bout which includes straight walking, curvilinear walking, non-strides portions and short breaks.

trajectories were initially gap-filled only for gaps shorter than 0.5 s and all marker trajectories were filtered using a zero-lag fourth order Butterworth filter (cut-off frequency 7 Hz). As a first approximation, ICs and FCs estimates were chosen in correspondence of the instants of local maxima and minima displacements of the heel and toe markers from the pelvis, respectively. The latter estimates were then refined based on the 3D marker velocities, as detailed in (Bonci et al., 2022). Stride length and speed were measured from the heel marker trajectories between two subsequent ICs of the same foot. Strides and walking bouts were then selected following the same criteria adopted for the INDIP. The quality check procedure followed on the different stereophotogrammetric systems led to systematic errors among the different sites <2.5 mm (Scott et al., 2021).

2.9 Statistical analysis

The validation was performed by comparing the results from the INDIP with those provided by the stereophotogrammetric system. The analysis was conducted by aggregating the DMOs values, computed for each walking bout, at cohort level and considering the seven structured tests and the simulated daily activities separately, being the latter the only test that included activities which are different from gait (Scott et al., 2022). It is important to note that, while for the seven structured tests it was expected to detect a single walking bout for each trial, for the simulated daily activities test, a single trial can lead to one or more walking bouts. Only the walking bouts detected by both the systems have been included in the analysis (99% for both structured tests and simulated daily activities).

For example, let us consider a specific cohort composed by N subjects, and let suppose that subject i performs several trials corresponding to a number of walking bouts equal to m_i. The total number of walking bouts for the considered cohort is then

$$M = \sum_{i=1}^{N} m_i$$

For each DMO, mean and standard deviation values were computed for both stereophotogrammetric and INDIP systems over the M observations equal to the total number of walking bout detected for a given population ($\overline{DMO}_{SP}$; $\overline{DMO}_{INDIP}$).

In addition, for each DMO, errors (E_j) and relative errors ($E\%_j$) for the jth walking bout were computed as:

$$E_j = DMO_{INDIP,j} - DMO_{SP,j} \quad (3)$$

$$E\%_j = \frac{DMO_{INDIP,j} - DMO_{SP,j}}{DMO_{SP,j}} \times 100 \quad (4)$$

where $DMO_{INDIP,j}$ and $DMO_{SP,j}$ are the DMO values obtained from the INDIP system and the stereophotogrammetric system, respectively, for the jth walking bout with j = 1: M.

As the temporal variables are indirectly derived from stereophotogrammetric system, it is important to note that the values of E_j and $E\%_j$ computed for the temporal DMOs should be regarded as differences between the two systems rather than actual errors.

A normality test (Shapiro-Wilk test) was used to determine, for each cohort and all the relevant DMOs, if errors were normally distributed (Mishra et al., 2019). As the large majority of errors showed a non-normal distribution, median value, median absolute value, and interquartile range value of the errors were computed over the M walking bouts detected for the relevant cohort to describe INDIP performance in terms of bias, accuracy, and precision (Walther and Moore, 2005), together with mean value and mean absolute value to allow the comparison with previous studies.

Finally, for each DMO and cohort, the absolute agreement between the two systems was tested using Intraclass Correlation Coefficients ($ICC_{2,1}$: two-way random effects model, absolute-agreement, 95% confidence intervals (Koo and Li, 2016)) computed using SPSS Software, Version 28.0.1.1. Values lower than 0.5, between 0.5 and 0.75, between 0.75 and 0.9, and larger than 0.90 were indicative of poor, moderate, good, and excellent agreement, respectively (Koo and Li, 2016). A statistical power analysis was performed in Stata 16.1 as described in (Scott et al., 2022) to determine the minimum number of walking bouts needed for the validation, according to the desired ICC and the confidence interval values. The values obtained for a confidence interval width of 0.1 were: 401 (ICC ≥ 0.7), 295 (ICC ≥ 0.75), 200 (ICC ≥ 0.8), 119 (ICC ≥ 0.85), 56 (ICC ≥ 0.9) and 16 (ICC ≥ 0.95) walking bouts.

3 Results

3.1 Sensor noise characterization

The boxplot distributions of the accelerometer STD, gyroscope STD, and gyroscope bias instability computed over the 72 IMUs included in the above-described characterization procedure are shown in Figure 5.

3.2 The INDIP performance in laboratory

Across the 128 participants recorded in the laboratory experiments, the majority were able to complete the full protocol (100% for HYA and COPD, 95% for HOA, PD and MS, 92% for CHF and 68% for PFF). Four participants were excluded from the analysis due to technical issues in the acquisitions linked to data loss or synchronization failure (1 MS, 1 CHF, 2 PFF). In addition, data from five participants were discarded due to different technical problems which affected PI data quality (1 PD, 2 MS, 1 CHF, 1 PFF). In the laboratory gait assessment, data obtained from 119/128 participants (completion percentages: 100% HYA and COPD, 95% HOA and PD, 94% MS, 90% CHF, 69% PFF) were included in the analysis.

Among the 119 subjects considered, 44 had at least one trial with a gap in a foot marker trajectory longer than 0.5 s. As a result, 129 trials, out of the total 1,132 trials recorded, required further quality checks prior to inclusion in the analysis. This additional quality check led to 79 of the 129 *trials with gaps* being discarded from the structured tests (27 HOA, 2 PD, 5 MS, 1 COPD, 14 CHF, 30 PFF) and 4 trials from the simulated daily activities (2 HOA, 1 MS, 1 PFF). Overall, 963 walking bouts were analyzed for the

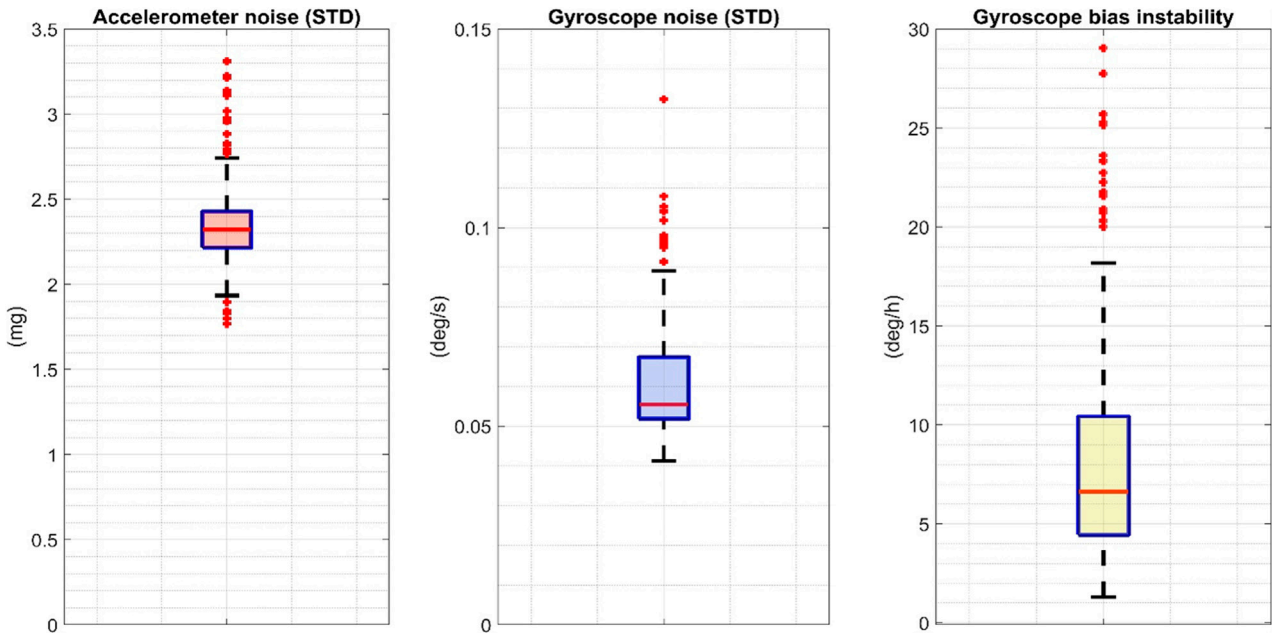

FIGURE 5
The boxplot distributions of the accelerometer and gyroscope STD and the gyroscope bias computed over 72 INDIP. STD: standard deviation.

TABLE 2 Number of Analyzed walking bouts and strides in laboratory (Structured and simulated daily activities tests) and real-world (2.5-h).

Cohort	*Laboratory*				*Real-world*	
	Structured tests		*SDA* test*			
	WBs (n)*	*Strides (n)*	*WBs* (n)*	*Strides (n)*	*WBs* (n)*	*Strides (n)*
HYA	189	2072	98	801	470	64,406
HOA	135	1,663	71	483	1,197	43,661
PD	157	2,219	67	593	557	26,812
MS	154	2084	49	494	484	16,493
COPD	135	1826	84	645	1,035	22,127
CHF	73	939	27	235	605	25,283
PFF	120	1946	35	433	531	15,273
TOTAL	963	12,749	431	3,684	4,879	213,945

*Abbreviations reported in the table: SDA, simulated daily activities; WBs, walking bouts.

structured tasks for a total of 12,749 strides, and 431 walking bouts for the simulated daily activities test including 3,684 strides (Table 2).

The results obtained from the comparison of INDIP and stereophotogrammetric systems are reported in Table 3 for the structured tests and in Table 4 for the simulated daily activities test. For each cohort and relevant DMO, descriptive statistics (M and STD) of the relevant DMOs values as estimated by INDIP and stereophotogrammetric system values are reported along with the agreement between distributions (ICC values). In addition, the following metrics were reported: mean error, mean absolute error and relative percentage values (*ME*, *MAE*, *ME%*, and *MAE%*); median error, median absolute error and relative percentage values (*MDE*, *MDAE*, *MDE%*, and *MDAE%*); interquartile range error and relative percentage value (*IQRE* and *IQRE%*).

3.2.1 Results from the structured tests

An excellent absolute agreement (ICC >0.95) was observed for the structured tests results in all cohorts and DMOs (Table 3). Moreover, the sample size resulted to be adequate in all cases. Considering the results obtained from all the cohorts, the

TABLE 3 Comparison between INDIP and stereophotogrammetric system for the relevant DMOs (structured tests).

DMO	Cohort	M ± STD * (INDIP)	M ± STD * (SP)*	*ME* (*ME* %) *	*MDE* (*MDE* %) *	*IQRE* (*IQRE%*)*	*MAE* (*MAE* %) *	*MDAE* (*MDAE%*) *	$ICC_{2,1}$ *
WB* duration (s)	HYA	7.16 ± 5.40	7.28 ± 5.41	−0.09 (−1.88%)	−0.03 (−0.52%)	0.06 (1.65%)	0.12 (2.39%)	0.03 (0.61%)	0.999
	HOA	7.95 ± 5.63	7.91 ± 5.63	−0.13 (−2.22%)	−0.03 (−0.41%)	0.09 (2.60%)	0.20 (3.09%)	0.04 (0.70%)	0.998
	PD	10.08 ± 7.60	10.29 ± 7.67	−0.07 (−0.91%)	−0.02 (−0.25%)	0.08 (1.42%)	0.26 (3.22%)	0.04 (0.51%)	0.998
	MS	9.80 ± 7.77	10.01 ± 7.83	−0.07 (−0.71%)	−0.01 (−0.11%)	0.08 (1.25%)	0.24 (2.82%)	0.03 (0.46%)	0.998
	COPD	8.93 ± 6.94	8.79 ± 6.88	−0.03 (−0.47%)	−0.01 (−0.10%)	0.06 (1.23%)	0.21 (2.92%)	0.03 (0.63%)	0.998
	CHF	9.16 ± 7.48	9.19 ± 7.35	−0.08 (−1.11%)	−0.03 (−0.42%)	0.07 (1.62%)	0.16 (1.89%)	0.05 (0.75%)	0.999
	PFF	11.58 ± 9.32	11.45 ± 8.96	0.13 (3.29%)	−0.02 (−0.33%)	0.10 (1.54%)	0.39 (4.35%)	0.05 (0.87%)	0.954
WB* length (m)	HYA	7.66 ± 5.56	7.48 ± 5.45	0.02 (0.19%)	0.05 (1.11%)	0.21 (2.78%)	0.22 (3.37%)	0.14 (2.18%)	0.998
	HOA	7.35 ± 5.41	7.11 ± 5.46	−0.06 (−0.44%)	0.03 (0.43%)	0.22 (4.79%)	0.24 (4.16%)	0.11 (2.50%)	0.998
	PD	7.37 ± 5.36	6.99 ± 5.21	0.00 (0.22%)	0.01 (0.20%)	0.29 (5.11%)	0.23 (3.96%)	0.15 (2.44%)	0.998
	MS	7.11 ± 5.28	7.04 ± 5.32	−0.03 (−0.26%)	0.01 (0.10%)	0.26 (4.79%)	0.25 (4.01%)	0.13 (2.46%)	0.997
	COPD	8.03 ± 6.39	7.90 ± 6.29	−0.01 (−0.45%)	0.01 (0.29%)	0.21 (3.61%)	0.21 (3.08%)	0.11 (1.80%)	0.999
	CHF	7.09 ± 5.18	6.70 ± 4.06	−0.04 (−0.30%)	0.02 (0.53%)	0.24 (4.48%)	0.20 (3.02%)	0.11 (2.25%)	0.997
	PFF	6.53 ± 4.74	5.56 ± 3.60	0.01 (1.05%)	0.01 (0.11%)	0.21 (4.17%)	0.29 (5.33%)	0.09 (1.89%)	0.975
Strides number	HYA	10.93 ± 8.97	11.04 ± 8.98	−0.08 (0.91%)	0.00 (0.00%)	0.00 (0.00%)	0.15 (1.64%)	0.00 (0.00%)	0.999
	HOA	12.42 ± 9.92	12.27 ± 9.86	−0.13 (−1.66%)	0.00 (0.00%)	0.00 (0.00%)	0.35 (3.03%)	0.00 (0.00%)	0.997
	PD	14.13 ± 11.68	14.53 ± 11.95	−0.17 (−0.88%)	0.00 (0.00%)	0.00 (0.00%)	0.41 (3.24%)	0.00 (0.00%)	0.998
	MS	13.38 ± 11.16	13.77 ± 11.31	−0.06 (−0.37%)	0.00 (0.00%)	0.00 (0.00%)	0.37 (3.10%)	0.00 (0.00%)	0.998
	COPD	13.53 ± 11.47	13.26 ± 11.37	−0.01 (0.01%)	0.00 (0.00%)	0.00 (0.00%)	0.30 (2.86%)	0.00 (0.00%)	0.998
	CHF	12.74 ± 10.80	12.64 ± 10.55	−0.02 (−0.59%)	0.00 (0.00%)	0.00 (0.00%)	0.25 (1.55%)	0.00 (0.00%)	0.998
	PFF	16.22 ± 13.80	16.15 ± 13.70	0.07 (2.71%)	0.00 (0.00%)	0.00 (0.00%)	1.00 (7.56%)	0.00 (0.00%)	0.970
Cadence (steps/min)	HYA	104.51 ± 18.04	103.45 ± 17.38	1.01 (0.92%)	0.30 (0.32%)	0.90 (0.87%)	1.21 (1.10%)	0.46 (0.46%)	0.990
	HOA	103.04 ± 17.36	102.50 ± 17.11	0.59 (0.58%)	0.23 (0.23%)	0.89 (0.85%)	0.96 (0.95%)	0.41 (0.38%)	0.995
	PD	93.64 ± 16.78	93.27 ± 16.66	0.36 (0.41%)	0.11 (0.10%)	0.76 (0.79%)	0.74 (0.80%)	0.27 (0.28%)	0.995
	MS	93.40 ± 18.48	93.55 ± 18.31	0.48 (0.69%)	0.08 (0.10%)	0.70 (0.78%)	0.89 (1.10%)	0.32 (0.33%)	0.994
	COPD	99.13 ± 18.03	98.96 ± 17.59	0.27 (0.26%)	0.10 (0.10%)	0.59 (0.61%)	0.53 (0.53%)	0.29 (0.29%)	0.998
	CHF	95.60 ± 17.14	94.43 ± 17.04	0.60 (0.61%)	0.22 (0.24%)	1.03 (1.20%)	1.19 (1.24%)	0.61 (0.59%)	0.992
	PFF	96.89 ± 19.53	96.52 ± 19.29	0.36 (0.33%)	0.34 (0.37%)	1.00 (1.02%)	0.91 (0.98%)	0.49 (0.52%)	0.998

(Continued on following page)

TABLE 3 (*Continued*) Comparison between INDIP and stereophotogrammetric system for the relevant DMOs (structured tests).

DMO	Cohort	M ± STD * (INDIP)	M ± STD * (SP)*	*ME* (*ME %*) *	*MDE* (*MDE %*) *	*IQRE* (*IQRE%*)*	*MAE* (*MAE %*) *	*MDAE* (*MDAE%*) *	$ICC_{2,1}$ *
Average Stride Length (m)	HYA	1.33 ± 0.17	1.32 ± 0.17	0.00 (0.29%)	0.01 (0.46%)	0.03 (2.19%)	0.03 (1.94%)	0.02 (1.73%)	0.980
	HOA	1.12 ± 0.16	1.13 ± 0.17	0.00 (0.19%)	0.00 (0.19%)	0.03 (2.97%)	0.03 (2.35%)	0.02 (1.44%)	0.968
	PD	1.04 ± 0.23	1.03 ± 0.23	0.01 (0.75%)	0.01 (0.92%)	0.04 (3.91%)	0.03 (2.58%)	0.02 (2.10%)	0.989
	MS	1.06 ± 0.22	1.06 ± 0.22	0.01 (1.09%)	0.01 (0.70%)	0.04 (3.75%)	0.03 (2.98%)	0.02 (1.96%)	0.978
	COPD	1.13 ± 0.15	1.13 ± 0.15	0.00 (0.08%)	0.01 (0.50%)	0.03 (3.09%)	0.02 (2.04%)	0.02 (1.49%)	0.986
	CHF	1.12 ± 0.26	1.12 ± 0.25	0.00 (0.02%)	0.00 (−0.04%)	0.04 (4.10%)	0.03 (2.46%)	0.02 (2.15%)	0.990
	PFF	0.88 ± 0.32	0.87 ± 0.32	0.00 (1.22%)	0.00 (0.27%)	0.03 (3.28%)	0.02 (3.85%)	0.01 (1.67%)	0.993
Walking Speed (m/s)	HYA	1.17 ± 0.30	1.15 ± 0.30	0.01 (1.22%)	0.01 (1.24%)	0.02 (2.07%)	0.02 (2.23%)	0.02 (1.82%)	0.993
	HOA	0.97 ± 0.25	0.97 ± 0.25	0.01 (0.95%)	0.01 (0.66%)	0.03 (3.27%)	0.02 (2.34%)	0.01 (1.62%)	0.989
	PD	0.82 ± 0.30	0.81 ± 0.29	0.01 (1.16%)	0.01 (1.19%)	0.03 (3.83%)	0.02 (2.67%)	0.02 (2.16%)	0.996
	MS	0.84 ± 0.29	0.84 ± 0.28	0.00 (0.31%)	0.01 (0.94%)	0.03 (3.47%)	0.02 (2.91%)	0.02 (2.07%)	0.994
	COPD	0.94 ± 0.25	0.94 ± 0.26	0.00 (0.30%)	0.01 (0.78%)	0.03 (2.87%)	0.02 (2.09%)	0.01 (1.64%)	0.992
	CHF	0.92 ± 0.34	0.90 ± 0.33	0.01 (0.67%)	0.00 (0.37%)	0.04 (4.18%)	0.02 (2.44%)	0.02 (2.01%)	0.996
	PFF	0.73 ± 0.35	0.72 ± 0.35	0.01 (1.57%)	0.00 (0.59%)	0.02 (3.39%)	0.02 (3.71%)	0.01 (1.74%)	0.996
Average Stance Duration (s)	HYA	0.78 ± 0.16	0.78 ± 0.17	0.00 (−0.02%)	0.00 (0.12%)	0.02 (2.38%)	0.02 (2.29%)	0.02 (2.02%)	0.990
	HOA	0.81 ± 0.16	0.80 ± 0.17	0.01 (1.30%)	0.01 (0.79%)	0.03 (3.88%)	0.02 (3.16%)	0.01 (2.05%)	0.978
	PD	0.89 ± 0.20	0.90 ± 0.21	−0.01 (−0.55%)	0.00 (−0.24%)	0.04 (4.15%)	0.03 (2.79%)	0.02 (2.28%)	0.984
	MS	0.91 ± 0.26	0.92 ± 0.27	−0.01 (1.64%)	−0.01 (−0.92%)	0.04 (4.16%)	0.03 (3.30%)	0.02 (2.20%)	0.975
	COPD	0.83 ± 0.16	0.84 ± 0.16	−0.01 (−1.00%)	−0.01 (−0.63%)	0.03 (4.17%)	0.02 (2.36%)	0.01 (1.84%)	0.986
	CHF	0.87 ± 0.20	0.89 ± 0.20	−0.01 (−1.76%)	−0.01 (−0.89%)	0.04 (4.24%)	0.03 (3.32%)	0.02 (2.21%)	0.976
	PFF	0.89 ± 0.26	0.90 ± 0.27	−0.01 (−1.48%)	−0.01 (−0.95%)	0.05 (5.81%)	0.04 (4.06%)	0.03 (2.93%)	0.975

*Abbreviations reported in the table: M ± STD: mean ± standard deviation; *ME (ME%)*: mean error (mean percentage error); *MDE (MDE%)*, median error (median percentage error); *IQRE (IQRE%)*, interquartile range error (interquartile range percentage error); *MAE (MAE%)*, mean absolute error (mean absolute percentage error); *MDAE (MDAE%)*, median absolute error (median absolute percentage error); $ICC_{2,1}$, intraclass correlation coefficient, SP, stereophotogrammetric; WB, walking bout.

structured tests showed, for all the DMOs, an *MDE%* between −1.0% and 1.3% and *ME%* between −2.22% and 3.29%. The absolute errors were very limited for all cohorts and DMOs, with *MDAE* values consistently lower than *MAE* values (*MDAE*: WB duration ≤0.05 s, WB length ≤0.14 m, average stance duration ≤0.03 s, average stride length ≤0.02 m, walking speed ≤0.02 m/s and cadence ≤0.61 steps/min; *MAE*: WB duration ≤0.39 s, WB length ≤0.29 m, average stance duration ≤0.04 s, average stride length ≤0.03 m, walking speed ≤0.02 m/s and cadence ≤1.21 steps/min).

In terms of percentage errors, we found *MDAE%* values <1% for WB duration and cadence, ≤2.1% for average stride length and walking speed, <3% for WB length and average stance duration. Stride number *MDAE%* observed are equal to zero in every case, as proof of a correct walking bout detection. The *MAE%* values were <5% across DMOs and cohorts except for slightly larger errors on stride numbers in PFF cohorts (7.6%, slowest cohort).

3.2.2 Results from the simulated daily activities test

Regarding this test, the same metrics are extracted for all the cohorts and DMOs (Table 4). The absolute agreement was excellent (ICC >0.90) in all the cohorts for WB length, average stride length, and walking speed, while it was between excellent and good for the remaining DMOs, except for few cases in which a moderate reliability, with ICC values ≥0.69, was observed (COPD, CHF for cadence and HOA, MS, and CHF for average stance duration, respectively). The sample size was adequate in all cohorts for WB length and walking speed, while analyses for some DMOs-cohorts combinations were under-powered (HOA and PFF for WB duration; PFF for stride number; HOA, PD, COPD, and CHF for cadence; HOA, MS, COPD, CHF, and PFF for average stance duration).

Strides number shows a zero bias for all cohorts (*ME* between −0.45 and 0.34), while the *MDAE* are between 0 (CHF,

TABLE 4 Comparison between INDIP and stereophotogrammetric system for the relevant DMOs (simulated daily activities test).

DMO	Cohort	M ± STD * (INDIP)	M ± STD * (SP)	*ME* (*ME* %) *	*MDE* (*MDE* %) *	*IQRE* (*IQRE* %) *	*MAE* (*MAE* %) *	*MDAE* (*MDAE%*) *	$ICC_{2,1}$ *
WB* duration (s)	HYA	7.83 ± 2.72	7.93 ± 2.71	−0.09 (−1.88%)	−0.03 (−0.52%)	0.72 (9.76%)	0.52 (6.49%)	0.22 (3.28%)	0.980
	HOA	6.00 ± 1.36	5.91 ± 1.36	−0.13 (−2.22%)	−0.03 (−0.41%)	0.78 (15.92%)	0.80 (14.73%)	0.41 (6.51%)	0.861
	PD	8.34 ± 3.46	8.68 ± 3.68	−0.07 (−0.91%)	−0.02 (−0.25%)	1.08 (13.23%)	0.89 (10.41%)	0.70 (7.54%)	0.963
	MS	9.20 ± 2.59	9.26 ± 2.68	−0.07 (−0.71%)	−0.01 (−0.11%)	1.39 (18.00%)	1.02 (12.56%)	0.69 (9.20%)	0.943
	COPD	6.94 ± 1.29	6.73 ± 1.22	−0.03 (−0.47%)	−0.01 (−0.10%)	1.18 (14.87%)	0.87 (13.24%)	0.08 (1.93%)	0.894
	CHF	10.62 ± 3.95	11.10 ± 4.33	−0.08 (−1.11%)	−0.03 (−0.42%)	0.13 (2.06%)	0.80 (6.64%)	0.06 (1.03%)	0.952
	PFF	10.60 ± 2.78	10.05 ± 2.73	0.13 (3.29%)	−0.02 (−0.33%)	1.44 (13.87%)	1.48 (20.03%)	0.66 (6.56%)	0.762
WB* length (m/s)	HYA	4.64 ± 1.35	4.30 ± 1.55	0.02 (0.19%)	0.05 (1.11%)	0.32 (8.49%)	0.26 (7.84%)	0.16 (4.21%)	0.970
	HOA	3.03 ± 0.54	3.18 ± 0.65	−0.06 (−0.44%)	0.03 (0.43%)	0.41 (14.38%)	0.33 (14.73%)	0.20 (5.94%)	0.938
	PD	3.59 ± 1.29	4.07 ± 2.03	0.00 (0.22%)	0.01 (0.20%)	0.56 (16.13%)	0.34 (10.46%)	0.24 (7.77%)	0.974
	MS	4.76 ± 1.53	4.03 ± 0.95	−0.03 (−0.26%)	0.01 (0.10%)	0.43 (17.84%)	0.30 (10.94%)	0.28 (7.41%)	0.981
	COPD	3.48 ± 1.14	3.39 ± 1.21	−0.01 (−0.45%)	0.01 (0.29%)	0.27 (8.42%)	0.19 (9.36%)	0.09 (3.75%)	0.980
	CHF	4.52 ± 1.64	4.22 ± 1.02	−0.04 (−0.30%)	0.02 (0.53%)	0.17 (6.79%)	0.19 (5.43%)	0.09 (2.65%)	0.981
	PFF	4.09 ± 1.78	3.63 ± 1.05	0.01 (1.05%)	0.01 (0.11%)	0.26 (8.82%)	0.34 (12.01%)	0.25 (6.82%)	0.944
Strides number	HYA	8.91 ± 3.25	9.09 ± 3.27	−0.08 (0.91%)	0.00 (0.00%)	1.00 (14.83%)	0.79 (8.62%)	1.00 (7.14%)	0.965
	HOA	7.12 ± 1.75	6.95 ± 1.89	−0.13 (−1.66%)	0.00 (0.00%)	1.00 (20.00%)	0.98 (15.20%)	1.00 (12.50%)	0.888
	PD	8.89 ± 3.78	9.08 ± 4.06	−0.17 (−0.88%)	0.00 (0.00%)	1.00 (13.29%)	0.97 (11.70%)	1.00 (9.76%)	0.962
	MS	11.14 ± 3.67	11.34 ± 3.57	−0.06 (−0.37%)	0.00 (0.00%)	2.00 (20.20%)	1.27 (11.80%)	1.00 (11.11%)	0.961
	COPD	7.87 ± 2.10	7.57 ± 2.19	−0.01 (0.01%)	0.00 (0.00%)	2.00 (20.00%)	1.07 (15.72%)	1.00 (9.09%)	0.912
	CHF	10.81 ± 3.80	11.32 ± 4.12	−0.02 (−0.59%)	0.00 (0.00%)	1.00 (11.11%)	0.73 (6.42%)	0.00 (0.00%)	0.968
	PFF	12.53 ± 4.02	11.91 ± 3.02	0.07 (2.71%)	0.00 (0.00%)	3.50 (35.00%)	2.34 (23.68%)	2.00 (17.64%)	0.815
Cadence (steps/min)	HYA	86.50 ± 9.94	85.27 ± 8.97	1.01 (0.92%)	0.30 (0.32%)	3.09 (3.74%)	2.72 (3.45%)	1.07 (1.39%)	0.929
	HOA	93.99 ± 8.97	91.64 ± 7.58	0.59 (0.58%)	0.23 (0.23%)	5.04 (5.92%)	4.36 (4.97%)	2.78 (2.62%)	0.867
	PD	83.40 ± 8.09	82.41 ± 10.18	0.36 (0.41%)	0.11 (0.10%)	3.35 (4.33%)	4.02 (4.61%)	2.14 (2.72%)	0.871
	MS	89.26 ± 8.38	87.63 ± 8.79	0.48 (0.69%)	0.08 (0.10%)	4.43 (5.01%)	3.14 (3.77%)	2.19 (2.45%)	0.902
	COPD	89.07 ± 9.54	86.32 ± 9.55	0.27 (0.26%)	0.10 (0.10%)	5.31 (6.29%)	4.87 (6.28%)	2.15 (2.42%)	0.733
	CHF	85.83 ± 11.23	82.27 ± 6.02	0.60 (0.61%)	0.22 (0.24%)	2.59 (2.74%)	3.26 (4.26%)	1.13 (1.37%)	0.740
	PFF	87.81 ± 10.31	88.50 ± 10.41	0.36 (0.33%)	0.34 (0.37%)	4.20 (4.32%)	3.63 (4.17%)	1.83 (2.39%)	0.918

(Continued on following page)

TABLE 4 (*Continued*) Comparison between INDIP and stereophotogrammetric system for the relevant DMOs (simulated daily activities test).

DMO	Cohort	M ± STD * (INDIP)	M ± STD * (SP)	*ME* (*ME %*) *	*MDE* (*MDE %*) *	*IQRE* (*IQRE %*) *	*MAE* (*MAE %*) *	*MDAE* (*MDAE%*) *	$ICC_{2,1}$ *
Average Stride Length (m)	HYA	0.99 ± 0.14	0.97 ± 0.14	0.00 (0.29%)	0.01 (0.46%)	0.06 (7.25%)	0.05 (7.20%)	0.04 (3.77%)	0.965
	HOA	0.83 ± 0.17	0.80 ± 0.11	0.00 (0.19%)	0.00 (0.19%)	0.09 (12.34%)	0.06 (9.96%)	0.04 (5.50%)	0.939
	PD	0.74 ± 0.13	0.72 ± 0.16	0.01 (0.75%)	0.01 (0.92%)	0.05 (8.07%)	0.05 (8.77%)	0.04 (5.71%)	0.963
	MS	0.81 ± 0.16	0.79 ± 0.13	0.01 (1.09%)	0.01 (0.70%)	0.09 (11.83%)	0.06 (7.88%)	0.04 (6.01%)	0.934
	COPD	0.82 ± 0.11	0.82 ± 0.12	0.00 (0.08%)	0.01 (0.50%)	0.05 (8.82%)	0.04 (6.99%)	0.03 (3.73%)	0.981
	CHF	0.80 ± 0.14	0.81 ± 0.13	0.00 (0.02%)	0.00 (−0.04%)	0.04 (6.51%)	0.05 (7.17%)	0.02 (2.21%)	0.927
	PFF	0.63 ± 0.12	0.62 ± 0.11	0.00 (1.22%)	0.00 (0.27%)	0.09 (16.07%)	0.05 (8.95%)	0.05 (8.89%)	0.939
Walking Speed (m/s)	HYA	0.73 ± 0.16	0.71 ± 0.16	0.01 (1.22%)	0.01 (1.24%)	0.05 (10.86%)	0.04 (8.24%)	0.03 (4.94%)	0.978
	HOA	0.66 ± 0.18	0.63 ± 0.11	0.01 (0.95%)	0.01 (0.66%)	0.06 (13.32%)	0.05 (11.21%)	0.03 (6.82%)	0.942
	PD	0.52 ± 0.13	0.51 ± 0.11	0.01 (1.16%)	0.01 (1.19%)	0.03 (8.38%)	0.03 (8.31%)	0.02 (5.20%)	0.975
	MS	0.61 ± 0.15	0.58 ± 0.13	0.00 (0.31%)	0.01 (0.94%)	0.08 (12.70%)	0.05 (9.14%)	0.03 (7.03%)	0.944
	COPD	0.61 ± 0.10	0.60 ± 0.10	0.00 (0.30%)	0.01 (0.78%)	0.04 (8.91%)	0.03 (8.23%)	0.02 (3.33%)	0.983
	CHF	0.58 ± 0.08	0.57 ± 0.10	0.01 (0.67%)	0.00 (0.37%)	0.05 (10.08%)	0.03 (6.60%)	0.02 (3.20%)	0.973
	PFF	0.46 ± 0.08	0.46 ± 0.07	0.01 (1.57%)	0.00 (0.59%)	0.06 (13.75%)	0.04 (8.91%)	0.03 (7.10%)	0.939
Average Stance Duration (s)	HYA	1.04 ± 0.11	1.08 ± 0.14	0.00 (−0.02%)	0.00 (0.12%)	0.09 (6.94%)	0.07 (6.61%)	0.05 (5.10%)	0.860
	HOA	0.97 ± 0.12	0.98 ± 0.12	0.01 (1.30%)	0.01 (0.79%)	0.12 (12.13%)	0.10 (9.72%)	0.06 (6.06%)	0.737
	PD	1.07 ± 0.12	1.09 ± 0.12	−0.01 (−0.55%)	0.00 (−0.24%)	0.11 (9.76%)	0.07 (5.96%)	0.05 (4.18%)	0.911
	MS	1.00 ± 0.14	1.05 ± 0.15	−0.01 (1.64%)	−0.01 (−0.92%)	0.11 (10.62%)	0.08 (7.81%)	0.06 (5.48%)	0.716
	COPD	1.03 ± 0.09	1.07 ± 0.09	−0.01 (−1.00%)	−0.01 (−0.63%)	0.07 (6.39%)	0.07 (6.44%)	0.03 (3.82%)	0.828
	CHF	1.10 ± 0.22	1.21 ± 0.35	−0.01 (−1.76%)	−0.01 (−0.89%)	0.06 (6.08%)	0.11 (7.65%)	0.03 (3.15%)	0.690
	PFF	1.01 ± 0.14	1.03 ± 0.15	−0.01 (−1.48%)	−0.01 (−0.95%)	0.11 (11.79%)	0.08 (8.13%)	0.05 (5.75%)	0.854

*Abbreviations reported in the table: M ± STD: mean ± standard deviation; *ME (ME%)*, mean error (mean percentage error); *MDE (MDE%)*, median error (median percentage error); *IQRE (IQRE%)*, interquartile range error (interquartile range percentage error); *MAE (MAE%)*, mean absolute error (mean absolute percentage error); *MDAE (MDAE%)*, median absolute error (median absolute percentage error); $ICC_{2,1}$, intraclass correlation coefficient; SP, stereophotogrammetric; WB, walking bout.

MAE 0.73) and 2 (PFF, *MAE* 2.34) across cohorts, with *MDAE%* ranging from 0% (CHF, *MAE%* 6.42%) to 17.64% (PFF, *MAE%* 23.68%). Due to the differences in strides number, also the *MDAE* and *MAE* obtained for the other DMOs were in general moderately higher with respect to those obtained for the structured tests. For instance, *MDAE* for walking speed ranged between 0.02 m/s and 0.03 m/s (*MAE* between 0.03 m/s and 0.05 m/s), while *MDAE%* ranged between 3.2% and 7.1% (*MAE* between 6.6% and 11.21%).

3.3 The INDIP real-world outcomes

The same participants were also involved in a 2.5-h unsupervised recording (except for the HYA for which we have a subset of 11/20 subjects) for a total of 119 participants. The duration of the acquisition reached the expected value in most of the cases (89%, the remaining 11% had a recording duration between 27 and 123 min). Five participants were excluded due to technical issues in the acquisitions (1 PD, 1 MS, 3 PFF), while 18 participants were discarded due to different technical problems which affected PI data quality during the recordings (3 HOA, 4 PD, 5 MS, 1 CHF, 5 PFF) (see Paragraph 2.6). Results on the real-world acquisitions are hence computed on 96/119 participants (81%). For the real-world experiments, 4,879 walking bouts were analyzed including 213,945 strides (Table 2).

Table 5 includes the characteristics (min, max and interquartile range values) of the walking bouts detected with the INDIP system in terms of WB duration, WB length and strides number for each cohort. Figure 6 shows the boxplots obtained for a subset of DMOs (cadence, average stride length and walking speed) for each group of participants. Results from

TABLE 5 INDIP Outcomes for duration, total length and strides number (2.5-h real world experiments).

	Cohort	Min-max values*	IQR* value
WB* duration (s)	HY	2.79–1,442.70	46.72
	HA	2.31–1,493.59	12.52
	PD	2.74–1741.60	14.90
	MS	2.82–814.49	15.55
	COPD	2.44–638.52	11.60
	CHF	2.36–1,090.32	13.76
	PFF	2.59–381.21	16.77
WB* length (m)	HY	0.75–2,105.02	42.47
	HA	0.51–1913.74	7.28
	PD	0.49–2,430.50	9.32
	MS	0.62–1,225.93	8.55
	COPD	0.60–699.69	6.28
	CHF	0.59–1,586.70	10.74
	PFF	0.76–425.96	7.71
Strides number	HY	4–2,779	74
	HA	4–2,450	17
	PD	4–3,101	20
	MS	4–1,634	20
	COPD	4–1,081	15
	CHF	4–1766	20
	PFF	4–643	22

*Abbreviations used in the table: IQR, interquartile range; Min, minimum; Max, maximum; WB, walking bout.

the usability questionnaires filled by the 11 HYA are reported in Appendix B.

4 Discussion

In this study, we presented and validated the INDIP, a multi-sensor wearable system specifically conceived for gait assessment under ecologically valid conditions. The system was deployed within the Mobilise-D project (Mobilise-D 2019) for assessing the technical validity of the DMOs estimated based on a single-device attached to the lower trunk for long-term daily-life mobility assessment (Mazzà et al., 2021; Micó-amigo et al., 2022; Scott et al., 2022).

4.1 INDIP hardware and algorithms

To ensure transparency, reproducibility and replicability, a thorough description of INDIP system hardware have been provided. Moreover, each of the state-of-the-art algorithms included in the INDIP computational pipeline has been previously described, validated under standard and controlled conditions (Trojaniello et al., 2014; Bertoli et al., 2018; Bertuletti et al., 2019), and specifically optimized for gait assessment. It is important to highlight that, to compute the DMOs according to the definition and the minimum requirements for strides and walking bouts (as agreed within the Mobilise-D consortium (Kluge et al., 2021)), it is necessary to perform a stride-by stride resolution gait analysis, independently of the DMOs aggregation level (e.g., across walking bout, across subjects, across cohort). Temporal gait events were directly measured from the foot-ground contacts detected using 16 force-resistive sensors integrated in the PIs, applying a clustering approach for increasing robustness to noise (Salis et al., 2021a). Similarly, spatial parameters were determined based on the double integration of accelerometric signals recorded by the IMUs attached to the feet, which may benefit from gravity removal and zero-velocity update techniques for noise reduction during walking (Sabatini, 2005; Skog et al., 2010; Rebula et al., 2013; Trojaniello et al., 2014).

4.2 INDIP calibration refinement and noise description

The quality and uniformity of the sensor data collected during the experiments were rigorously verified. In fact, the performances of low-cost miniaturized IMUs, commonly employed in human movement monitoring, aren't as stable as those of IMUs used in

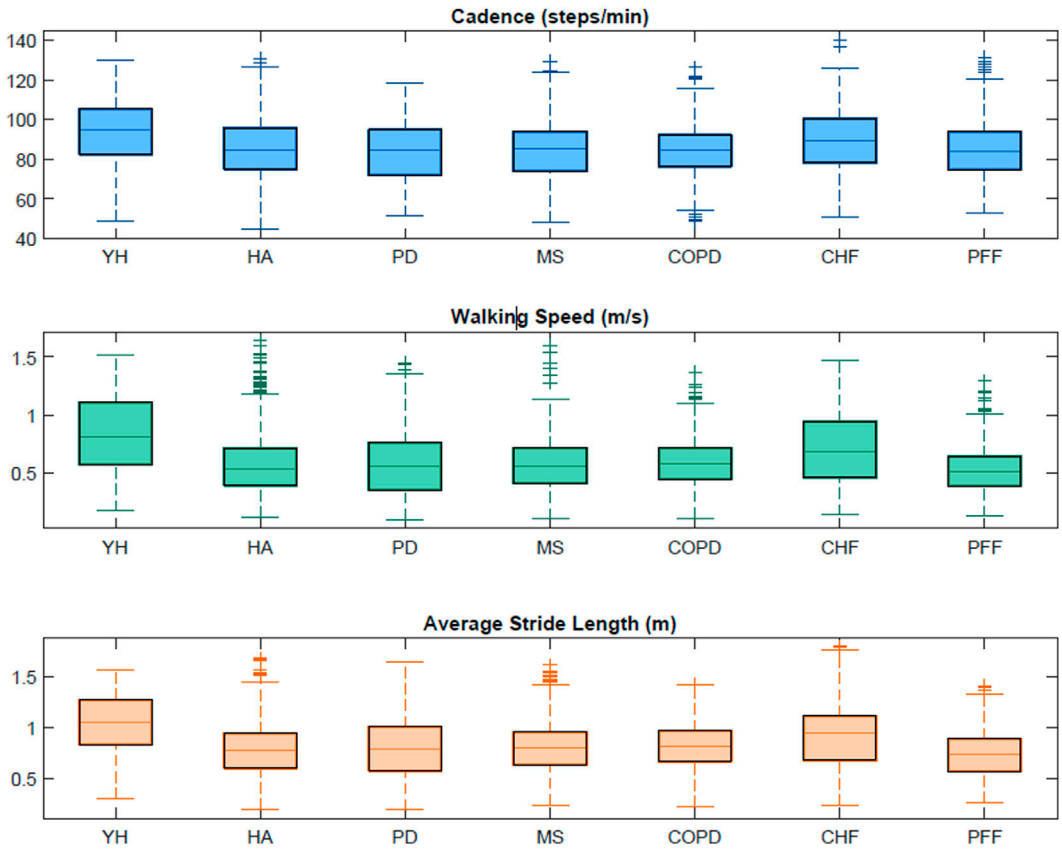

FIGURE 6
Boxplots obtained from the INDIP system for cadence, average stride length and walking speed for each cohort in the 2.5-h acquisitions.

navigation applications (Nez et al., 2016). For this reason, it is good practice—when possible—to perform appropriate quality checks, and to eventually refine calibration parameters based on in-field procedures proposed in the literature (Stančin and Tomažič, 2014). In this validation study, sensor characterization and recalibration were performed on all the 72 IMUs used by the five laboratories to verify that each sensor had similar metrological performance and thus facilitating the comparison of the results obtained for the different centers. Furthermore, the description of the noise statistics for both the accelerometers and gyroscopes deployed enabled the setting of reference values for sensor stochastic noise, and the elimination of those sensors which did not satisfy metrological requirements (two IMUs with STD values exceeding by 15% the STD maximum values found for the accelerometers and the gyroscopes distributions–3.31 mg and 0.13 dps, respectively).

4.3 INDIP performance validation

A key aspect of this study concerns the efforts devoted to the assessment of the INDIP system performance (Mazzà et al., 2021). In principle, when establishing a new reference method, attention should be paid in validating the estimated DMOs under conditions similar to those of its intended use, that in this context are represented by real-world mobility. However, in practice, this is often not possible due to the lack of well-established valid gold standard solutions for the entire set of gait metrics of interest (Del Din et al., 2016). To overcome this paradox, we tested the INDIP system through an experimental protocol specifically designed and validated (Scott et al., 2022) for simulating several real-world walking conditions in terms of: 1). Complexity and heterogeneity of the motor tests recorded including not only straight walking but also turnings, obstacles, different surfaces, standing and sitting on a chair and intermittent gait due to interaction with objects of the typical home daily life; 2). Types of target populations analyzed (seven different cohorts including normal gait in young and older adults, neurological disorders, orthopedic pathologies, and cardio-respiratory disorders); 3). Broad range of walking speeds, from 0.46 m/s (PFF, simulated daily activities test) to 1.15 m/s (HYA, structured tests) on average; 4). Technical reproducibility (multi-centric data collection carried on five different gait analysis laboratories).

In general, the INDIP system showed very good performance, similar across motor tests and cohorts, supporting the robustness of algorithm's estimate for a large variety of gait patterns. In particular, the results of the structured motor tests showed excellent concurrent validity between the stereophotogrammetry and INDIP estimates, with ICC values ranging between 0.95 and 0.99 across cohorts and DMOs. Similarly, the accuracy was very high for all the DMOs-cohorts combinations, with *MDAE%* less than 2.93% (Table 3). Precision as represented by interquartile range values was very good

for all DMOs and cohorts (<5.2%) with the largest dispersion observed for average stance duration in PFF (5.81%), which is also the cohort with the most frequent use of walking aids (in general, 13/19 PFF patients recruited were walking aid users, Table 1).

As expected, slightly larger errors were observed for the simulated daily activities test, which is characterized by multiple shorter walking bouts separated by motor activities other than walking (i.e., setting the table, moving chair and other objects, etc.). On average, the WB length for this test (3–4 m) was half that observed for the structured tests, resulting in an inevitable increase in DMOs relative errors. For instance, a difference of a single stride between the stereophotogrammetric system and INDIP system led to a relative error from 7.14% to 12.50% depending on the specific cohort analyzed. In general, concurrent validity was excellent for all cohorts for both average stride length and walking speed (ICC >0.94) whereas a larger variability was observed for average stance duration and cadence (ICC values between 0.71 and 0.93). Accuracy level was also good with *MDAE* of 1-2 strides for stride number, smaller than 0.05 m for the average stride length (*MDAE%* ≤ 8.89%), and smaller than 0.03 m/s for walking speed (*MDAE%* ≤ 7.10%) across cohorts.

As the DMOs error distributions were negatively skewed, mean errors were higher with respect to median errors. In fact, the last ones are less sensitive to outliers due to the asymmetry that characterizes error distributions and the data cleaning procedure applied. Interestingly, the INDIP system showed similar performance across tests and cohorts. These findings support the robustness of the algorithm's estimate for a large variety of different gait patterns. It should be also highlighted that the INDIP system performance was assessed on relatively short walking bouts (length <8 m; number of strides <16.5) which represent critical and challenging experimental conditions compared to motor tests including longer walking bout characterized by more regular and predictable gait patterns (Micó-amigo et al., 2022). This is the worst-case situation, thereby yielding the most conservative estimates.

4.4 Comparison with the literature

The choice of reporting both mean and median errors enabled a direct comparison of the results with studies based on different metrics (Trojaniello et al., 2014; Bertoli et al., 2018; Bonci et al., 2022; Micó-Amigo et al., 2022). It is interesting noting that the errors associated with the spatial-temporal parameters estimated by the INDIP were in general larger than those reported by (Trojaniello et al., 2014) and (Bertoli et al., 2018), from which INDIP IMU-based algorithms were derived and refined. Although a direct errors comparison is not possible as errors were computed at different aggregation levels (stride-level versus walking bout level), it is possible to observe that, in Bertoli et al. (Bertoli et al., 2018), stride length mean absolute errors were on average 2% (about 25 mm) for PD patients, compared to errors of 30 mm (structured tests) and 50 mm (simulated daily activities test) found with the INDIP system for the same cohort. Such differences may be explained considering that the original methods (Trojaniello et al., 2014; Bertoli et al., 2018) were validated on gait data recorded for 1 min while the subject was walking on a 12-m-long straight walkway, without including much more complex and challenging motor tests as in the present study. These observations further support the importance of testing the proposed methods under conditions like those usually encountered in real world scenarios (intermittent walking including turning, short walking bouts, breaks and higher gait variability).

In the last decades, several methods based on wearable sensors for mobility assessment (Iosa et al., 2016) have been developed, with a particular attention to feet/shanks IMUs approaches. However, in most of the studies, validation was limited to straight walking, normal gait, or to the evaluation of temporal parameters only. For example, Gastaldi and colleagues (Gastaldi et al., 2015) compared the results obtained from two IMUs with those of a footswitch-based system (STEP 32 footswitches); data were collected on one healthy subject while walking on a 12 m straight path for three times, obtaining relative errors below 5% for cadence computed at trial level. Also Zhou and colleagues (Zhou et al., 2020) tested an algorithm based on two feet mounted IMUs (Physiolog→5 IMUs, Gait Up) against an OptoGait system, using straight walk data collected on five young healthy participants. The stride-by-stride comparison led to root mean square errors of 0.05 m (3%) for stride length. The results obtained with the INDIP system under similar conditions (healthy participants for the structured tests), showed smaller errors both for cadence (MAE% about 1%) and average stride length (MAE 0.03 m). Jakob and colleagues (Jakob et al., 2021) validated a wearable system (Portabiles-HCT GaitLab-System, including two IMUs positioned inside the shoes) on 33 PD patients during straight walk, using the stereophotogrammetry as reference. The method performance was evaluated in terms of ICC values and results were excellent (0.986 for walking speed and 0.985 for stride length) but lower than found with the INDIP system (ICC of 0.996 for walking speed and 0.989 for average stride length in PD patients during structured tests).

Recently, Romijnders and colleagues (Romijnders et al., 2021) stressed the importance of assessing the performance of methods for daily-life use during curved walking and dual-task conditions. With this purpose, they proposed and validated a shank IMU-based algorithm for gait events detection on HOA, PD patients and stroke patients walking in three conditions (straight walk, slalom walk, and dual task walk along an elliptical path). Very good performances were found in terms of recall, precisions against the stereophotogrammetric system (recall between 85% and 100%, precision 95%–100% for HOA and PD). The INDIP system showed similar or better performance, in terms of accuracy based on the number of detected strides (97% for HOA and 98% for PD), across more complex motor tasks.

More recently, it has become evident that there is a need of extending the validation during real-world conditions, comparing IMU-based methods against pressure insoles for the estimation of temporal parameters. For example, Storm and colleagues (Storm, Buckley, and Mazzà, 2016) validated two algorithms, one based on two shank IMUs and the other on one waist IMU, using pressure insoles as reference. Data were collected on ten healthy participants, both indoor and outdoor, while performing straight walking and curvilinear walking, for a total of five different tasks. Among the gait parameters presented, also stance duration was computed, obtaining an average absolute error around 0.04 s for the shank method and around 0.03 s for the waist method across all the tasks. Another relevant work is that proposed by Roth and colleagues (Roth et al., 2021b), in which they

validated a pipeline based on foot mounted IMUs against force sensitive resistor pressure insoles. Their performance was evaluated using data collected on 20 healthy participants in supervised real-world conditions (level walking, stairs ascending and stairs descending at normal, slow and fast speed). The authors reported mean absolute error on stance duration about 0.02 s on level walking, 0.03 s ascending, 0.02 s descending, comparable with those obtained from the INDIP based method for the average stance duration in the structured tests (MAE 0.02 s for both HYA and HOA).

Some studies have proposed to use a multi-technology approach for gait analysis (Schepers et al., 2009; Van Meulen et al., 2016; Li et al., 2018; Refai et al., 2018; Tang et al., 2019; Duong et al., 2022), but very few studies characterized the performance of those systems in estimating DMOs against a ground truth reference. An interesting but preliminary study was presented by Li and colleagues (Li et al., 2018), who developed a multi-sensor system including three force sensors (positioned at the heel, arch and forefoot to detect IC and FC), an IMU and four range sensors for each foot. The study involved four healthy male participants and the stereophotogrammetric system was used as reference, obtaining average relative errors - computed among all subjects and trials—of 9.34% for stride length and 5.90% for stride velocity on straight walks (against a MAE% of 2.23% for walking speed and 1.94% for average stride length in HYA from INDIP system). A multi-sensor system with a sensor configuration similar to the INDIP has been recently proposed by Duong and colleagues (*SportSole II)* (Duong et al., 2022). It includes two instrumented insoles, with eight force sensitive resistor elements, each connected to an IMU attached to the shoe. Data were collected on eleven HYA while performing a series of different activities (including tasks with straight walk, curves and stairs). However, the system performance was validated only for selected gait portions (the subject walking on the instrumented walkway during straight or curvilinear portions), and on normal gait. Data were processed using a support vector regression (SVR) based algorithm, obtaining a good performance (*MAE%* structured session: 2.97% for stride length and 3.16% for stride velocity; *MAE%* unstructured session: 3.55% for stride length and 3.59% for stride velocity), but lower than that obtained with the INDIP for the structured tests (*MAE%* 1.94% for average stride length and 2.23% for walking speed). In general, compared to previous studies, the INDIP method showed better or similar performances in the DMOs estimation based on a more complex validation design—both in terms of motor activities analyzed or motor gait impairments diversity—than what is currently being achieved.

4.5 INDIP usability in the real-world

Consistency of INDIP outputs was tested during 2.5 h of unsupervised acquisitions on the same participants involved in the laboratory experiments, while acceptability of the device, wearability and usability factors were also examined for the HYA participants (Appendix B). Regarding the 2.5 h real-world experiments, a wider range of WB durations was explored (from a minimum of 2.3 s to a maximum of 1741.6 s), which leads to WB lengths ranging from 0.49 m to 2,430.50 m. The minimum number of strides (four in all cohorts) was determined by the walking bout definition while a maximum value of 3,101 strides was observed for a PD patient. Extracted stride length values ranged from 0.19 m to 1.8 m (for definition the minimum stride length is 0.15 m) along with a very broad range of walking speeds from very slow (0.1 m/s) to very fast (1.6 m/s) and cadence values ranging from 44.69 steps/min (HOA) to 139.95 steps/min (CHF). It is important to notice that the values obtained for this subset of DMOs resulted to be consistent with those found in literature (Sofuwa et al., 2005; Panizzolo et al., 2014; Thingstad et al., 2015; Dujmovic et al., 2017; Iwakura et al., 2019). In general, during the 2.5 h acquisition, the INDIP resulted to be well accepted and no major technical or usability issues were declared.

4.6 Limitations and methodological choices

The findings of this study must be evaluated considering some limitations and specific methodological choices:

- The INDIP system in its full configuration requires sensors to be attached to the feet, shanks and lower trunk and sensor redundancy clearly limits wearability. For this reason, the INDIP is more suitable for a complete description of mobility performance rather than for long-term monitoring, for which a single-IMU solution is certainly preferable.
- The INDIP sensor redundancy was exploited for identifying gait events and detecting strides from pressure, inertial, and distance signals. For this study, it was decided to prioritize sensitivity to avoid missing events. However, stride detection specificity could be increased by selecting only strides identified by all the three types of sensors (i.e., gait events detected from both PI and foot mounted IMU, and non-zero DS measure during the stride interval).
- In this study, the distance sensors have not been properly integrated in a sensor fusion process. These sensors provide the inter-leg distance measure as further information (Bertuletti et al., 2018; Rossanigo et al., 2023), but the validation of this gait parameter was out of the scope of the present study.
- The PIs used are based on a low-cost technology (force sensitive resistor) with an expected lifetime of about 30 h, followed by an inevitable deterioration of the performances. Therefore, when the signal quality was no longer considered sufficient, PIs data was not used, and the trial was discarded from the here-presented analysis. The number of discarded acquisitions can be reduced ensuring the proper functionality of the adopted PIs before each data acquisition.
- The technical complexity associated to the implementation of multi-center experimental sessions and, in particular, problems related to the simultaneous use and synchronization of different technologies and sensors, the collection of a large number of trials in patients with mobility deficits and the presence of marker visibility issues led to discard about 13% of the participants' data.
- Further analysis on INDIP outcomes could be performed to explore potential correlations between the results accuracy and the use of walking aids.

5 Conclusion

This work concerned the validation of a novel multi-sensor wearable system for digital mobility assessment in ecological environments. Its performance was evaluated based on a various

and complex experimental protocol specifically designed for mobility assessment. Experiments included selected cohorts of participants with various conditions affecting gait characteristics performing a complex battery of motor tests designed to produce a heterogeneous and broad range of gait patterns. Results showed overall good/excellent reliability and high repeatability and accuracy for the DMOs analyzed across populations, walking speeds and walking bouts. The INDIP system is therefore a valuable candidate to collect reference standard data for the analysis of gait in real-world conditions.

Data availability statement

The datasets presented in this study can be found in online repositories. The names of the repository/repositories and accession number(s) can be found below: Data sample INDIP Validation Paper [Data set]. Zenodo. https://doi.org/10.5281/zenodo.7802795.

Ethics statement

The studies involving human participants were reviewed and approved by Ethics approvals: University of Sheffield Research Ethics Committee, Application number 029143; The Newcastle upon Tyne Hospitals NHS Foundation Trust and Sheffield Teaching Hospitals NHS Foundation Trust: London—Bloomsbury Research Ethics committee, 19/LO/1,507; Tel Aviv Sourasky Medical Center: the Helsinki Committee, 0551-19TLV; Robert Bosch Foundation for Medical Research: Medical Faculty of the University of Tübingen, 647/2019BO2; University of Kiel: Medical Faculty of Kiel University, D540/19. The patients/participants provided their written informed consent to participate in this study.

Author contributions

FS, SB, TB, CM, and AC designed the study. FS, SB, TB, MC, KS, LA, EB, EG, CH, and LS conducted the experiments, acquiring and pre-processing the data. FS analysed the experimental data. FS, SB, TB, MC, and AC interpreted the results and drafted the article. CM, KS, LA, SD, SK, WM, AM, LP, BV, and UD made important intellectual contributions during revision. All authors have reviewed the manuscript and approved the submitted version.

Funding

This work was supported by the Mobilise-D project that has received funding from the Innovative Medicines Initiative 2 Joint Undertaking (JU) under grant agreement No. 820820. This JU receives support from the European Union's Horizon 2020 research and innovation program and the European Federation of Pharmaceutical Industries and Associations (EFPIA). Content in this publication reflects the authors view and neither IMI nor the European Union, EFPIA, or any Associated Partners are responsible for any use that may be made of the information contained herein. LA, SD, AY, and LR are also supported by the National Institute for Health Research (NIHR) Newcastle Biomedical Research Centre (BRC) based at Newcastle Upon Tyne Hospital NHS Foundation Trust and Newcastle University. The work was also supported by the NIHR/Wellcome Trust Clinical Research Facility (CRF) infrastructure at Newcastle upon Tyne Hospitals NHS Foundation Trust. All opinions are those of the authors and not the funders. A-EC, JG-A, and SK, all researchers from the Barcelona Institute for Global Health received support from the Spanish Ministry of Science, Innovation and Universities through the "Centro de Excelencia Severo Ochoa 2019–2023" Programme (CEX 2018-000806-S), and support from the Generalitat de Catalunya through the CERCA Programme.

Acknowledgments

The authors thank all members of the Mobilise-D WP2 work-package for the work performed and the inputs provided. They also thank all the participants in the study for their contribution.

Conflict of interest

AM and FK are employees of, and may hold stock in, Novartis. BME reports consulting activities with adidas AG, Siemens AG, SiemensHealthineers AG, WSAudiology GmbH outside of the study. He is a shareholder in Portabiles HealthCare Technologies GmbH. In addition, BME holds a patent related to gait assessment. LP and LC are co-founders and own shares of mHealth Technologies (https://mhealthtechnologies.it/). LS and CB are consultants of Philipps Healthcare, Bosch Healthcare, Eli Lilly, Gait-up.

The remaining authors declare that the research was conducted in the absence of any commercial or financial relationships that could be construed as a potential conflict of interest.

Publisher's note

Supplementary material

The Supplementary Material for this article can be found online at: https://www.frontiersin.org/articles/10.3389/fbioe.2023.1143248/full#supplementary-material

References

221 e S.r.l (2020). *221 e S.r.l.* Padova, Italy: Products Overview. Accessed in 2020. Available at: https://www.221e.com/wp-content/themes/221e-theme/pdf/products_overview.pdf.

Atrsaei, A., Dadashi, F., Mariani, B., Gonzenbach, R., and Aminian, K. (2021). Toward a remote assessment of walking bout and speed: Application in patients with multiple sclerosis. *IEEE J. Biomed. Health Inf.* 25 (11), 4217–4228. doi:10.1109/JBHI.2021.3076707

Bertoli, M., Cereatti, A., Trojaniello, D., Avanzino, L., Pelosin, E., Del Din, S., et al. (2018). Estimation of spatio-temporal parameters of gait from magneto-inertial measurement units: Multicenter validation among Parkinson, mildly cognitively impaired and healthy older adults. *Biomed. Eng. Online* 17 (1), 58–14. doi:10.1186/s12938-018-0488-2

Bertuletti, S., Cereatti, A., Comotti, D., Caldara, M., and Della Croce, U. (2017). Static and dynamic accuracy of an innovative miniaturized wearable platform for short range distance measurements for human movement applications. *Sensors* 17 (7), 1492. doi:10.3390/s17071492

Bertuletti, S., Della Croce, U., and Cereatti, A. (2018). A wearable solution for accurate step detection based on the direct measurement of the inter-foot distance. *J. Biomech.* 84, 274–277. doi:10.1016/j.jbiomech.2018.12.039

Bonci, T., Keogh, A., Del Din, S., Scott, K., and Mazzà, C. (2020). An objective methodology for the selection of a device for continuous mobility assessment. *Sensors* 20 (22), 6509. doi:10.3390/s20226509

Bonci, T., Salis, F., Scott, K., Alcock, L., Becker, C., Bertuletti, S., et al. (2022). An algorithm for accurate marker-based gait event detection in healthy and pathological populations during complex motor tasks. *Front. Bioeng. Biotechnol.* 10, 868928. doi:10.3389/fbioe.2022.868928

Bourgeois, A. B., Mariani, B., Aminian, K., Zambelli, P. Y., and Newman, C. J. (2014). Spatio-temporal gait analysis in children with cerebral palsy using, foot-worn inertial sensors. *Gait Posture* 39 (1), 436–442. doi:10.1016/j.gaitpost.2013.08.029

Buso, V., Hopper, L., Benois-Pineau, J., Plans, P. M., and Mégret, R. (2015). "Recognition of Activities of Daily Living in natural "at home" scenario for assessment of Alzheimer's disease patients," in Proceeding of the IEEE International Conference on Multimedia & Expo Workshops (ICMEW), Turin, Italy, 29 June 2015 - 03 July 2015 (IEEE). doi:10.1109/ICMEW.2015.7169861

Caruso, M., Sabatini, A. M., Knaflitz, M., Gazzoni, M., Della Croce, U., and Cereatti, A. (2020). Orientation estimation through magneto-inertial sensor fusion: A heuristic approach for suboptimal parameters tuning. *IEEE Sens. J.* 21 (3), 3408–3419. doi:10.1109/JSEN.2020.3024806

Caruso, M., Sabatini, A. M., Laidig, D., Seel, T., Knaflitz, M., Della Croce, U., et al. (2021a). Analysis of the accuracy of ten algorithms for orientation estimation using inertial and magnetic sensing under optimal conditions: One size does not fit all. *Sensors* 21 (7), 2543. doi:10.3390/s21072543

Caruso, M., Sabatini, A. M., Knaflitz, M., Della Croce, U., and Cereatti, A. (2021b). Extension of the rigid-constraint method for the heuristic suboptimal parameter tuning to ten sensor fusion algorithms using inertial and magnetic sensing. *Sensors* 21 (18), 6307. doi:10.3390/s21186307

Del Din, S., Godfrey, A., Mazzà, C., Lord, S., and Rochester, L. (2016). Free-living monitoring of Parkinson's disease: Lessons from the field. *Mov. Disord.* 31 (9), 1293–1313. doi:10.1002/mds.26718

Della Croce, U., and Cappozzo, A. (2000). A spot check for estimating stereophotogrammetric errors. *Med. Biol. Eng. Comput.* 38 (3), 260–266. doi:10.1007/BF02347045

Dujmovic, I., Radovanovic, S., Martinovic, V., Dackovic, J., Maric, G., Mesaros, S., et al. (2017). Gait pattern in patients with different multiple sclerosis phenotypes. *Mult. Scler. Relat. Disord.* 13, 13–20. doi:10.1016/j.msard.2017.01.012

Duong, T. T. H., Uher, D., Montes, J., and Zanotto, D. (2022). Ecological validation of machine learning models for spatiotemporal gait analysis in free-living environments using instrumented insoles. *IEEE Robot. Autom. Lett.* 7 (4), 10834–10841. doi:10.1109/LRA.2022.3188895

El-Sheimy, N., Hou, H., and Niu, X. (2008). Analysis and modeling of inertial sensors using Allan variance. *IEEE Trans. Instrum. Meas.* 57 (1), 140–149. doi:10.1109/TIM.2007.908635

FeetMe Devices (2022a). *Feetme clinical applications*. Available at: https://feetmehealth.com/clinical-research/ ([accessed in 2022].

FeetMe Devices (2022b). *Feetme insoles*. Available at: https://feetmehealth.com/insoles/ ([accessed in 2022].

Ferraris, F., Grimaldi, U., and Parvis, M. (1995). Procedure for effortless in-field calibration of three-axial rate gyro and accelerometers. *Sens. Mat.* 7 (5), 311–330.

Full, K., Leutheuser, H., Schlessman, J., Armitage, R., and Eskofier, B. M. (2015). "Comparative study on classifying gait with a single trunk-mounted inertial-magnetic measurement unit," in Proceeding of the IEEE 12th International Conference on Wearable and Implantable Body Sensor Networks (BSN), Cambridge (MA), USA, 09-12 June 2015. doi:10.1109/BSN.2015.7299375

Galperin, I., Hillel, I., Del Din, S., Bekkers, E. M., Nieuwboer, A., Abbruzzese, G., et al. (2019). Associations between daily-living physical activity and laboratory-based assessments of motor severity in patients with falls and Parkinson's disease. *Park. Relat. Disord.* 62, 85–90. doi:10.1016/j.parkreldis.2019.01.022

Gastaldi, L., Agostini, V., Lisco, G., Knaflitz, M., and Tadaro, S. (2015). "Comparison between a MIMUs system and a gold standard electromechanical system," in *Eight asian pacific conference on Biomechanics* (Japan: Sapporo). doi:10.1299/jsmeapbio.2015.8.114

Giannouli, E., Bock, O., Mellone, S., and Zijlstra, W. (2016). Mobility in old age: Capacity is not performance. *BioMed Res. Int.* 2016, 1–8. doi:10.1155/2016/3261567

Hausdorff, J. M., Ladin, Z., and Wei, J. Y. (1995). Footswitch system for measurement of the temporal parameters of gait. *J. Biomech.* 28 (3), 347–351. doi:10.1016/0021-9290(94)00074-E

Hickey, A., Del Din, S., Rochester, L., and Godfrey, A. (2016). Detecting free-living steps and walking bouts: Validating an algorithm for macro gait analysis. *Physiol. Meas.* 38 (1), N1–N15. doi:10.1088/1361-6579/38/1/N1

Hillel, I., Gazit, E., Nieuwboer, A., Avanzino, L., Rochester, L., Cereatti, A., et al. (2019). Is every-day walking in older adults more analogous to dual-task walking or to usual walking? Elucidating the gaps between gait performance in the lab and during 24/7 monitoring. *Eur. Rev. Aging Phys. Act.* 16 (6), 6–12. doi:10.1186/s11556-019-0214-5

Hundza, S. R., Hook, W. R., Harris, C. R., Mahajan, S. V., Leslie, P. A., Spani, C. A., et al. (2014). Accurate and reliable gait cycle detection in Parkinson's disease. *IEEE Trans. Neural Syst. Rehabil. Eng.* 22 (1), 127–137. doi:10.1109/TNSRE.2013.2282080

IEEE (2017). *IEEE 2700-2017 standard for sensor performance parameter definitions*. Available at: https://standards.ieee.org/ieee/2700/6770/.

Iosa, M., Picerno, P., Paolucci, S., and Morone, G. (2016). Wearable inertial sensors for human movement analysis. *Expert Rev. Med. Devices* 17 (7), 641–659. doi:10.1080/17434440.2016.1198694

Iwakura, M., Okura, K., Shibata, K., Kawagoshi, A., Sugawara, K., Takahashi, H., et al. (2019). Gait characteristics and their associations with clinical outcomes in patients with chronic obstructive pulmonary disease. *Gait Posture* 74, 60–65. doi:10.1016/j.gaitpost.2019.08.012

Jakob, V., Kuderle, A., Kluge, F., Klucken, J., Eskofier, B. M., Winkler, J., et al. (2021). Validation of a sensor-based gait analysis system with a gold-standard motion capture system in patients with Parkinson's disease. *Sensors* 21 (22), 7680. doi:10.3390/s21227680

Kluge, F., Del Din, S., Cereatti, A., GaBner, H., Hansen, C., Helbostad, J. L., et al. (2021). Consensus based framework for digital mobility monitoring. *PLoS One* 16 (8), e0256541. doi:10.1371/journal.pone.0256541

Koo, T. K., and Li, M. Y. (2016). A guideline of selecting and reporting intraclass correlation coefficients for reliability research. *J. Chiropr. Med.* 15 (2), 155–163. doi:10.1016/j.jcm.2016.02.012

Laudani, L., Vannozzi, G., Sawacha, Z., Della Croce, U., Cereatti, A., and Macaluso, A. (2013). Association between physical activity levels and physiological factors underlying mobility in young, middle-aged and older individuals living in a city district. *PLoS One* 8 (9), e74227. doi:10.1371/journal.pone.0074227

Li, G., Liu, T., and Yi, J. (2018). Wearable sensor system for detecting gait parameters of abnormal gaits: A feasibility study. *IEEE Sensors Journ.* 18 (10), 4234–4241. doi:10.1109/JSEN.2018.2814994

Lyons, G. M., Culhane, K. M., Hilton, D., Grace, P. A., and Lyons, D. (2005). A description of an accelerometer-based mobility monitoring technique. *Med. Eng. Phys.* 27 (6), 497–504. doi:10.1016/j.medengphy.2004.11.006

Madgwick, S. O. H., Harrison, A. J. L., and Vaidyanathan, R. (2011). "Estimation of IMU and MARG orientation using a gradient descent algorithm," in Proceeding of the IEEE Int. Conf. Rehabil. Robot., Zurich, Switzerland, 29 June 2011 - 01 July 2011. doi:10.1109/ICORR.2011.5975346

Martindale, C. F., Sprager, S., and Eskofier, B. M. (2019). Hidden Markov model-based smart annotation for benchmark cyclic activity recognition database using wearables. *Sensors* 19 (8), 1820. doi:10.3390/s19081820

Mazzà, C., Alcock, L., Aminian, K., Becker, C., Bertuletti, S., Bonci, T., et al. (2021). Technical validation of real-world monitoring of gait: A multicentric observational study. *BMJ Open* 11 (12), e050785. doi:10.1136/bmjopen-2021-050785

Micó-Amigo, M. E., Bonci, T., Paraschiv-Ionescu, A., Ullrich, M., Kirk, C., Soltani, A., et al. (2022). *Assessing real-world gait with digital technology? Validation, insights and recommendations from the mobilise-D consortium*. Durham, North Carolina: Research Square. doi:10.21203/rs.3.rs-2088115/v1

Mishra, P., Pandey, C. M., Singh, U., Gupta, A., Sahu, C., and Keshri, A. (2019). Descriptive statistics and normality tests for statistical data. *Ann. Card. Anaesth.* 22 (1), 67–72. doi:10.4103/aca.ACA_157_18

Mobbs, R. J., Perring, J., Raj, S. M., Maharaj, M., Yoong, N. K. M., Sy, L. W., et al. (2022). Gait metrics analysis utilizing single-point inertial measurement units: A systematic review. *Mhealth* 8 (9), 9–2. doi:10.21037/mhealth-21-17

Mobilise-D (2019). *Mobilise-D project*. Available at: https://www.mobilise-d.eu/.

Nez, A., Fradet, L., Laguillaumie, P., Monnet, T., and Lacouture, P. (2016). Comparison of calibration methods for accelerometers used in human motion analysis. *Med. Eng. Phys.* 38 (11), 1289–1299. doi:10.1016/j.medengphy.2016.08.004

NURVV (2022). *Nurv run smart insoles*. Available at: https://www.nurvv.com/en-gb/products/nurvv-run-insoles-trackers/.

Pacini, G., Bisi, M. C., Stagni, R., and Fantozzi, S. (2018). Analysis of the performance of 17 algorithms from a systematic review: Influence of sensor position, analysed variable and computational approach in gait timing estimation from IMU measurements. *Gait Posture* 66, 76–82. doi:10.1016/j.gaitpost.2018.08.025

Panizzolo, F. A., Maiorana, A. J., Naylor, L. H., Dembo, L., Lloyd, D. G., Green, D. J., et al. (2014). Gait analysis in chronic heart failure: The calf as a locus of impaired walking capacity. *J. Biomech.* 47 (15), 3719–3725. doi:10.1016/j.jbiomech.2014.09.015

Peruzzi, A., Della Croce, U., and Cereatti, A. (2011). Estimation of stride length in level walking using an inertial measurement unit attached to the foot: A validation of the zero velocity assumption during stance. *J. Biomech.* 44 (10), 1991–1994. doi:10.1016/j.jbiomech.2011.04.035

Picerno, P., Cereatti, A., and Cappozzo, A. (2011). A spot check for assessing static orientation consistency of inertial and magnetic sensing units. *Gait Posture* 33 (3), 373–378. doi:10.1016/j.gaitpost.2010.12.006

Polhemus, A., Ortiz, L. D., Brittain, G., Chynkiamis, N., Salis, F., GaBner, H., et al. (2021). Walking on common ground: A cross-disciplinary scoping review on the clinical utility of digital mobility outcomes. *npj Digit. Med.* 4 (1), 149. doi:10.1038/s41746-021-00513-5

Rebula, J. R., Ojeda, L. V., Adamczyk, P. G., and Kuo, A. D. (2013). Measurement of foot placement and its variability with inertial sensors. *Gait Posture* 38 (4), 974–980. doi:10.1016/j.gaitpost.2013.05.012

Refai, M. I. M., van Beijnum, B. J. F., Buurke, J. H., and Veltink, P. H. (2018). Gait and dynamic balance sensing using wearable foot sensors. *IEEE Trans. Neural Syst. Rehabil. Eng.* 27 (2), 218–227. doi:10.1109/TNSRE.2018.2885309

Reggi, L., Palmerini, L., Chiari, L., and Mellone, S. (2022). Real-world walking speed assessment using a mass-market RTK-GNSS receiver. *Front. Bioeng. Biotechnol.* 501, 1–9. doi:10.3389/fbioe.2022.87320

Romijnders, R., Warmerdam, E., Hansen, C., Welzel, J., Schmidt, G., and Maetzler, W. (2021). Validation of IMU-based gait event detection during curved walking and turning in older adults and Parkinson's Disease patients. *J. Neuroeng. Rehabil.* 18 (1), 28–10. doi:10.1186/s12984-021-00828-0

Rossanigo, R., Caruso, M., Bertuletti, S., Deriu, F., Knaflitz, M., Della Croce, U., et al. (2023). Base of support, step length and stride width estimation during walking using an inertial and infrared wearable system. *Sensors* 23 (8), 3921. doi:10.3390/s23083921

Rossanigo, R., Caruso, M., Salis, F., Bertuletti, S., Della Croce, U., and Cereatti, A. (2021). "An optimal procedure for stride length estimation using foot-mounted magneto-inertial measurement units," in Proceeding of the IEEE International Symposium on Medical Measurements and Applications (MeMeA), Lausanne, Switzerland, 23-25 June 2021 (IEEE). doi:10.1109/MeMeA52024.2021.9478604

Roth, N., Martindale, C. F., Gaßner, H., Kohl, Z., and Klucken, J. (2018). Synchronized sensor insoles for clinical gait analysis in home-monitoring applications. *Curr. Dir. Biomed. Eng.* 4 (1), 433–437. doi:10.1515/cdbme-2018-0103

Roth, N., Kuderle, A., Ullrich, M., Gladow, T., Marxreiter, F., Klucken, J., et al. (2021a). Hidden Markov Model based stride segmentation on unsupervised free-living gait data in Parkinson's disease patients. *J. Neuroeng. Rehabil.* 18 (1), 93–15. doi:10.1186/s12984-021-00883-7

Roth, N., Küderle, A., Prossel, D., Gassner, H., Eskofier, B. M., and Kluge, F. (2021b). An inertial sensor-based gait analysis pipeline for the assessment of real-world stair ambulation parameters. *Sensors* 21 (19), 6559. doi:10.3390/s21196559

Sabatini, A. M. (2005). Quaternion-based strap-down integration method for applications of inertial sensing to gait analysis. *Med. Biol. Eng. Comput.* 43 (1), 94–101. doi:10.1007/BF02345128

Salis, F., Bertuletti, S., Bonci, T., Della Croce, U., Mazzà, C., and Cereatti, A. (2021a). A method for gait events detection based on low spatial resolution pressure insoles data. *J. Biomech.* 127, 110687. doi:10.1016/j.jbiomech.2021.110687

Salis, F., Bertuletti, S., Scott, K., Caruso, M., Bonci, T., Buckley, E., et al. (2021b). "A wearable multi-sensor system for real world gait analysis," in Proceeding of the IEEE 43rd Annual International Conference of the IEEE Engineering in Medicine & Biology Society (EMBC), Mexico, 01-05 Nov 2021 (IEEE), 7020–7023. doi:10.1109/EMBC46164.2021.9630392

Schepers, H. M., Van Asseldonk, E. H., Buurke, J. H., and Veltink, P. H. (2009). Ambulatory estimation of center of mass displacement during walking. *Ieee. Trans. Biomed. Eng.* 56 (4), 1189–1195. doi:10.1109/TBME.2008.2011059

Scott, K., Bonci, T., Alcock, L., Buckley, E., Hansen, C., Gazit, E., et al. (2021). A quality control check to ensure comparability of stereophotogrammetric data between sessions and systems. *Sensors* 21 (24), 8223. doi:10.3390/s21248223

Scott, K., Bonci, T., Salis, F., Alcock, L., Buckley, E., Gazit, E., et al. (2022). Design and validation of a multi-task, multi-context protocol for real-world gait simulation. *J. NeuroEngineering Rehabil.* 19, 141. doi:10.1186/s12984-022-01116-1

Skog, I., Nilsson, J., and Peter, H. (2010). "Evaluation of zero-velocity detectors for foot-mounted inertial navigation systems," in Proceeding of the Int. Conf. on Indoor Positioning and Indoor Navigation (IPIN), Zurich, Switzerland, 15-17 Sept 2010 (IEEE). doi:10.1109/IPIN.2010.5646936

Skog, I., Peter, H., Nilsson, J., and Rantakokko, J. O. (2010). Zero-velocity detection — an algorithm evaluation. *Ieee. Trans. Biomed. Eng.* 57 (11), 2657–2666. doi:10.1109/TBME.2010.2060723

Sofuwa, O., Nieuwboer, A., Desloovere, K., Willems, A. M., Chavret, F., and Jonkers, I. (2005). Quantitative gait analysis in Parkinson's disease: Comparison with a healthy control group. *Arch. Phys. Med. Rehabil.* 86 (5), 1007–1013. doi:10.1016/j.apmr.2004.08.012

Stančin, S., and Tomažič, S. (2014). Time-and computation-efficient calibration of MEMS 3D accelerometers and gyroscopes. *Sensors* 14 (8), 14885–14915. doi:10.3390/s140814885

Storm, F. A., Buckley, C. J., and Mazzà, C. (2016). Gait event detection in laboratory and real-life settings: Accuracy of ankle and waist sensor-based methods. *Gait Posture* 50, 42–46. doi:10.1016/j.gaitpost.2016.08.012

Tang, W., Fulk, G., Zeigler, S., Zhang, T., and Sazonov, E. (2019). "Estimating berg balance scale and mini balance evaluation system test scores by using wearable shoe sensors," in Proceeding of the 2019 IEEE EMBS International Conference on Biomedical & Health Informatics (BHI), Chicago, IL, USA, 19-22 May 2019 (IEEE). doi:10.1109/BHI.2019.8834631

Terrier, P., Ladetto, Q., Merminod, B., and Schutz, Y. (2000). High-precision satellite positioning system as a new tool to study the biomechanics of human locomotion. *J. Biomech.* 33 (12), 1717–1722. doi:10.1016/S0021-9290(00)00133-0

Thingstad, P., Egerton, T., Ihlen, E. F., Taraldsen, K., Moe-nilssen, R., and Helbostad, J. L. (2015). Identification of gait domains and key gait variables following hip fracture. *BMC Geriatr.* 15 (1), 150–157. doi:10.1186/s12877-015-0147-4

Trojaniello, D., Cereatti, A., Pelosin, E., Avanzino, L., Mirelman, A., Hausdorff, J. M., et al. (2014). Estimation of step-by-step spatio-temporal parameters of normal and impaired gait using shank-mounted magneto-inertial sensors: Application to elderly, hemiparetic, parkinsonian and choreic gait. *J. Neuroeng. Rehabil.* 11 (1), 152. doi:10.1186/1743-0003-11-152

Unsal, D., and Demirbas, K. (2012). "Estimation of deterministic and stochastic IMU error parameters," in Proceeding of the IEEE/ION Position, Location and Navigation Symposium, Myrtle Beach, SC, USA, 23-26 Apr 2012 (IEEE). doi:10.1109/PLANS.2012.6236828

Van Meulen, F. B., Weenk, D., Buurke, J. H., Van Beijnum, B. F., and Veltink, P. H. (2016). Ambulatory assessment of walking balance after stroke using instrumented shoes. *J. Neuroeng. Rehabil.* 13 (48), 48–10. doi:10.1186/s12984-016-0146-5

Viceconti, M., Hernandez Penna, S., Dartee, W., Mazza, C., Caulfield, B., Becker, C., et al. (2020). Toward a regulatory qualification of real-world mobility performance biomarkers in Parkinson's patients using digital mobility outcomes. *Sensors* 20 (20), 5920. doi:10.3390/s20205920

Walther, B. A., and Moore, J. L. (2005). The concepts of bias, precision and accuracy, and their use in testing the performance of species richness estimators, with a literature review of estimator performance. *Ecography* 28 (6), 815–829. doi:10.1111/j.2005.0906-7590.04112.x

Wang, C., Wang, X., Long, Z., Yuan, J., Qian, Y., and Li, J. (2016). Estimation of temporal gait parameters using a wearable microphone-sensor-based system. *Sensors* 16 (12), 2167. doi:10.3390/s16122167

World Health Organization (2001). *International classification of functioning, disability and health*. Geneva, Switzerland: ICF.

Yang, S., Zhang, J., Novak, A. C., Brouwer, B., and Li, Q. (2013). Estimation of spatio-temporal parameters for post-stroke hemiparetic gait using inertial sensors. *Gait Posture* 37 (3), 354–358. doi:10.1016/j.gaitpost.2012.07.032

Zhou, L., Tunca, C., Fischer, E., Brahms, C. M., Ersoy, C., Granacher, U., et al. (2020). "Validation of an IMU gait analysis algorithm for gait monitoring in daily life situations," in Proceeding of the The 42nd Annual International Conference of the IEEE Engineering in Medicine & Biology Society (EMBC), Montreal, QC, Canada, 20-24 Jul. 2020 (IEEE). doi:10.1109/EMBC44109.2020.9176827

Zijlstra, W., and Hof, A. L. (2003). Assessment of spatio-temporal gait parameters from trunk accelerations during human walking. *Gait Posture* 18 (2), 1–10. doi:10.1016/S0966-6362(02)00190-X

Zok, M., Mazzà, C., and Della Croce, U. (2004). Total body centre of mass displacement estimated using ground reactions during transitory motor tasks: Application to step ascent. *Med. Eng. Phys.* 26 (9), 791–798. doi:10.1016/j.medengphy.2004.07.005

References

[1] L. Laudani, G. Vannozzi, Z. Sawacha, U. della Croce, A. Cereatti, and A. Macaluso, "Association between Physical Activity Levels and Physiological Factors Underlying Mobility in Young, Middle-Aged and Older Individuals Living in a City District," *PLoS One*, vol. 8, no. 9, Sep. 2013, doi: 10.1371/journal.pone.0074227.

[2] A. Polhemus *et al.*, "Walking on common ground: a cross-disciplinary scoping review on the clinical utility of digital mobility outcomes," *npj Digital Medicine*, vol. 4, no. 1. Nature Research, Dec. 01, 2021. doi: 10.1038/s41746-021-00513-5.

[3] M. Rantakokko, M. Mä nty, and T. Rantanen, "Mobility decline in old age," *Exerc Sport Sci Rev*, vol. 41, no. 1, pp. 19–25, 2013, [Online]. Available: www.acsm-essr.org

[4] M. Y. Osoba, A. K. Rao, S. K. Agrawal, and A. K. Lalwani, "Balance and gait in the elderly: A contemporary review," *Laryngoscope Investigative Otolaryngology*, vol. 4, no. 1. John Wiley and Sons Inc, pp. 143–153, Feb. 01, 2019. doi: 10.1002/lio2.252.

[5] F. W. Booth, C. K. Roberts, and M. J. Laye, "Lack of exercise is a major cause of chronic diseases," *Compr Physiol*, vol. 2, no. 2, pp. 1143–1211, Apr. 2012, doi: 10.1002/cphy.c110025.

[6] S. Studenski *et al.*, "Gait Speed and Survival in Older Adults." [Online]. Available: https://jamanetwork.com/

[7] S. L. M. Fritz, "White Paper: 'Walking Speed: the Sixth Vital Sign,'" *Journal of Geriatric Physical Therapy*, vol. 32, no. 2, pp. 2–5, 2009.

[8] A. Peppe, C. Chiavalon, P. Pasqualetti, D. Crovato, and C. Caltagirone, "Does gait analysis quantify motor rehabilitation efficacy in Parkinson's disease patients?," *Gait Posture*, vol. 26, no. 3, pp. 452–462, Sep. 2007, doi: 10.1016/j.gaitpost.2006.11.207.

[9] J. R. Gage, " The Role of Gait Analysis in the Treatment of Cerebral Palsy. ," *Journal of Pediatric Orthopaedics* , vol. 14, no. 6, pp. 701–702, 1994.

[10] A. Atrsaei *et al.*, "Gait speed in clinical and daily living assessments in Parkinson's disease patients: performance versus capacity," *NPJ Parkinsons Dis*, vol. 7, no. 1, Dec. 2021, doi: 10.1038/s41531-021-00171-0.

[11] E. Giannouli, O. Bock, S. Mellone, and W. Zijlstra, "Mobility in old age: Capacity is not performance," *Biomed Res Int*, vol. 2016, 2016, doi: 10.1155/2016/3261567.

[12] I. Galperin *et al.*, "Associations between daily-living physical activity and laboratory-based assessments of motor severity in patients with falls and Parkinson's disease," *Parkinsonism Relat Disord*, vol. 62, pp. 85–90, May 2019, doi: 10.1016/j.parkreldis.2019.01.022.

[13] World Health Organization, "International Classification of Functioning, Disability and Health," 2001.

[14] I. Hillel *et al.*, "Is every-day walking in older adults more analogous to dual-task walking or to usual walking? Elucidating the gaps between gait performance in the lab and during 24/7 monitoring," *European Review of Aging and Physical Activity*, vol. 16, no. 1, May 2019, doi: 10.1186/s11556-019-0214-5.

[15] L. Rochester *et al.*, "A Roadmap to Inform Development, Validation and Approval of Digital Mobility Outcomes: The Mobilise-D Approach," *Digit Biomark*, vol. 4, pp. 13–27, Nov. 2020, doi: 10.1159/000512513.

[16] "Mobilise-D," 2019.

[17] C. F. Martindale, S. Sprager, and B. M. Eskofier, "Hidden markov model-based smart annotation for benchmark cyclic activity recognition database using wearables," *Sensors (Switzerland)*, vol. 19, no. 8, Apr. 2019, doi: 10.3390/s19081820.

[18] H. Leutheuser, D. Schuldhaus, and B. M. Eskofier, "Hierarchical, Multi-Sensor Based Classification of Daily Life Activities: Comparison with State-of-the-Art Algorithms Using a Benchmark Dataset," *PLoS One*, vol. 8, no. 10, Oct. 2013, doi: 10.1371/journal.pone.0075196.

[19] S. Engel and F. Zipp, “Preventing disease progression in multiple sclerosis—insights from large real-world cohorts,” *Genome Medicine*, vol. 14, no. 1. BioMed Central Ltd, Dec. 01, 2022. doi: 10.1186/s13073-022-01044-8.

[20] M. J. Sá, “Exercise therapy and multiple sclerosis: a systematic review,” *Journal of Neurology*, vol. 261, no. 9. Dr. Dietrich Steinkopff Verlag GmbH and Co. KG, pp. 1651–1661, Sep. 01, 2014. doi: 10.1007/s00415-013-7183-9.

[21] A. Mendes and M. J. Sá, “View and review Classical immunomodulatory therapy in multiple sclerosis How it acts, how it works,” 2011.

[22] M. J. Sá, J. Guimarães, P. Abreu, A. Mendes, and E. B. Souto, “Etiopathogenesis, Classical Immunotherapy and Innovative Nanotherapeutics for Inflammatory Neurological Disorders,” 2011.

[23] H. Wiendl *et al.*, “Basic and escalating immunomodulatory treatments in multiple sclerosis: Current therapeutic recommendations,” *Journal of Neurology*, vol. 255, no. 10. pp. 1449–1463, Oct. 2008. doi: 10.1007/s00415-008-0061-1.

[24] D. Centonze, L. Leocani, and P. Feys, “Advances in physical rehabilitation of multiple sclerosis,” *Current Opinion in Neurology*, vol. 33, no. 3. Lippincott Williams and Wilkins, pp. 255–261, 2020. doi: 10.1097/WCO.0000000000000816.

[25] J. Tollár *et al.*, “Exercise Effects on Multiple Sclerosis Quality of Life and Clinical-Motor Symptoms,” *Med Sci Sports Exerc*, vol. 52, no. 5, pp. 1007–1014, May 2020, doi: 10.1249/MSS.0000000000002228.

[26] B. Amatya, F. Khan, and M. Galea, “Rehabilitation for people with multiple sclerosis: An overview of Cochrane Reviews,” *Cochrane Database of Systematic Reviews*, vol. 2019, no. 1. John Wiley and Sons Ltd, Jan. 14, 2019. doi: 10.1002/14651858.CD012732.pub2.

[27] C. Dettmers, M. Sulzmann, A. Ruchay-Plössl, R. Gütler, and M. Vieten, “Endurance exercise improves walking distance in MS patients with fatigue,” *Acta Neurol Scand*, vol. 120, no. 4, pp. 251–257, Oct. 2009, doi: 10.1111/j.1600-0404.2008.01152.x.

[28] I. Baert *et al.*, “Responsiveness and clinically meaningful improvement, according to disability level, of five walking measures after rehabilitation in multiple sclerosis: A European multicenter study,” *Neurorehabil Neural Repair*, vol. 28, no. 7, pp. 621–631, 2014, doi: 10.1177/1545968314521010.

[29] A. Kalron *et al.*, “A personalized, intense physical rehabilitation program improves walking in people with multiple sclerosis presenting with different levels of disability: A retrospective cohort,” *BMC Neurol*, vol. 15, no. 1, Mar. 2015, doi: 10.1186/s12883-015-0281-9.

[30] M. Pau *et al.*, “Quantitative assessment of the effects of 6 months of adapted physical activity on gait in people with multiple sclerosis: a randomized controlled trial,” *Disabil Rehabil*, vol. 40, no. 2, pp. 144–151, Jan. 2018, doi: 10.1080/09638288.2016.1244291.

[31] C. Leone *et al.*, “Effects of rehabilitation on gait pattern at usual and fast speeds depend on walking impairment level in multiple sclerosis,” *Int J MS Care*, vol. 20, no. 5, pp. 199–209, Sep. 2018, doi: 10.7224/1537-2073.2015-078.

[32] R. Sacco, R. Bussman, P. Oesch, J. Kesselring, and S. Beer, “Assessment of gait parameters and fatigue in MS patients during inpatient rehabilitation: A pilot trial,” *J Neurol*, vol. 258, no. 5, pp. 889–894, May 2011, doi: 10.1007/s00415-010-5821-z.

[33] R. W. Motl, D. C. Smith, J. Elliott, M. Weikert, D. Dlugonski, and J. J. Sosnoff, “Combined training improves walking mobility in persons with significant disability from multiple sclerosis: A pilot study,” *Journal of Neurologic Physical Therapy*, vol. 36, no. 1. pp. 32–37, Mar. 2012. doi: 10.1097/NPT.0b013e3182477c92.

[34] K. K. Patterson *et al.*, “Gait Asymmetry in Community-Ambulating Stroke Survivors,” *Arch Phys Med Rehabil*, vol. 89, no. 2, pp. 304–310, Feb. 2008, doi: 10.1016/j.apmr.2007.08.142.

[35] D. Chen *et al.*, “Bring Gait Lab to Everyday Life: Gait Analysis in Terms of Activities of Daily Living,” *IEEE Internet Things J*, vol. 7, no. 2, pp. 1298–1312, Feb. 2020, doi: 10.1109/JIOT.2019.2954387.

[36] H. Yu, J. Riskowski, R. Brower, and T. Sarkodie-Gyan, “Gait variability while walking with three different speeds,” in *2009 IEEE International Conference on Rehabilitation Robotics, ICORR 2009*, 2009, pp. 823–827. doi: 10.1109/ICORR.2009.5209486.

[37] O. Beauchet *et al.*, “Gait variability among healthy adults: Low and high stride-to-stride variability are both a reflection of gait stability,” *Gerontology*, vol. 55, no. 6, pp. 702–706, Nov. 2009, doi: 10.1159/000235905.

[38] S. Chen, J. Lach, B. Lo, and G. Z. Yang, “Toward Pervasive Gait Analysis With Wearable Sensors: A Systematic Review,” *IEEE Journal of Biomedical and Health Informatics*, vol. 20, no. 6. Institute of Electrical and Electronics Engineers Inc., pp. 1521–1537, Nov. 01, 2016. doi: 10.1109/JBHI.2016.2608720.

[39] T. Bonci, A. Keogh, S. Del Din, K. Scott, and C. Mazzà, “An objective methodology for the selection of a device for continuous mobility assessment,” *Sensors (Switzerland)*, vol. 20, no. 22, pp. 1–16, Nov. 2020, doi: 10.3390/s20226509.

[40] R. J. Mobbs *et al.*, “Gait metrics analysis utilizing single-point inertial measurement units: a systematic review,” *mHealth*, vol. 8. AME Publishing Company, Jan. 01, 2022. doi: 10.21037/mhealth-21-17.

[41] V. Agostini, M. Knaflitz, L. Antenucci, G. Lisco, L. Gastaldi, and S. Tadano, “Wearable sensors for gait analysis,” in *2015 IEEE International Symposium on Medical Measurements and Applications, MeMeA 2015 - Proceedings*, Institute of Electrical and Electronics Engineers Inc., Jun. 2015, pp. 146–150. doi: 10.1109/MeMeA.2015.7145189.

[42] D. Trojaniello *et al.*, “Estimation of step-by-step spatio-temporal parameters of normal and impaired gait using shank-mounted magneto-inertial sensors: application to elderly, hemiparetic, parkinsonian and choreic gait,” 2014. [Online]. Available: http://www.jneuroengrehab.com/content/11/1/152

[43] M. Bertoli *et al.*, “Estimation of spatio-temporal parameters of gait from magneto-inertial measurement units: Multicenter validation among

Parkinson, mildly cognitively impaired and healthy older adults," *Biomed Eng Online*, vol. 17, no. 1, May 2018, doi: 10.1186/s12938-018-0488-2.

[44] Lin Zhou *et al.*, "Validation of an IMU Gait Analysis Algorithm for Gait Monitoring in Daily Life Situations," 2020.

[45] V. Jakob *et al.*, "Validation of a sensor-based gait analysis system with a gold-standard motion capture system in patients with parkinson's disease," *Sensors*, vol. 21, no. 22, Nov. 2021, doi: 10.3390/s21227680.

[46] R. Romijnders, E. Warmerdam, C. Hansen, J. Welzel, G. Schmidt, and W. Maetzler, "Validation of IMU-based gait event detection during curved walking and turning in older adults and Parkinson's Disease patients," *J Neuroeng Rehabil*, vol. 18, no. 1, Dec. 2021, doi: 10.1186/s12984-021-00828-0.

[47] A. Atrsaei, F. Dadashi, B. Mariani, R. Gonzenbach, and K. Aminian, "Toward a Remote Assessment of Walking Bout and Speed: Application in Patients with Multiple Sclerosis," *IEEE J Biomed Health Inform*, vol. 25, no. 11, pp. 4217–4228, Nov. 2021, doi: 10.1109/JBHI.2021.3076707.

[48] F. A. Storm, C. J. Buckley, and C. Mazzà, "Gait event detection in laboratory and real life settings: Accuracy of ankle and waist sensor based methods," *Gait Posture*, vol. 50, pp. 42–46, Oct. 2016, doi: 10.1016/j.gaitpost.2016.08.012.

[49] N. Roth, A. Küderle, D. Prossel, H. Gassner, B. M. Eskofier, and F. Kluge, "An inertial sensor-based gait analysis pipeline for the assessment of real-world stair ambulation parameters," *Sensors*, vol. 21, no. 19, Oct. 2021, doi: 10.3390/s21196559.

[50] N. Roth *et al.*, "Hidden Markov Model based stride segmentation on unsupervised free-living gait data in Parkinson's disease patients," *J Neuroeng Rehabil*, vol. 18, no. 1, Dec. 2021, doi: 10.1186/s12984-021-00883-7.

[51] V. Buso, L. Hopper, J. Benois-Pineau, P.-M. Plans, and R. Mégret, "RECOGNITION OF ACTIVITIES OF DAILY LIVING IN NATURAL

‘AT HOME’ SCENARIO FOR ASSESSMENT OF ALZHEIMER’S DISEASE PATIENTS.”

[52] K. Full, H. Leutheuser, J. Schlessman, R. Armitage, and B. M. Eskofier, “Comparative study on classifying gait with a single trunk-mounted inertial-magnetic measurement unit,” in *2015 IEEE 12th International Conference on Wearable and Implantable Body Sensor Networks, BSN 2015*, Institute of Electrical and Electronics Engineers Inc., Oct. 2015. doi: 10.1109/BSN.2015.7299375.

[53] A. Hickey, S. Del Din, L. Rochester, and A. Godfrey, “Detecting free-living steps and walking bouts: Validating an algorithm for macro gait analysis,” *Physiol Meas*, vol. 38, no. 1, pp. N1–N15, Jan. 2017, doi: 10.1088/1361-6579/38/1/N1.

[54] J. Bae and M. Tomizuka, “Gait phase analysis based on a Hidden Markov Model,” *Mechatronics*, vol. 21, no. 6, pp. 961–970, 2011, doi: 10.1016/j.mechatronics.2011.03.003.

[55] K. Kong and M. Tomizuka, “A gait monitoring system based on air pressure sensors embedded in a shoe,” *IEEE/ASME Transactions on Mechatronics*, vol. 14, no. 3, pp. 358–370, 2009, doi: 10.1109/TMECH.2008.2008803.

[56] J. M. Hausdorff, Z. Ladin, and J. Y. Weis, “FOOTSWITCH SYSTEM FOR MEASUREMENT OF THE TEMPORAL PARAMETERS OF GAIT,” 1995.

[57] M. M. Skelly and H. J. Chizeck, “Real-time gait event detection for paraplegic FES walking,” *IEEE Transactions on Neural Systems and Rehabilitation Engineering*, vol. 9, no. 1, pp. 59–68, 2001, doi: 10.1109/7333.918277.

[58] V. Agostini, G. Balestra, and M. Knaflitz, “Segmentation and classification of gait cycles,” *IEEE Transactions on Neural Systems and Rehabilitation Engineering*, vol. 22, no. 5, pp. 946–952, Sep. 2014, doi: 10.1109/TNSRE.2013.2291907.

[59] “Tekscan® F-Scan® System web page,” *http://www.tekscan.com.*

[60] “Novel® Pedar® System Web Page,” *http://www.novel.de*.

[61] B. T. Smith, D. J. Coiro, R. Finson, R. R. Betz, and J. McCarthy, "Evaluation of force-sensing resistors for gait event detection to trigger electrical stimulation to improve walking in the child with cerebral palsy," *IEEE Transactions on Neural Systems and Rehabilitation Engineering*, vol. 10, no. 1, pp. 22–29, 2002, doi: 10.1109/TNSRE.2002.1021583.

[62] B. J. Braun *et al.*, "Validation and reliability testing of a new, fully integrated gait analysis insole," *J Foot Ankle Res*, vol. 8, no. 1, Sep. 2015, doi: 10.1186/s13047-015-0111-8.

[63] N. Carbonaro, F. Lorussi, and A. Tognetti, "Assessment of a smart sensing shoe for gait phase detection in level walking," *Electronics (Switzerland)*, vol. 5, no. 4, Dec. 2016, doi: 10.3390/electronics5040078.

[64] S. Crea, M. Donati, S. M. M. De Rossi, C. Maria Oddo, and N. Vitiello, "A wireless flexible sensorized insole for gait analysis," *Sensors (Switzerland)*, vol. 14, no. 1, pp. 1073–1093, Jan. 2014, doi: 10.3390/s140101073.

[65] R. Agarwal, A. Aggarwal, and R. Gupta, "A Wireless Sensorized Insole Design for Spatio-Temporal Gait Analysis," *Neurophysiology*, vol. 52, no. 3, pp. 212–221, May 2020, doi: 10.1007/s11062-020-09873-2.

[66] M. E. Morris, R. Iansek, T. A. Matyas, J. J. Summers, and M. Morris, "Stride length regulation in Parkinson's disease Normalization strategies and underlying mechanisms," 1996. [Online]. Available: https://academic.oup.com/brain/article/119/2/551/382456

[67] M. Montero-Odasso *et al.*, "Gait Velocity as a Single Predictor of Adverse Events in Healthy Seniors Aged 75 Years and Older," 2005. [Online]. Available: https://academic.oup.com/biomedgerontology/article/60/10/1304/553147

[68] A. Rodríguez-Molinero *et al.*, "The spatial parameters of gait and their association with falls, functional decline and death in older adults: a prospective study," *Sci Rep*, vol. 9, no. 1, Dec. 2019, doi: 10.1038/s41598-019-45113-2.

[69] D. Trojaniello, A. Cereatti, and U. Della Croce, "Accuracy, sensitivity and robustness of five different methods for the estimation of gait temporal parameters using a single inertial sensor mounted on the lower trunk," *Gait*

Posture, vol. 40, no. 4, pp. 487–492, 2014, doi: 10.1016/j.gaitpost.2014.07.007.

[70] A. Soltani, H. Dejnabadi, M. Savary, and K. Aminian, "Real-World Gait Speed Estimation Using Wrist Sensor: A Personalized Approach," *IEEE J Biomed Health Inform*, vol. 24, no. 3, pp. 658–668, Mar. 2020, doi: 10.1109/JBHI.2019.2914940.

[71] T. T. H. Duong, D. Uher, J. Montes, and D. Zanotto, "Ecological Validation of Machine Learning Models for Spatiotemporal Gait Analysis in Free-Living Environments Using Instrumented Insoles," *IEEE Robot Autom Lett*, vol. 7, no. 4, pp. 10834–10841, Oct. 2022, doi: 10.1109/LRA.2022.3188895.

[72] M. I. Mohamed Refai, B. J. F. van Beijnum, J. H. Buurke, and P. H. Veltink, "Gait and Dynamic Balance Sensing Using Wearable Foot Sensors," *IEEE Trans Neural Syst Rehabil Eng*, vol. 27, no. 2, pp. 218–227, Feb. 2019, doi: 10.1109/TNSRE.2018.2885309.

[73] "Feetme Insoles," 2022.

[74] "NURVV," 2022.

[75] A. Holzinger, M. Plass, K. Holzinger, G. C. Crisan, C.-M. Pintea, and V. Palade, "A glass-box interactive machine learning approach for solving NP-hard problems with the human-in-the-loop," Aug. 2017, [Online]. Available: http://arxiv.org/abs/1708.01104

[76] J. and J. M. B. Perry, *Gait analysis. Normal and pathological function 2nd ed.*, California: Slack. 2010.

[77] M. W. Whittle, *Gait analysis: an introduction.* 2014.

[78] É. Watelain, "Human gait: From clinical gait analysis to diagnosis assistance," *Movement & Sport Sciences*, vol. n° 98, no. 4, p. 3, 2017, doi: 10.3917/sm.098.0003.

[79] U. Della Croce, A. Cereatti, and M. Mancini, "Gait Parameters Estimated Using Inertial Measurement Units," in *Handbook of Human Motion*, Springer International Publishing, 2017, pp. 1–21. doi: 10.1007/978-3-319-30808-1_163-1.

[80] V. T. , R. H. J. , T. F. , & L. J. Inman, *Human walking*. 1981.

[81] A. , & B. B. R. Fasano, "Gait disorders.," *CONTINUUM: Lifelong Learning in Neurology*, vol. 19, no. 5, pp. 1344–1382, 2013.

[82] Y. Celik, S. Stuart, W. L. Woo, and A. Godfrey, "Gait analysis in neurological populations: Progression in the use of wearables," *Medical Engineering and Physics*, vol. 87. Elsevier Ltd, pp. 9–29, Jan. 01, 2021. doi: 10.1016/j.medengphy.2020.11.005.

[83] K. Kamiya *et al.*, "Gait speed has comparable prognostic capability to six-minute walk distance in older patients with cardiovascular disease," *Eur J Prev Cardiol*, vol. 25, no. 2, pp. 212–219, Jan. 2018, doi: 10.1177/2047487317735715.

[84] F. M. , C. D. Carol L. Richards, "Gait in Stroke: Assessment and Rehabilitation," *Clin Geriatr Med*, vol. 15, no. 4, pp. 833–856, 1999.

[85] W. Pirker and R. Katzenschlager, "Gait disorders in adults and the elderly: A clinical guide," *Wiener Klinische Wochenschrift*, vol. 129, no. 3–4. Springer-Verlag Wien, pp. 81–95, Feb. 01, 2017. doi: 10.1007/s00508-016-1096-4.

[86] "Parkinson's Europe website," *https://www.parkinsonseurope.org/about-parkinsons/what-is-parkinsons/*, 2022.

[87] B. R. Bloem, M. S. Okun, and C. Klein, "Parkinson's disease," *The Lancet*, vol. 397, no. 10291. Elsevier B.V., pp. 2284–2303, Jun. 12, 2021. doi: 10.1016/S0140-6736(21)00218-X.

[88] A. Mirelman *et al.*, "Gait impairments in Parkinson's disease," *The Lancet Neurology*, vol. 18, no. 7. Lancet Publishing Group, pp. 697–708, Jul. 01, 2019. doi: 10.1016/S1474-4422(19)30044-4.

[89] Y. Okuma, "Freezing of gait in Parkinson's disease," *Journal of Neurology*, vol. 253, no. SUPPL. 7. Dec. 2006. doi: 10.1007/s00415-006-7007-2.

[90] "Associazione Italiana Sclerosi Multipla Website," *https://www.aism.it/cosa_e_la_sclerosi_multipla*, 2022.

[91] M. J. Socie and J. J. Sosnoff, “Gait Variability and Multiple Sclerosis,” *Mult Scler Int*, vol. 2013, pp. 1–7, 2013, doi: 10.1155/2013/645197.

[92] M. Coca-Tapia, A. Cuesta-Gómez, F. Molina-Rueda, and M. Carratalá-Tejada, “Gait pattern in people with multiple sclerosis: A systematic review,” *Diagnostics*, vol. 11, no. 4, Apr. 2021, doi: 10.3390/diagnostics11040584.

[93] N. G. La Rocca, “Impact of Walking Impairment in Multiple Sclerosis Perspectives of Patients and Care Partners.”

[94] “WHO website ,” *https://www.who.int/news-room/fact-sheets/detail/chronic-obstructive-pulmonary-disease-(copd)*, 2022.

[95] James C. Hogg and Wim Timens, “The Pathology of Chronic Obstructive Pulmonary Disease,” *Annual Review of Pathology: Mechanisms of Disease*, vol. 4, pp. 435–459, 2009.

[96] J. M. Yentes, K. K. Schmid, D. Blanke, D. J. Romberger, S. I. Rennard, and N. Stergiou, “Gait mechanics in patients with chronic obstructive pulmonary disease,” *Respir Res*, vol. 16, no. 1, Feb. 2015, doi: 10.1186/s12931-015-0187-5.

[97] M. Zago, C. Sforza, D. R. Bonardi, E. E. Guffanti, and M. Galli, “Gait analysis in patients with chronic obstructive pulmonary disease: a systematic review,” *Gait and Posture*, vol. 61. Elsevier B.V., pp. 408–415, Mar. 01, 2018. doi: 10.1016/j.gaitpost.2018.02.007.

[98] “Congestive Heart Failure,” *https://www.ncbi.nlm.nih.gov/books/NBK430873/*.

[99] E. B. Ozcan *et al.*, “Impaired Balance and Gait Characteristics in Patients With Chronic Heart Failure,” *Heart Lung Circ*, vol. 31, no. 6, pp. 832–840, Jun. 2022, doi: 10.1016/j.hlc.2021.10.015.

[100] S. W. Davies, C. A. Greig, S. L. Jordan, D. W. Grieve, and D. P. Lipkin, “Short-stepping gait in severe heart failure,” *Heart*, vol. 68, no. 11, pp. 469–472, 1992, doi: 10.1136/hrt.68.11.469.

[101] “Hip Fracture overview,” *https://www.ncbi.nlm.nih.gov/books/NBK557514/*, 2022.

[102] L. Rodrigues, F. H. Cornelis, and S. Chevret, “Hip fracture prevention in osteoporotic elderly and cancer patients: An on-line french survey evaluating current needs,” *Medicina (Lithuania)*, vol. 56, no. 8, pp. 1–12, Aug. 2020, doi: 10.3390/medicina56080397.

[103] M. , & J. A. Parker, “Hip Fracture,” *Bmj*, vol. 333, no. 7557, pp. 27–30, 2006.

[104] P. Thingstad, T. Egerton, E. F. Ihlen, K. Taraldsen, R. Moe-Nilssen, and J. L. Helbostad, “Identification of gait domains and key gait variables following hip fracture,” *BMC Geriatr*, vol. 15, no. 1, Nov. 2015, doi: 10.1186/s12877-015-0147-4.

[105] N. Herssens, E. Verbecque, A. Hallemans, L. Vereeck, V. Van Rompaey, and W. Saeys, “Do spatiotemporal parameters and gait variability differ across the lifespan of healthy adults? A systematic review,” *Gait and Posture*, vol. 64. Elsevier B.V., pp. 181–190, Jul. 01, 2018. doi: 10.1016/j.gaitpost.2018.06.012.

[106] C. L. Christiansen and J. E. Stevens-Lapsley, “Weight-bearing asymmetry in relation to measures of impairment and functional mobility for people with knee osteoarthritis,” *Arch Phys Med Rehabil*, vol. 91, no. 10, pp. 1524–1528, 2010, doi: 10.1016/j.apmr.2010.07.009.

[107] F. Kluge *et al.*, “Consensus based framework for digital mobility monitoring,” *PLoS One*, vol. 16, no. 8 August, Aug. 2021, doi: 10.1371/journal.pone.0256541.

[108] M. A. D. Brodie *et al.*, “Wearable pendant device monitoring using new wavelet-based methods shows daily life and laboratory gaits are different,” *Med Biol Eng Comput*, vol. 54, no. 4, pp. 663–674, Apr. 2016, doi: 10.1007/s11517-015-1357-9.

[109] W. Zijlstra and A. L. Hof, “Assessment of spatio-temporal gait parameters from trunk accelerations during human walking.” [Online]. Available: www.elsevier.com/locate/gaitpost

[110] S. C. Miff ’, S. A. Gard, and D. S. Childress, “The Effect of Step Length, Cadence, and Walking Speed on the Trunk’s Vertical Excursion.”

[111] F. Saibene and A. E. Minetti, “Biomechanical and physiological aspects of legged locomotion in humans,” *European Journal of Applied Physiology*, vol. 88, no. 4–5. Springer Verlag, pp. 297–316, 2003. doi: 10.1007/s00421-002-0654-9.

[112] Y. P. Ivanenko, N. Dominici, and F. Lacquaniti, “Development of independent walking in toddlers,” 2007. [Online]. Available: www.acsm-essr.org

[113] D. A. Winter, *Biomechanics and motor control of human movement.* . John Wiley & Sons, 2009.

[114] A. Muro-de-la-Herran, B. García-Zapirain, and A. Méndez-Zorrilla, “Gait analysis methods: An overview of wearable and non-wearable systems, highlighting clinical applications,” *Sensors (Switzerland)*, vol. 14, no. 2. pp. 3362–3394, Feb. 19, 2014. doi: 10.3390/s140203362.

[115] A. A. Hulleck, D. Menoth Mohan, N. Abdallah, M. El Rich, and K. Khalaf, “Present and future of gait assessment in clinical practice: Towards the application of novel trends and technologies,” *Front Med Technol*, vol. 4, Dec. 2022, doi: 10.3389/fmedt.2022.901331.

[116] B. Toro, C. Nester, and P. Farren, “A review of observational gait assessment in clinical practice”, doi: 10.1080/0959398039221901.

[117] D. M. Mohan, A. H. Khandoker, S. A. Wasti, S. Ismail Ibrahim Ismail Alali, H. F. Jelinek, and K. Khalaf, “Assessment Methods of Post-stroke Gait: A Scoping Review of Technology-Driven Approaches to Gait Characterization and Analysis,” *Frontiers in Neurology*, vol. 12. Frontiers Media S.A., Jun. 08, 2021. doi: 10.3389/fneur.2021.650024.

[118] T. A. L. Wren, C. A. Tucker, S. A. Rethlefsen, G. E. Gorton, and S. Õunpuu, “Clinical efficacy of instrumented gait analysis: Systematic review 2020 update,” *Gait Posture*, vol. 80, pp. 274–279, Jul. 2020, doi: 10.1016/j.gaitpost.2020.05.031.

[119] A. Carriero, A. Zavatsky, J. Stebbins, T. Theologis, and S. J. Shefelbine, “Determination of gait patterns in children with spastic diplegic cerebral palsy using principal components,” *Gait Posture*, vol. 29, no. 1, pp. 71–75, Jan. 2009, doi: 10.1016/j.gaitpost.2008.06.011.

[120] L. Middleton, A. A. Buss, A. Bazin, and M. S. Nixon, “A floor sensor system for gait recognition,” in *Proceedings - Fourth IEEE Workshop on Automatic Identification Advanced Technologies, AUTO ID 2005*, 2005, pp. 171–180. doi: 10.1109/AUTOID.2005.2.

[121] C. J. van Uden and M. P. Besser, “Test-retest reliability of temporal and spatial gait characteristics measured with an instrumented walkway system (GAITRite ®),” 2004. [Online]. Available: http://www.biomedcentral.com/1471-2474/5/13

[122] M. Gabel, R. Gilad-Bachrach, E. Renshaw, and A. Schuster, “Full body gait analysis with Kinect,” in *Proceedings of the Annual International Conference of the IEEE Engineering in Medicine and Biology Society, EMBS*, 2012, pp. 1964–1967. doi: 10.1109/EMBC.2012.6346340.

[123] M. W. Whittle, “Chapter 4-Methods of gait analysis.,” in *Gait analysis*, 2007.

[124] K. A. , & P. M. B. Lamkin-Kennard, “Sensors: Naturaland Synthetic Sensors,” in *Biomechatronics*, 2019, pp. 81–107.

[125] D. A. Bruening and S. T. Ridge, “Automated event detection algorithms in pathological gait,” *Gait Posture*, vol. 39, no. 1, pp. 472–477, Jan. 2014, doi: 10.1016/j.gaitpost.2013.08.023.

[126] M. Lempereur *et al.*, “A new deep learning-based method for the detection of gait events in children with gait disorders: Proof-of-concept and concurrent validity,” *J Biomech*, vol. 98, Jan. 2020, doi: 10.1016/j.jbiomech.2019.109490.

[127] R. , C. M. H. , & M. L. G. Wellmon, “Gait assessment and training.,” in *Physical Rehabilitation*, St. Louis: Elsevier., 2007.

[128] Robert Wellmon, “Chapter 32 - Gait Assessment and Training,” in *Physical Rehabilitation Evidence-Based Examination, Evaluation, and Intervention*, 2007, pp. 844–876.

[129] A. L. Adkin, J. S. Frank, M. G. Carpenter, and G. W. Peysar, “Postural control is scaled to level of postural threat,” 2000. [Online]. Available: www.elsevier.com/locate/gaitpost

[130] A. J. Parker, “Stereoscopic Vision,” *Encyclopedia of Neuroscience*. pp. 411–417, 2009.

[131] A. Küderle, N. Roth, J. Zlatanovic, M. Zrenner, B. Eskofier, and F. Kluge, “The placement of foot-mounted IMU sensors does affect the accuracy of spatial parameters during regular walking,” *PLoS One*, vol. 17, no. 6 June, Jun. 2022, doi: 10.1371/journal.pone.0269567.

[132] M. Moro, G. Marchesi, F. Hesse, F. Odone, and M. Casadio, “Markerless vs. Marker-Based Gait Analysis: A Proof of Concept Study,” *Sensors*, vol. 22, no. 5, Mar. 2022, doi: 10.3390/s22052011.

[133] T. Bonci *et al.*, “An Algorithm for Accurate Marker-Based Gait Event Detection in Healthy and Pathological Populations During Complex Motor Tasks,” *Front Bioeng Biotechnol*, vol. 10, Jun. 2022, doi: 10.3389/fbioe.2022.868928.

[134] M. Iosa, P. Picerno, S. Paolucci, and G. Morone, “Wearable inertial sensors for human movement analysis,” *Expert Review of Medical Devices*, vol. 13, no. 7. Taylor and Francis Ltd, pp. 641–659, Jul. 02, 2016. doi: 10.1080/17434440.2016.1198694.

[135] Y. Hutabarat, D. Owaki, and M. Hayashibe, “Recent Advances in Quantitative Gait Analysis Using Wearable Sensors: A Review,” *IEEE Sens J*, vol. 21, no. 23, pp. 26470–26487, Dec. 2021, doi: 10.1109/JSEN.2021.3119658.

[136] A. , L. L. , & S. G. Medeiros, “An Introduction to Wearable Sensor Technology.,” in *Intelligent Internet of Things for Healthcare and Industry* , Cham: Springer International Publishing., 2022, pp. 189–198.

[137] L. C. Benson, C. A. Clermont, E. Bošnjak, and R. Ferber, “The use of wearable devices for walking and running gait analysis outside of the lab: A systematic review,” *Gait and Posture*, vol. 63. Elsevier B.V., pp. 124–138, Jun. 01, 2018. doi: 10.1016/j.gaitpost.2018.04.047.

[138] J. H. R. L. & M. S. G. Fernie, “Footswitches,” in *Disability Proceedings of a Seminar on Rehabilitation of the Disabled*, 1979, pp. 136–140.

[139] J. L. Chen *et al.*, “Plantar Pressure-Based Insole Gait Monitoring Techniques for Diseases Monitoring and Analysis: A Review,” *Advanced*

Materials Technologies, vol. 7, no. 1. John Wiley and Sons Inc, Jan. 01, 2022. doi: 10.1002/admt.202100566.

[140] "Tekscan solutions for pressure mapping," *https://www.tekscan.com/products-solutions/pressure-offloading-foot-function*.

[141] A. Muro-de-la-Herran, B. García-Zapirain, and A. Méndez-Zorrilla, "Gait analysis methods: An overview of wearable and non-wearable systems, highlighting clinical applications," *Sensors (Switzerland)*, vol. 14, no. 2. pp. 3362–3394, Feb. 19, 2014. doi: 10.3390/s140203362.

[142] P. Esser, H. Dawes, J. Collett, M. G. Feltham, and K. Howells, "Assessment of spatio-temporal gait parameters using inertial measurement units in neurological populations," *Gait Posture*, vol. 34, no. 4, pp. 558–560, Oct. 2011, doi: 10.1016/j.gaitpost.2011.06.018.

[143] M. Khedr and N. El-Sheimy, "A smartphone step counter using IMU and magnetometer for navigation and health monitoring applications," *Sensors (Switzerland)*, vol. 17, no. 11, Nov. 2017, doi: 10.3390/s17112573.

[144] Erdem et al, "Gait Analysis Using Smartwatches," in *IEEE 30th International Symposium on Personal, Indoor and Mobile Radio Communications (PIMRC Workshops).*, 2019.

[145] S. Stankoski, M. Gjoreski, J. Archer William, and B. Hayes Canterbury, "Smart Glasses for Gait Analysis in Parkinson's Disease: A preliminary study", doi: 10.1101/2022.10.22.22281214.

[146] T. Seel, M. Kok, and R. S. McGinnis, "Inertial sensors—applications and challenges in a nutshell," *Sensors (Switzerland)*, vol. 20, no. 21. MDPI AG, pp. 1–5, Sep. 01, 2020. doi: 10.3390/s20216221.

[147] W. Zijlstra and A. L. Hof, "Assessment of spatio-temporal gait parameters from trunk accelerations during human walking." [Online]. Available: www.elsevier.com/locate/gaitpost

[148] D. Trojaniello, A. Cereatti, and U. Della Croce, "Accuracy, sensitivity and robustness of five different methods for the estimation of gait temporal parameters using a single inertial sensor mounted on the lower trunk," *Gait*

Posture, vol. 40, no. 4, pp. 487–492, 2014, doi: 10.1016/j.gaitpost.2014.07.007.

[149] P. Catalfamo, S. Ghoussayni, and D. Ewins, "Gait event detection on level ground and incline walking using a rate gyroscope," *Sensors*, vol. 10, no. 6, pp. 5683–5702, Jun. 2010, doi: 10.3390/s100605683.

[150] B. Mariani, M. C. Jiménez, F. J. G. Vingerhoets, and K. Aminian, "On-shoe wearable sensors for gait and turning assessment of patients with parkinson's disease," *IEEE Trans Biomed Eng*, vol. 60, no. 1, pp. 155–158, 2013, doi: 10.1109/TBME.2012.2227317.

[151] M. Zago *et al.*, "Machine-learning based determination of gait events from foot-mounted inertial units," *Sensors (Switzerland)*, vol. 21, no. 3, pp. 1–13, Feb. 2021, doi: 10.3390/s21030839.

[152] M. Z. Arshad, A. Jamsrandorj, J. Kim, and K. R. Mun, "Gait Events Prediction Using Hybrid CNN-RNN-Based Deep Learning Models through a Single Waist-Worn Wearable Sensor," *Sensors*, vol. 22, no. 21, Nov. 2022, doi: 10.3390/s22218226.

[153] R. Romijnders, E. Warmerdam, C. Hansen, G. Schmidt, and W. Maetzler, "A Deep Learning Approach for Gait Event Detection from a Single Shank-Worn IMU: Validation in Healthy and Neurological Cohorts," *Sensors*, vol. 22, no. 10, May 2022, doi: 10.3390/s22103859.

[154] R. J. Mobbs *et al.*, "Gait metrics analysis utilizing single-point inertial measurement units: a systematic review," *mHealth*, vol. 8. AME Publishing Company, Jan. 01, 2022. doi: 10.21037/mhealth-21-17.

[155] S. Yang, J. T. Zhang, A. C. Novak, B. Brouwer, and Q. Li, "Estimation of spatio-temporal parameters for post-stroke hemiparetic gait using inertial sensors," *Gait Posture*, vol. 37, no. 3, pp. 354–358, Mar. 2013, doi: 10.1016/j.gaitpost.2012.07.032.

[156] S. R. Hundza *et al.*, "Accurate and reliable gait cycle detection in parkinson's disease," *IEEE Transactions on Neural Systems and Rehabilitation Engineering*, vol. 22, no. 1, pp. 127–137, Jan. 2014, doi: 10.1109/TNSRE.2013.2282080.

[157] A. Brégou Bourgeois, B. Mariani, K. Aminian, P. Y. Zambelli, and C. J. Newman, "Spatio-temporal gait analysis in children with cerebral palsy using, foot-worn inertial sensors," *Gait Posture*, vol. 39, no. 1, pp. 436–442, Jan. 2014, doi: 10.1016/j.gaitpost.2013.08.029.

[158] T. M. Mok, F. Cornish, and J. Tarr, "Too Much Information: Visual Research Ethics in the Age of Wearable Cameras," *Integr Psychol Behav Sci*, vol. 49, no. 2, pp. 309–322, May 2015, doi: 10.1007/s12124-014-9289-8.

[159] P. Catalfamo, D. Moser, S. Ghoussayni, and D. Ewins, "Detection of gait events using an F-Scan in-shoe pressure measurement system," *Gait Posture*, vol. 28, no. 3, pp. 420–426, 2008, doi: 10.1016/j.gaitpost.2008.01.019.

[160] E. Martini *et al.*, "Pressure-sensitive insoles for real-time gait-related applications," *Sensors (Switzerland)*, vol. 20, no. 5, Mar. 2020, doi: 10.3390/s20051448.

[161] M. Benocci, L. Rocchi, E. Farella, L. Chiari, and L. Benini, "A wireless system for gait and posture analysis based on pressure insoles and inertial measurement units," in *2009 3rd International Conference on Pervasive Computing Technologies for Healthcare - Pervasive Health 2009, PCTHealth 2009*, 2009. doi: 10.4108/ICST.PERVASIVEHEALTH2009.6032.

[162] N. Roth, C. F. Martindale, H. Gaßner, Z. Kohl, J. Klucken, and B. M. Eskofer, "Synchronized sensor insoles for clinical gait analysis in home-monitoring applications," *Current Directions in Biomedical Engineering*, vol. 4, no. 1, pp. 433–437, Sep. 2018, doi: 10.1515/cdbme-2018-0103.

[163] S. Del Din, A. Godfrey, C. Mazzà, S. Lord, and L. Rochester, "Free-living monitoring of Parkinson's disease: Lessons from the field," *Movement Disorders*, vol. 31, no. 9, pp. 1293–1313, Sep. 2016, doi: 10.1002/mds.26718.

[164] F. A. Storm, K. P. S. Nair, A. J. Clarke, J. M. Van der Meulen, and C. Mazzà, "Free-living and laboratory gait characteristics in patients with multiple sclerosis," *PLoS One*, vol. 13, no. 5, May 2018, doi: 10.1371/journal.pone.0196463.

[165] I. Hillel *et al.*, “Is every-day walking in older adults more analogous to dual-task walking or to usual walking? Elucidating the gaps between gait performance in the lab and during 24/7 monitoring,” *European Review of Aging and Physical Activity*, vol. 16, no. 1, May 2019, doi: 10.1186/s11556-019-0214-5.

[166] V. V. Shah *et al.*, “Laboratory versus daily life gait characteristics in patients with multiple sclerosis, Parkinson’s disease, and matched controls,” *J Neuroeng Rehabil*, vol. 17, no. 1, Dec. 2020, doi: 10.1186/s12984-020-00781-4.

[167] C. Tunca, N. Pehlivan, N. Ak, B. Arnrich, G. Salur, and C. Ersoy, “Inertial sensor-based robust gait analysis in non-hospital settings for neurological disorders,” *Sensors (Switzerland)*, vol. 17, no. 4, Apr. 2017, doi: 10.3390/s17040825.

[168] A. Rampp, J. Barth, S. Schülein, K. G. Gaßmann, J. Klucken, and B. M. Eskofier, “Inertial Sensor-Based Stride Parameter Calculation From Gait Sequences in Geriatric Patients,” *IEEE Trans Biomed Eng*, vol. 62, no. 4, pp. 1089–1097, Apr. 2015, doi: 10.1109/TBME.2014.2368211.

[169] C. M. Kanzler *et al.*, “Inertial sensor based and shoe size independent gait analysis including heel and toe clearance estimation,” in *Proceedings of the Annual International Conference of the IEEE Engineering in Medicine and Biology Society, EMBS*, Institute of Electrical and Electronics Engineers Inc., Nov. 2015, pp. 5424–5427. doi: 10.1109/EMBC.2015.7319618.

[170] F. Kluge, H. Gaßner, J. Hannink, C. Pasluosta, J. Klucken, and B. M. Eskofier, “Towards mobile gait analysis: Concurrent validity and test-retest reliability of an inertial measurement system for the assessment of spatio-temporal gait parameters,” *Sensors (Switzerland)*, vol. 17, no. 7, Jul. 2017, doi: 10.3390/s17071522.

[171] P. Terrier, Q. Ladetto, B. Merminod, and Y. Schutz, “High-precision satellite positioning system as a new tool to study the biomechanics of human locomotion,” 2000.

[172] L. Reggi, L. Palmerini, L. Chiari, and S. Mellone, “Real-World Walking Speed Assessment Using a Mass-Market RTK-GNSS Receiver,” *Front Bioeng Biotechnol*, vol. 10, Mar. 2022, doi: 10.3389/fbioe.2022.873202.

[173] H. M. Schepers, H. F. J. M. Koopman, and P. H. Veltink, “Ambulatory Assessment of Ankle and Foot Dynamics,” *IEEE Trans Biomed Eng*, vol. 54, no. 5, pp. 895–902, 2007, doi: 10.1109/TBME.2006.889769.

[174] F. B. Van Meulen, D. Weenk, J. H. Buurke, B. J. F. Van Beijnum, and P. H. Veltink, “Ambulatory assessment of walking balance after stroke using instrumented shoes,” *J Neuroeng Rehabil*, vol. 13, no. 1, May 2016, doi: 10.1186/s12984-016-0146-5.

[175] G. Li, T. Liu, and J. Yi, “Wearable Sensor System for Detecting Gait Parameters of Abnormal Gaits: A Feasibility Study,” *IEEE Sens J*, vol. 18, no. 10, pp. 4234–4241, May 2018, doi: 10.1109/JSEN.2018.2814994.

[176] W. , Tang, G. , Fulk, S. , Zeigler, T. , Zhang, and E. Sazonov, “Estimating Berg Balance Scale and Mini Balance Evaluation System Test Scores by Using Wearable Shoe Sensors.,” IEEE EMBS International Conference on Biomedical & Health Informatics (BHI), Ed., Chicago, IL, USA, , May 2019.

[177] J. M. Potter, A. L. Evans, and G. Duncan, “Gait Speed and Activities of Daily Living Function in Geriatric Patients,” 1995.

[178] N. G. Lee, T. W. Kang, and H. J. Park, “Relationship Between Balance, Gait, and Activities of Daily Living in Older Adults With Dementia,” *Geriatr Orthop Surg Rehabil*, vol. 11, 2020, doi: 10.1177/2151459320929578.

[179] D. Tan, M. Danoudis, J. McGinley, and M. E. Morris, “Relationships between motor aspects of gait impairments and activity limitations in people with Parkinson’s disease: A systematic review,” *Parkinsonism and Related Disorders*, vol. 18, no. 2. pp. 117–124, Feb. 2012. doi: 10.1016/j.parkreldis.2011.07.014.

[180] P. , R. O. , W. S. , L. M. , & K. P. Raiss, “Range of motion of shoulder and elbow in activities of daily life in 3D motion analysis. ,” *Z Orthop Unfall*, vol. 145, no. 4, pp. 493–498, 2007.

[181] M. C. M. Klotz *et al.*, “Motion capture of the upper extremity during activities of daily living in patients with spastic hemiplegic cerebral palsy,”

Gait Posture, vol. 38, no. 1, pp. 148–152, May 2013, doi: 10.1016/j.gaitpost.2012.11.005.

[182] F. S. Ayachi, H. P. Nguyen, C. Lavigne-Pelletier, E. Goubault, P. Boissy, and C. Duval, "Wavelet-based algorithm for auto-detection of daily living activities of older adults captured by multiple inertial measurement units (IMUs)," *Physiol Meas*, vol. 37, no. 3, pp. 442–461, Feb. 2016, doi: 10.1088/0967-3334/37/3/442.

[183] J. I. Serrano, S. Lambrecht, M. D. del Castillo, J. P. Romero, J. Benito-León, and E. Rocon, "Identification of activities of daily living in tremorous patients using inertial sensors," *Expert Syst Appl*, vol. 83, pp. 40–48, Oct. 2017, doi: 10.1016/j.eswa.2017.04.032.

[184] H. Nguyen, K. Lebel, S. Bogard, E. Goubault, P. Boissy, and C. Duval, "Using Inertial Sensors to Automatically Detect and Segment Activities of Daily Living in People with Parkinson's Disease," *IEEE Transactions on Neural Systems and Rehabilitation Engineering*, vol. 26, no. 1, pp. 197–204, Jan. 2018, doi: 10.1109/TNSRE.2017.2745418.

[185] B. Kirking, M. El-Gohary, and Y. Kwon, "The feasibility of shoulder motion tracking during activities of daily living using inertial measurement units," *Gait Posture*, vol. 49, pp. 47–53, Sep. 2016, doi: 10.1016/j.gaitpost.2016.06.008.

[186] R. M. Chapman, M. T. Torchia, J. E. Bell, and D. W. Van Citters, "Assessing Shoulder Biomechanics of Healthy Elderly Individuals during Activities of Daily Living Using Inertial Measurement Units: High Maximum Elevation Is Achievable but Rarely Used," *J Biomech Eng*, vol. 141, no. 4, Apr. 2019, doi: 10.1115/1.4042433.

[187] L. Uhlenberg, S. Hassan Gangaraju, and O. Amft, "IMUAngle: Joint Angle Estimation with Inertial Sensors in Daily Activities," in *Proceedings - International Symposium on Wearable Computers, ISWC*, Association for Computing Machinery, Sep. 2022, pp. 64–68. doi: 10.1145/3544794.3558470.

[188] A. K. Bourke *et al.*, "Energy expenditure estimation using accelerometry and heart rate for multiple sclerosis and healthy older adults," in *Proceedings - 11th International Conference on Wearable and Implantable*

Body Sensor Networks Workshops, BSN Workshops 2014, Institute of Electrical and Electronics Engineers Inc., Dec. 2014, pp. 1–5. doi: 10.1109/BSN.Workshops.2014.18.

[189] M. Hedegaard, A. Anvari-Moghaddam, B. K. Jensen, C. B. Jensen, M. K. Pedersen, and A. Samani, "Prediction of energy expenditure during activities of daily living by a wearable set of inertial sensors," *Med Eng Phys*, vol. 75, pp. 13–22, Jan. 2020, doi: 10.1016/j.medengphy.2019.10.006.

[190] J. M. Hausdorff, M. E. Cudkowicz, R. Firtion, J. Y. Wei, and A. L. Goldberger, "Gait variability and basal ganglia disorders: Stride-to-stride variations of gait cycle timing in Parkinson's disease and Huntington's disease," *Movement Disorders*, vol. 13, no. 3, pp. 428–437, May 1998, doi: 10.1002/mds.870130310.

[191] S. I. Yaniger, "Force Sensing resistors™ a review of the technology," in *Electro International, ELECTR 1991 - Conference Record*, Institute of Electrical and Electronics Engineers Inc., 1991, pp. 666–668. doi: 10.1109/ELECTR.1991.718294.

[192] D. J. Van Den Heever, K. Schreve, and C. Scheffer, "Tactile sensing using force sensing resistors and a super-resolution algorithm," *IEEE Sens J*, vol. 9, no. 1, pp. 29–35, Jan. 2009, doi: 10.1109/JSEN.2008.2008891.

[193] J. , & F. J. Fraden, *Handbook of modern sensors: physics, designs, and applications* , vol. 3. New York: Springer, 2010.

[194] S. Stassi, V. Cauda, G. Canavese, and C. F. Pirri, "Flexible tactile sensing based on piezoresistive composites: A review," *Sensors (Switzerland)*, vol. 14, no. 3. MDPI AG, pp. 5296–5332, Mar. 14, 2014. doi: 10.3390/s140305296.

[195] D. Giovanelli and E. Farella, "Force Sensing Resistor and Evaluation of Technology for Wearable Body Pressure Sensing," *J Sens*, vol. 2016, 2016, doi: 10.1155/2016/9391850.

[196] D. K. Shaeffer, "MEMS inertial sensors: A tutorial overview," *IEEE Communications Magazine*, vol. 51, no. 4, pp. 100–109, 2013.

[197] B. E. Boser and R. T. Howe, “Surface Micromachined Accelerometers,” 1996.

[198] J. A. Geen, S. J. Sherman, J. F. Chang, and S. R. Lewis, “Single-chip surface micromachined integrated gyroscope with 50°/h allan deviation,” in *IEEE Journal of Solid-State Circuits*, Dec. 2002, pp. 1860–1866. doi: 10.1109/JSSC.2002.804345.

[199] T. K. Sethuramalingam and A. Vimalajuliet, “Design of MEMS based capacitive accelerometer,” in *ICMET 2010 - 2010 International Conference on Mechanical and Electrical Technology, Proceedings*, 2010, pp. 565–568. doi: 10.1109/ICMET.2010.5598424.

[200] Z. Mohammed, I. (Abe) M. Elfadel, and M. Rasras, “Monolithic multi degree of freedom (MDoF) capacitive MEMS accelerometers,” *Micromachines*, vol. 9, no. 11. MDPI AG, Nov. 16, 2018. doi: 10.3390/mi9110602.

[201] C. , & S. A. Acar, *MEMS vibratory gyroscopes: structural approaches to improve robustness.* . Springer Science & Business Media., 2008.

[202] H. C. Corben and P. Stehle, “Chapter 1, Section 5,” in *Classical Mechanics* , Wiley, Ed., 1960.

[203] W. A. Gill, I. Howard, I. Mazhar, and K. McKee, “A Review of MEMS Vibrating Gyroscopes and Their Reliability Issues in Harsh Environments,” *Sensors*, vol. 22, no. 19. MDPI, Oct. 01, 2022. doi: 10.3390/s22197405.

[204] J. Bernstein, S. Cho, A. T. King, A. Kourepenis, P. Maciel, and M. Weinberg, “Micromachined comb-drive tuning fork rate gyroscope,” in *IEEE Micro Electro Mechanical Systems*, Publ by IEEE, 1993, pp. 143–148. doi: 10.1109/memsys.1993.296932.

[205] R. , & O. R. Antonello, “MEMS gyroscopes for consumer and industrial applications.,” in *Microsensors*, Intech, 2011, pp. 253–280.

[206] S. Bertuletti, A. Cereatti, D. Comotti, M. Caldara, and U. Della Croce, “Static and dynamic accuracy of an innovative miniaturized wearable platform for short range distance measurements for human movement applications,” *Sensors (Switzerland)*, vol. 17, no. 7, Jul. 2017, doi: 10.3390/s17071492.

[207] M. , L. S. , C. O. , & H. R. P. Hansard, *Time-of-flight cameras: principles, methods and applications.* . Springer Science & Business Media., 2012.

[208] S. , C. A. , C. M. , & D. C. U. Bertuletti, "Measurement of the inter-foot distance using a Time-of-Flight proximity sensor: Preliminary evaluation during leg oscillation exercises.," in *Proceedings of the GNB Conference*, Naples, 2016, pp. 20–22.

[209] "221e S.r.l., Padova, Italy. Products Overview.," *https://www.221e.com/*, 2020.

[210] F. Salis *et al.*, "A multi-sensor wearable system for the assessment of diseased gait in real-world conditions," *Front Bioeng Biotechnol*, vol. 11, p. 518, 2023, doi: 10.3389/fbioe.2023.1143248.

[211] F. Salis, S. Bertuletti, T. Bonci, U. Della Croce, C. Mazzà, and A. Cereatti, "A method for gait events detection based on low spatial resolution pressure insoles data," *J Biomech*, vol. 127, Oct. 2021, doi: 10.1016/j.jbiomech.2021.110687.

[212] K. Scott *et al.*, "Design and validation of a multi-task, multi-phase protocol for real-world gait simulation."

[213] C. Mazzà *et al.*, "Technical validation of real-world monitoring of gait: A multicentric observational study," *BMJ Open*, vol. 11, no. 12, Dec. 2021, doi: 10.1136/bmjopen-2021-050785.

[214] Y. C. Learmonth, D. D. Dlugonski, L. A. Pilutti, B. M. Sandroff, and R. W. Motl, "The reliability, precision and clinically meaningful change of walking assessments in multiple sclerosis," *Multiple Sclerosis Journal*, vol. 19, no. 13, pp. 1784–1791, 2013, doi: 10.1177/1352458513483890.

[215] F. Ayoubi, C. P. Launay, C. Annweiler, and O. Beauchet, "Fear of Falling and Gait Variability in Older Adults: A Systematic Review and Meta-Analysis," *Journal of the American Medical Directors Association*, vol. 16, no. 1. Elsevier Inc., pp. 14–19, Jan. 01, 2015. doi: 10.1016/j.jamda.2014.06.020.